Texas Tech University
Multidisciplinary Research in Transportation

Implementation of Concrete Overlay Evaluation and Design

Niwesh Koirala, Chuljin Hwang, Heejun Lee, Jeonghee Nam,
Christopher Jabonero and Moon Won

Performed in cooperation with the Texas Department of Transportation and the Federal Highway Administration

Research Project 5-6910-01
Research Report 5-6910-01 R1
http://www.techmrt.ttu.edu/reports.php

1. Report No. FHWA/TX-24/5-6910-01-1	2. Government Accession No.	3. Recipient's Catalog No.
4. Title and Subtitle Implementation of CRCP Overlay on CPCD		5. Report Date July 2023 6. Performing Organization Code
7. Author(s) Niwesh Koirala, Chuljin Hwang, Heejun Lee, Jeonghee Nam, Christopher Jabonero and Moon Won		8. Performing Organization Report No. 5-6910-01
9. Performing Organization Name and Address Texas Tech Center for Multidisciplinary Research in Transportation Texas Tech University Box 41023 Lubbock, TX 79409		10. Work Unit No. (TRAIS) 11. Contract or Grant No.
12. Sponsoring Agency Name and Address Texas Department of Transportation Research and Technology Implementation Division Box 5080 Austin, TX 78763-5080		13. Type of Report and Period Covered Technical Report September 2019-August 2023 14. Sponsoring Agency Code
15. Supplementary Notes Project performed in cooperation with the Texas Department of Transportation and the Federal Highway Administration		

16. Abstract

The performance of 7-in CRCP overlay on CPCD in US 75 in Sherman, which was built in 2010, has been quite satisfactory. Encouraged by the satisfactory performance of the project, TxDOT Paris District decided to build another CRCP overlay on CPCD in US 82 in Paris. This project is in the westbound direction of US 82 – consisting of 2 main lanes and asphalt shoulders for both inside and outside – from Kiamichi Railroad to FM 79, approximately 0.9 miles. The structural evaluation of the existing 9-in CPCD was conducted in November 2019, and the construction of 5-in CRCP overlay started in May 2023. The construction of overlay in the outside lane started on May 30, 2023, and the inside lane construction started late August of 2023. Temperature profiling indicated a significant insulating effect of the CRCP overlay, reducing temperature variations and joint movements in the CPCD layer. Key findings included (1) good bonding between CRCP and CPCD interface when concrete with reasonable workability was placed, while quite poor bonding when concrete with excessive slump was placed, (2) considerable reduction in slab deflections by placing 5-in CRCP overlay, and (3) significant level of reflection cracking in CRCP at existing transverse contraction joints. For various reasons, the variability in construction operations and concrete material properties was larger than expected and is reflected in the early behavior of CRCP overlay. At this point, it is not known whether the large variability in materials and construction and resulting early-age behavior will have appreciable effects on long-term performance. The performance of this section will be monitored in the TxDOT rigid pavement research project (0-7147).

17. Key Word	18. Distribution Statement
Bonded concrete overlay, CPCD, CRCP, reflection cracking, bond strength	No restrictions. This document is available to the public through the National Technical Information Service, Springfield, Virginia 22161 www.ntis.gov

19. Security Classif. (of this report)	20. Security Classif. (of this page)	21. No. of Pages	22. Price

Form DOT F 1700.7 (8-72) Reproduction of completed page authorized.

IMPLEMENTATION OF CONCRETE OVERLAY EVALUATION AND DESIGN

by

Niwesh Koirala,
Chuljin Hwang,
and
Heejun Lee

Graduate Students
Texas Tech University

Jeonghee Nam, Ph.D.
Research Associate
Texas Tech University

Christopher Jabonero, Ph.D.
Post-Doctoral Researcher
Texas Tech University

Moon Won, P.E., Ph.D.
Professor
Texas Tech University

Project Report 5-6910-01-1
Project Number 5-6910-01

Performed in Cooperation with the
Texas Department of Transportation
and the
Federal Highway Administration

Center for Multidisciplinary Research in Transportation
Department of Civil. and Environmental and Construction Engineering
Texas Tech University
Box 41023
Lubbock, TX 79409-1023

AUTHORS' DISCLAIMER
The contents of this report reflect the views of the authors who are responsible for the facts and the accuracy of the data presented herein. The contents do not necessarily reflect the official view of policies of the Texas Department of Transportation or the Federal Highway Administration. This report does not constitute a standard, specification, or regulation.

PATENT DISCLAIMER
There was no invention or discovery conceived or first actually reduced to practice in the course of or under this contract, including any art, method, process, machine, manufacture, design or composition of matter, or any new useful improvement thereof, or any variety of plant which is or may be patentable under the patent laws of the United States of America or any foreign country.

ENGINEERING DISCLAIMER
Not intended for construction, bidding, or permit purposes.

TRADE NAMES AND MANUFACTURERS' NAMES
The United States Government and the State of Texas do not endorse products or manufacturers. Trade or manufacturers' names appear herein solely because they are considered essential to the object of this report.

ACKNOWLEDGMENTS

The authors express their appreciation to the members of the Project Team, Messrs. Andy Naranjo, Ruben Carrasco, and Pangil Choi, and Ms. Rachel Cano. The support provided by Mr. Austin Shatto, and the Paris Area Office personnel is appreciated.

PRODUCTS

This report contains recommended revisions to Pavement Manual in Appendix A.

Table of Contents

List of Figures

List of Tables

Chapter 1 Introduction

1.1 Background

As of 2023, the Texas Department of Transportation (TxDOT) has 3225 lane miles of plain jointed concrete pavement (JCP or CPCD) in service(TxDOT, 2023). Even though CPCD has been used extensively in other states, its use has been limited in Texas, primarily due to better performance of continuously reinforced concrete pavement (CRCP) as well as few options available for rehabilitation when CPCD reaches a terminal condition. As for the rehabilitation options for CPCD, asphalt concrete (AC) overlay has been utilized most extensively, with crack and seat, rubblization, and removal and replacement occasionally implemented. The popularity of AC overlay is primarily due to the low cost of rehabilitation and fast opening to traffic after AC overlay (Ryu et al., 2013). On the other hand, AC overlay has the disadvantage of reflection cracking at existing transverse contraction joints. Reflection cracking in AC overlays on CPCD degrades the ride quality and often requires the removal and replacement of the AC layer on a regular basis. Crack and seat and rubblization with subsequent AC overlay are not always effective. Removal and replacement of CPCD with CPCD or other pavement types could be quite expensive. An effective rehabilitation method for old CPCD that will provide a better long-term performance for a reasonable cost is needed.

Findings from the AASHO Road Test and TxDOT research project 0-6274, Project Level Performance Database for Rigid Pavements in Texas, Phase II, indicate superior performance of rigid pavement or CRCP when the slab support condition is adequate (AASHO, 1962; Choi et al., 2013). Old CPCD could provide excellent support for CRCP overlays. There are 2 overlay types: bonded and unbonded concrete overlays (BCO and UBCO, respectively). In bonded concrete overlay, both existing and overlaid slabs are supposed to behave as a monolithic slab, whereas in unbonded overlay, existing slabs and asphalt interlayer become good base layers under the overlay. In BCO, a full bond should be achieved between CRCP and CPCD, while in UBCO, bond between them is not needed. Primarily due to this difference, UBCO provides a more reliable option than BCO. In other words, UBCO is more forgiving than BCO. In other words, minor imperfections in materials and construction quality during concrete placement may not compromise the performance of UBCO as much as that of BCO. On the other hand, per current rigid pavement designs, UBCO requires much larger slab thickness than BCO. Along with the 2-in ASB layer needed in UBCO, the construction cost of UBCO is more than that of BCO, as well as a difficulty meeting overhead bridge clearance requirement for UBCO. Accordingly, UBCO and BCO have their own advantages and disadvantages.

Bonded CRCP overlay on CPCD has rarely been utilized for the rehabilitation of CPCD. The first known CRCP overlay on jointed reinforced concrete pavement is on IH 75 in Macon, Georgia constructed in late 1970s. However, the project was not a part of research studies, and no good technical information has ever been recorded. In that project, no surface preparation was executed prior to the placement of new concrete, thus it was neither bonded nor unbonded

overlay project. The first known bonded CRCP on CPCD was placed on US 75 in Sherman in 2010 as shown in Figure 1 (Ryu et al., 2011).

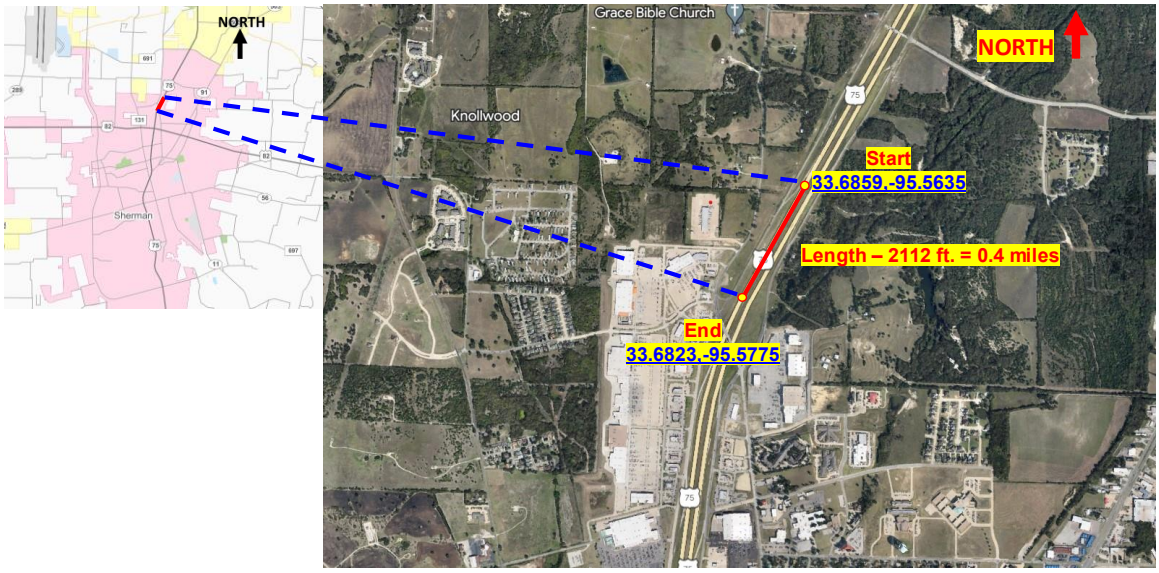

Figure 1 Testing location on US75 in Sherman

The half-mile long CPCD section on US 75 southbound that was selected for the rehabilitation is located just south of Exit 64. The 10-in CPCD was completed in 1984. The roadway consisted of 10-in concrete slab with 15-ft joint spacing on 6-in flexible base and lime treated subgrade. Dowels were used at transverse joints for load transfer. The section has two 12-ft wide lanes in each direction, with 4-ft inside and 10-ft outside shoulders. Originally, shoulders were 1-in AC layer on 8-in flexible base. In 1998, tied concrete shoulders were retrofitted with 10-in CPCD with matching 15-ft joint spacing on 6-in flexible base. When the pavement design was developed in the early 1980s for this section, the average annual daily traffic (AADT) was 11,000 and 20-year projected AADT (in 2004) was 16,200. The pavement was designed with 20-year design life with the above projected traffic. Actual ADT in 2004 was 55,000, which is more than 3-fold the projected design traffic for 2004. From 2002 until 2010, the TxDOT Sherman Area Office spent on average between half a million and one million dollars per year for routine maintenance of the CPCD in US 75. Repairs in this section required various lane closures for an average of 3 months per year. With the assumption that the same level of repairs would be needed for the next 20 years, the cost of maintenance was projected to be 10 to 20 million dollars, even without adjustments for inflation. Road user cost due to the lane closures for the next 20 years was estimated at over 70 million dollars. Considering the financial constraints TxDOT was facing at that time, this level of cost was not acceptable and a better rehabilitation method that was cost-effective and that would provide a long-term good performance with minimal maintenance was needed. At that time, no other feasible rehabilitation options were identified for a CPCD in a poor structural condition, and a 7-in CRCP bonded overlay was selected. 7-in CRCP was placed on the inside lane and inside shoulder first. The concrete

placement was completed in one day, on May 21, 2010. After the concrete gained adequate strength and all the preparation for its opening to traffic was completed, the traffic was switched to the newly placed inside lane in mid-June of 2010. There were issues with concrete during the construction of the outside lane and outside shoulder. The concrete delivered was quite dry, and some portion of the 7-in concrete overlay was removed and replaced. Still, the performance of this overlay has been satisfactory, with no distresses in the inside lane, and a few distresses that occurred over existing transverse contraction joints in the outside lane, after 13 years of heavy truck traffic. In 2022, the AADT in the southbound of this section was 31,208 vehicles per day with 15% trucks, which is about 4,680 trucks per day in the southbound lanes, which is equivalent to approximately 2.4 million ESALs per year. In this estimation, an equivalent axle load factor of 1.4 was selected per truck; however, there are no WIM stations in this area with no information on truck weights. Actual ESAL numbers could be higher, considering overweight trucks recorded in Texas highways.

For the rehabilitation of CPCD in US 75 in Sherman, detailed evaluations of the existing condition of the CPCD were made with FWD. The deflections obtained are shown in Figure 2. It illustrates quite poor structural conditions at some joints and cracks. It is to be noted that in this project, dowels were used at transverse contraction joints, which quite possibly keeps deflections low and load transfer efficiency (LTE) over 70 %. Even though most large deflections were at transverse repair joints and cracks, some were at transverse contraction joints, indicating poor slab support. There were two major issues in this pavement section: one is poor drainage and the other poor materials in the flex base. The PI values of the base materials in this section were quite high, and the combination of high PI and poor drainage (high moisture content) was a primary cause for distress and a poor condition of the CPCD. In CPCD sections in US 75 managed by the Sherman Area Office, this section was in the worst condition, and was selected for the 7-in CRCP BCO. The thought was that, if 7-in CRCP BCO could provide good performance in this section, the same overlay design could be applied to the rest of the CPCD sections managed by the Sherman Area Office. However, large deflections at contraction joints/repair joints/cracks were a major concern for CRCP bonded overlay, especially a potential for reflection cracking. No information was available regarding whether reflection cracking in CRCP might compromise the performance of CRCP overlay. To address this uncertainty concerning a potential problem with reflection cracking, it was decided that 2-ft wide non-woven fabric be placed on transverse contraction joints and repair joints. This decision was based on neither past experience nor theoretical analyses. This decision was solely based on the engineering judgement of the pavement designer. The placement of this fabric is not without potential problems. It will actually cause debonding between old and new concrete, increasing slab deflections and potential distresses. As of the writing of this report, there are 30 repairs done in the outside lane, but none in the inside lane. In other words, the difference in the performance for more than 13 years between inside and outside lanes is significant.

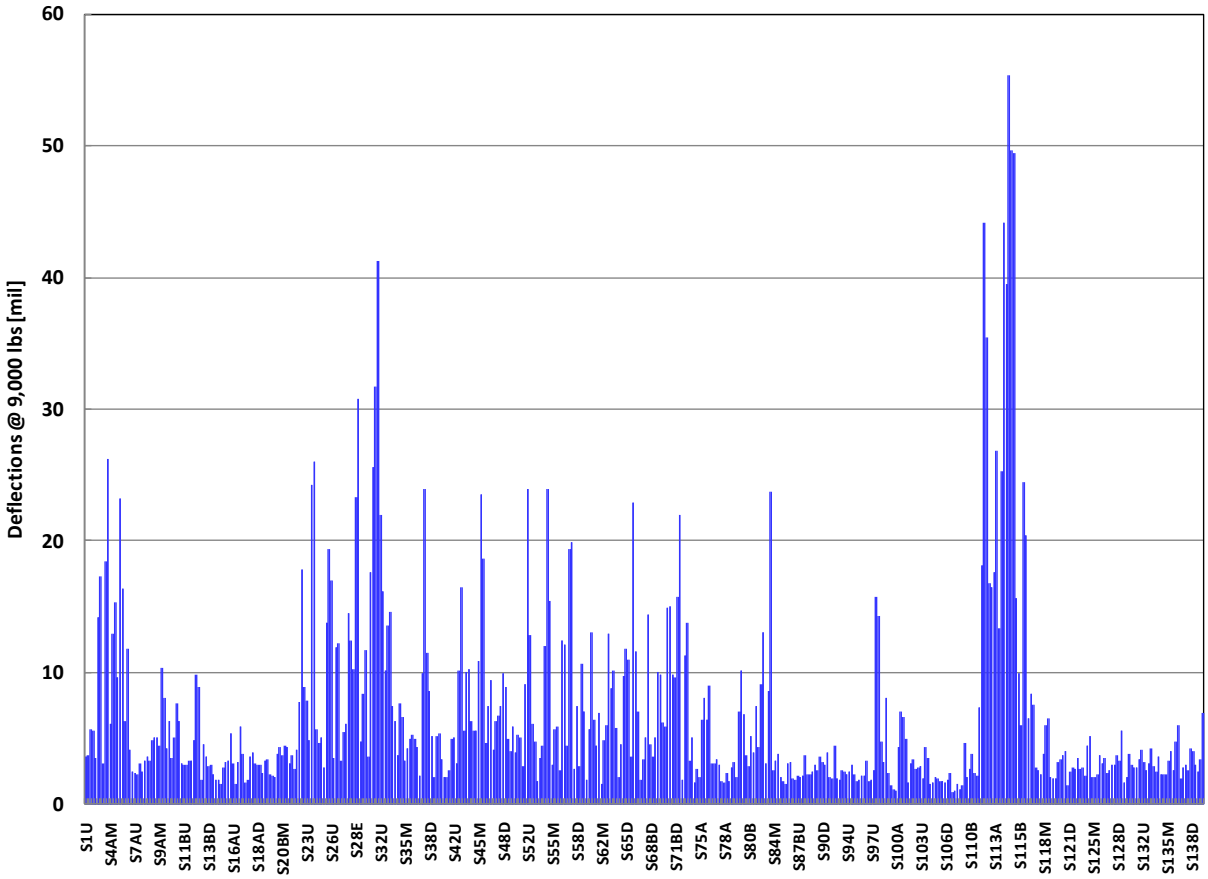

Figure 2 Deflections measured using FWD machine in US 75 in Sherman

Since the truck traffic is mostly in the outside lane, it could be construed that the truck traffic was the primary cause for the difference. On the other hand, there were a number of issues during the construction of the outside lane, while the inside lane construction went smoothly with no issues. Accordingly, construction quality might explain the difference. Or it could be the combination of both – i.e., truck traffic and construction quality caused a big difference in the performance of inside and outside lanes. The use of fabric does not explain the difference in the performance of the two lanes since fabric was placed in both lanes. However, the performance of the repairs of distresses in the outside lane, which consisted of removing deteriorated concrete in the overlay and non-woven fabric, followed by cleaning the surface of CPCD and placing new concrete, has been excellent, indicating that the use of fabric was not needed to prevent or retard reflection cracking. The tentative conclusion from the US 75 experimental project is that (1) bonded CRCP overlay on CPCD could be a good rehabilitation option, (2) construction quality is an important factor for the good performance of bonded CRCP overlay on CPCD, and (3) the use of non-woven fabric is not needed. Encouraged by the satisfactory performance of this 7-in CRCP bonded overlay on CPCD under heavy truck traffic, the Paris District identified a section of Loop

286 in Paris between US 82 and US 271 as a potential candidate for CRCP bonded overlay on CPCD as shown in Figure 3.

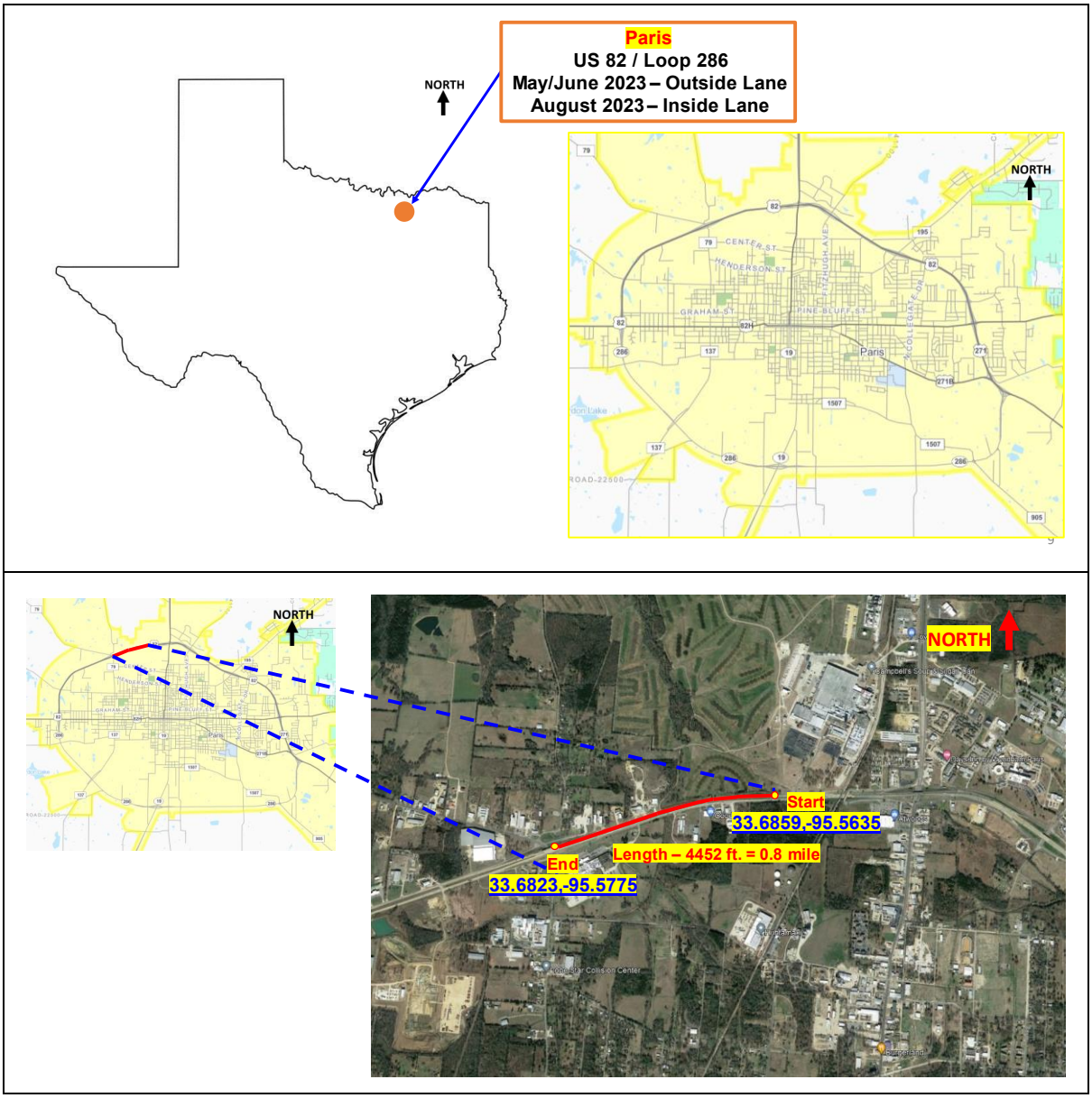

Figure 3 Testing Location in US82/Loop 286 Paris

This 9-in CPCD + 1-in ACP + 6-in flexible base was placed in the late 1970s or early 1980s. Even though the design life of this CPCD was 20 years, it served more than twice the design life. The distresses and needed repairs in this project were mostly at transverse contraction joints. The Paris District considered CRCP bonded overlay as an effective rehabilitation option for this section.

1.2 Objectives

The primary objective of this project was to (1) develop a pavement design, and materials and construction specifications, (2) develop pavement design details, (3) develop early-age monitoring plan for CRCP bonded overlay behavior, and (4) conduct early-age performance evaluations. Due to the short amount of time left in this implementation project, long-term performance cannot be evaluated in this project. Rather, long-term performance will be monitored under the current TxDOT rigid pavement database project, 0-7147.

Chapter 2 Evaluation of Existing Pavement & CRCP Overlay Design

2.1 Pavement Information of existing CPCD

Table 1 summarizes the existing pavement information. The Plans, Specifications, and Estimates (PS&E) were obtained from CSJ 1690-01-041. The existing CPCD was constructed probably in the late 1970s or in the early 1980s and has been in service for more than 43 years, which was earlier mentioned to have exceeded the 20-year design life.

Table 1 Pavement Information on existing CPCD

Attribute	Information
CSJ	1690-01-041
District	Paris
County	Lamar
Highway	US 82
Existing Pavement Construction	Plan Prepared → 1977 Construction → Late 1970s or Early 1980s
Pavement Type	CPCD
Pavement Thickness	9-in CPCD+1-in ACP + 6-in flexible base
Shoulder Type	2-in Asphalt shoulder
Steel design – longitudinal tie bar	#4 bars of length 30-inch at 30-inch c-c
Steel design – transverse tie bar	1-1/8th inch diameter of length 20 inches at 12-inch c-c

The existing highway has four lanes with two lanes in each direction. Figure 4 shows the cross section of the westbound direction of the existing pavement consisting of two 12 feet wide lanes, a 10 feet wide outside shoulder and 4 feet wide inside shoulder. The shoulder consists of a two inches asphalt layer placed over a flexible base. The existing main lanes are a 9-inch CPCD on a 1-inch asphalt concrete pavement (ACP) and 6-inch flexible base. The joint spacing is 15-ft, with dowels placed at transverse contraction joints.

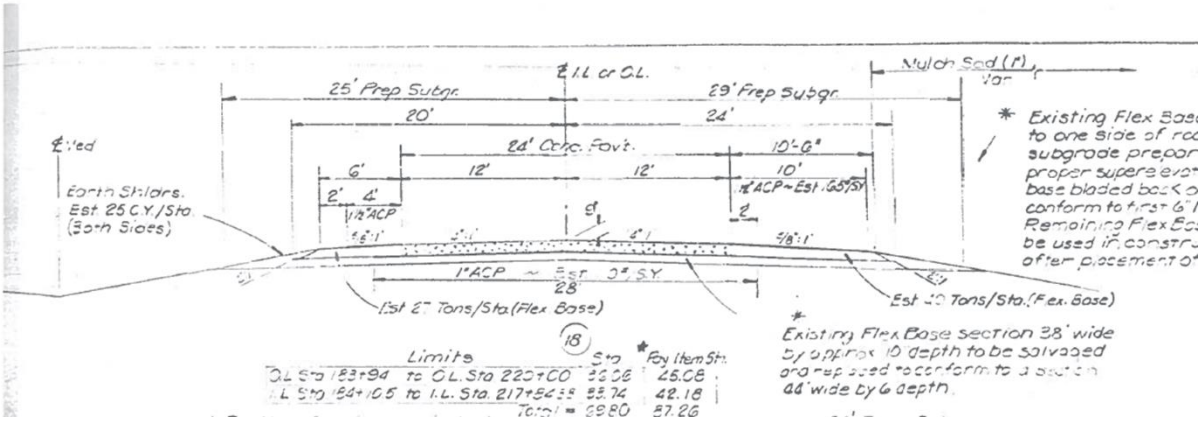

Figure 4 Cross-section of WB direction of existing pavement with two lanes

As shown in Figure 5, existing CPCD slabs are tied longitudinally with 30-in long #4 bars placed at 30 inches center to center. For the transverse joints, 1-1/8-inch-diameter by 20-inch-long smooth dowel bars were installed at 12-in spacing.

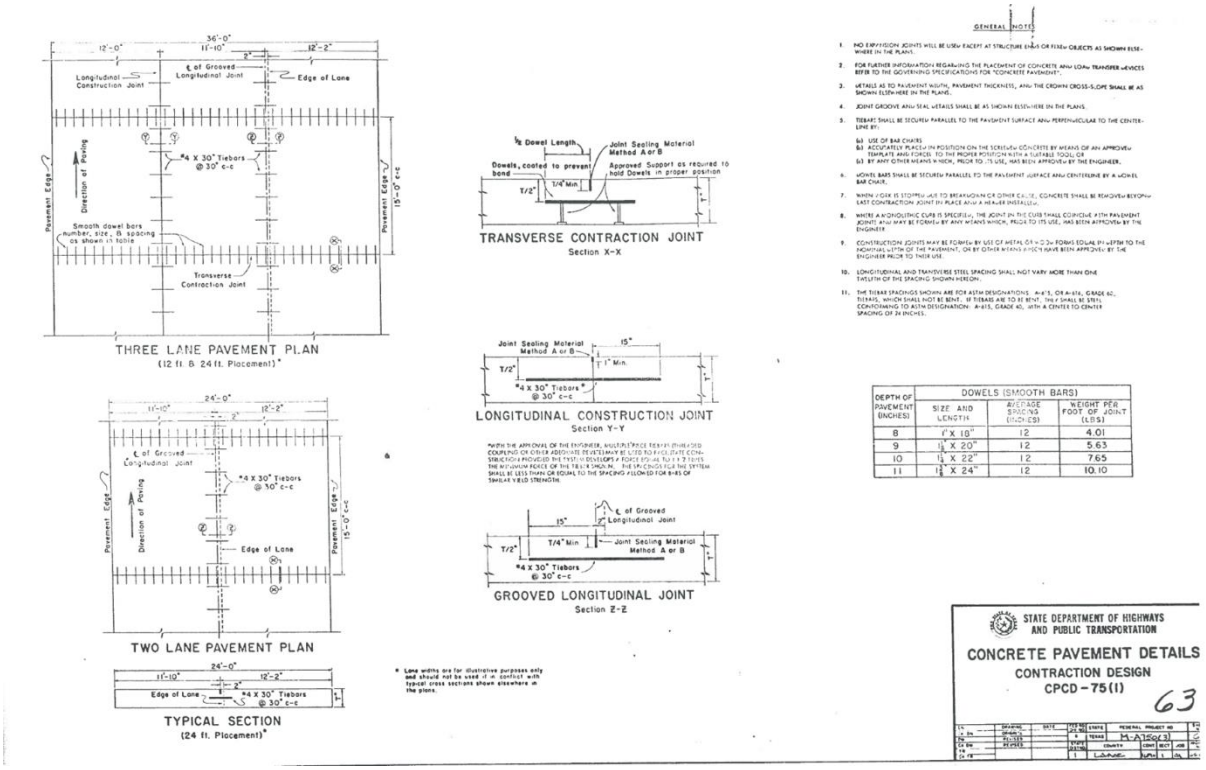

Figure 5 Reinforcement detail of the existing CPCD

2.2 Visual survey of existing CPCD

The research team conducted a preliminary evaluation in November 2019. Paris District team proposed that the test section shall be from [33.6859, -95.5635] up to [33.6823, - 95.5775]. This is a westbound segment covering a total length of 4452 feet (approximately 0.85 mi). The highway segment selected for the overlay has a good overall pavement condition other than concrete repairs done mostly at transverse contraction joints.

Figure 6 shows typical pavement condition. Figure 6-(a) shows the driveway to the Campbell Soup Company where the beginning of the test section is located. This is a two-lane highway where most of the trucks drive through the outside lane. It was observed that even though most of the truck traffic uses the outside lane, repair sections are also observed in the inside lane as shown in Figure 6-(b) and (c). This indicates that the distresses were not necessarily due to structural issues, but potentially due to a joint issue in the CPCD. Figure 6-(d) shows similar types of concrete patches in the outside lane as the inside lane, which supports the assumption that joint failures necessitated the repairs. Furthermore, it can also be observed that these are full depth repairs, mostly in the outside lane as shown in Figure 6-(e) and (f).

(a)

(b)

(c)

(d)

(e)

(f)

Figure 6 Existing CPCD condition on Loop 286

2.3 Slab Deflection on existing CPCD

Pavement structural evaluation was also conducted along with visual survey. Slab deflections of existing CPCD were measured using Falling weight Deflectometer (FWD) as shown in Figure 7.

Figure 7 FWD testing on existing CPCD

The initial plan was to perform FWD testing throughout the project limits. However, due to time constraints of the traffic control setup, the research team was unable to carry out the original plan. Instead, three short segments within the project limits were identified and FWD test was conducted. Figure 8 shows the three locations: Location 1 covering 10 slabs, Location 2 covering 53 slabs and Location 3 covering 25 slabs.

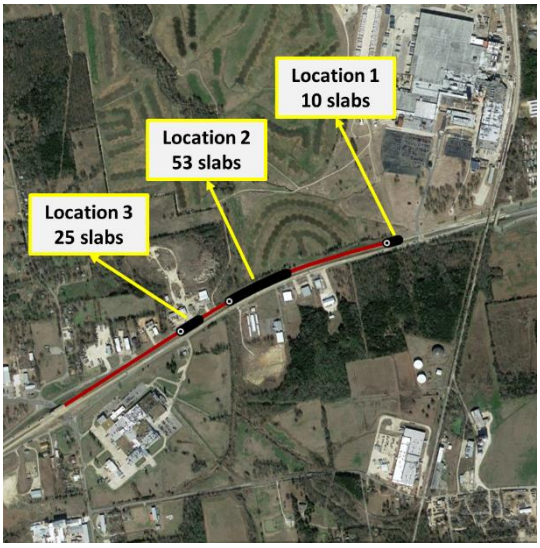

Figure 8 FWD Testing locations in existing CPCD

During the FWD testing, deflections were measured along the outer wheel-path of the lane at three different locations on each slab namely: (1) after the joint (downstream); (2) middle of the slab (mid-slab); and (3) before the succeeding joint (upstream) as shown in Figure 9. For the repaired sections, the joints were considered as a regular joint so that upstream and downstream deflections were measured at repair joints. Subsequently, analysis was performed from the acquired data that included estimation of the modulus of subgrade reaction, load transfer efficiency (LTE), and deflection comparisons.

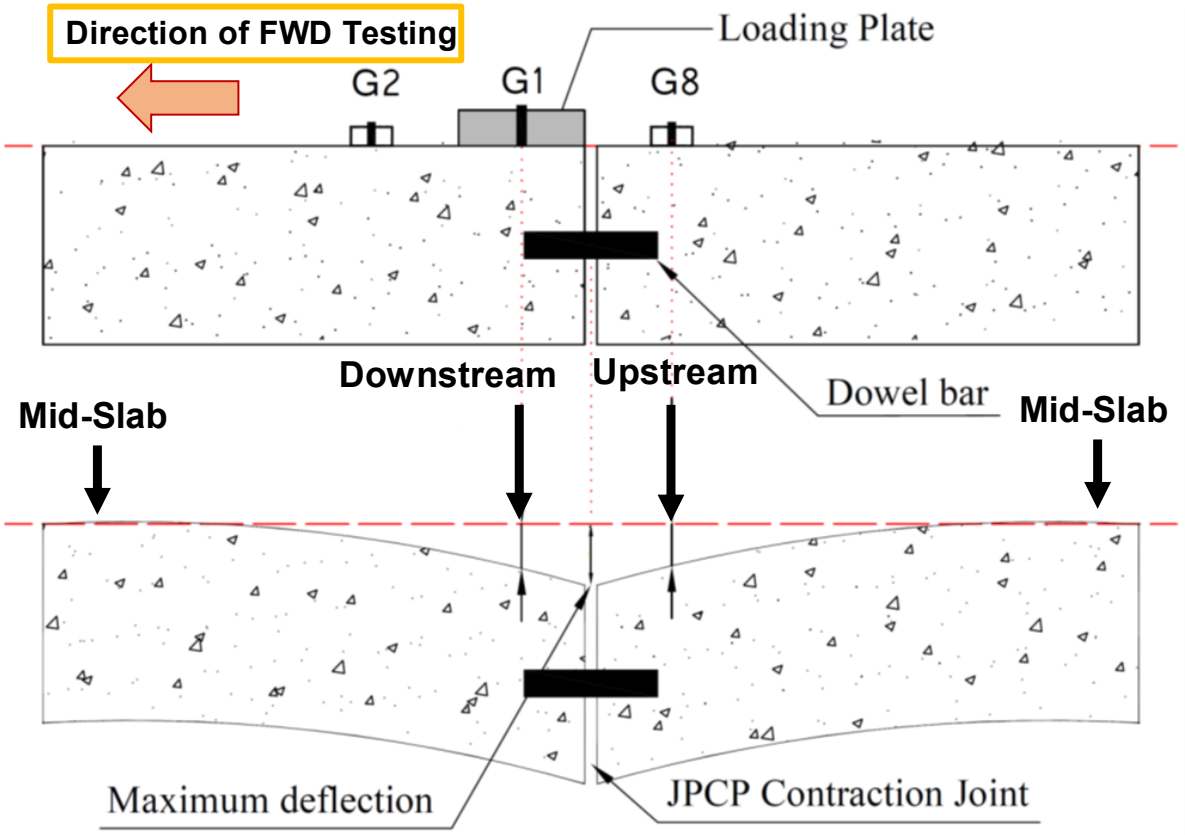

Figure 9 FWD testing protocol

In Location 1 as shown in Figure 10, the deflection of 37 points were measured. Figure 11 shows the measured deflections in Location 1 segment. It is observed that 2 larger deflections are between 2 smaller deflections. The 2 larger deflections are those evaluated at a joint, and the other 2 smaller deflections are at mid-slabs. Most of the mid-slab deflections are about 4 mils, while the joint deflections vary from 4 to 8 mils. The variations at transverse contraction joints or repair joints may be attributed to various conditions of joints – some may be locked, and some may be fully separated. It can be recalled in the specifications that the dowels shall be coated or smooth. This is to prevent bonding of the dowel bar and concrete. However, when the dowel bars are bonded to the concrete at both sides of joints, joint movements are restrained, forcing slabs on both side of the joint behave like a continuous slab ("locked joints"). With this, some joints in Location 1 are potentially locked, resulting deflections comparable to those mid-slabs. Such

behavior suggests potential issues with dowel installation. It was also noticed that the LTE values obtained at those suspected locked joints were relatively high.

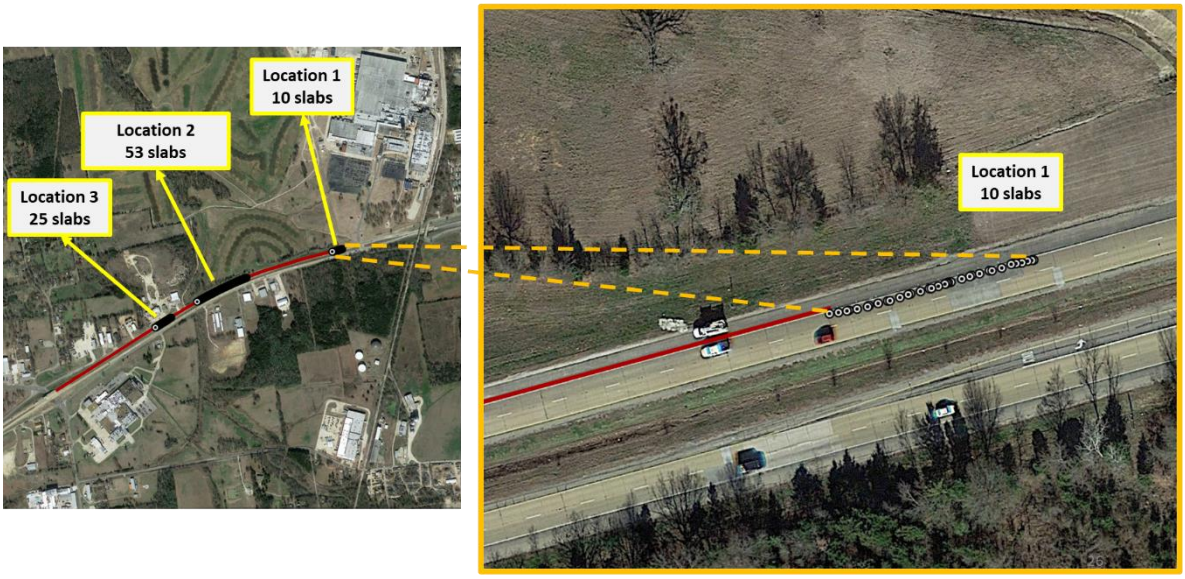

Figure 10 FWD drops in location 1

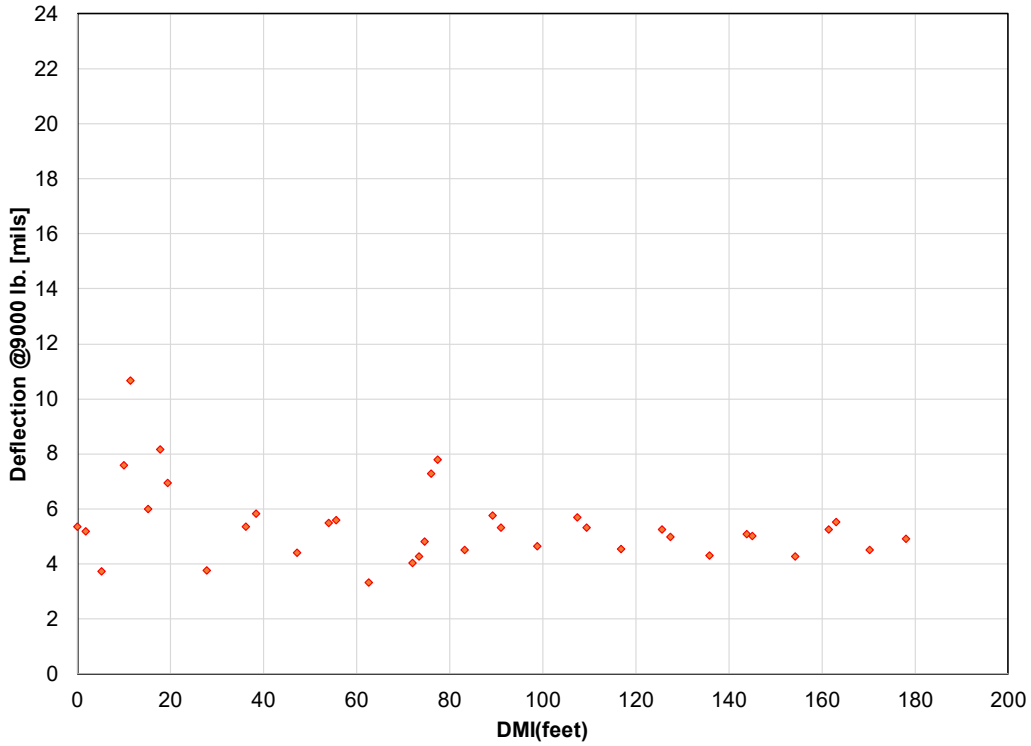

Figure 11 Location 1 FWD deflections

The Location 2 segment, shown in Figure 12, had a total of 180 points covering 53 slabs. Figure 13 shows the measured deflections across the entire segment. It can be observed that the first 300

feet of the segment have high deflections. The deflection recorded went up to 20 mils. Pavement condition information shows that these areas are repaired slabs, which indicates that the repairs were not done properly. Meanwhile, the deflections mid-slabs recorded after the first 300 feet of the segment were relatively consistent which ranges from 4 to 4.5 mils.

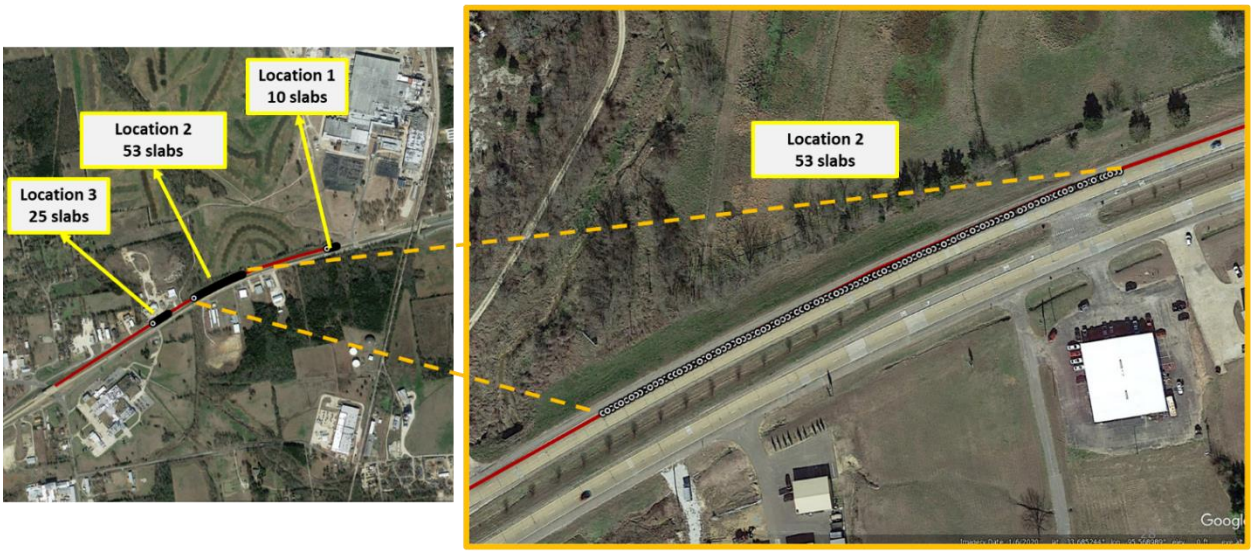

Figure 12 FWD drops in Location 2

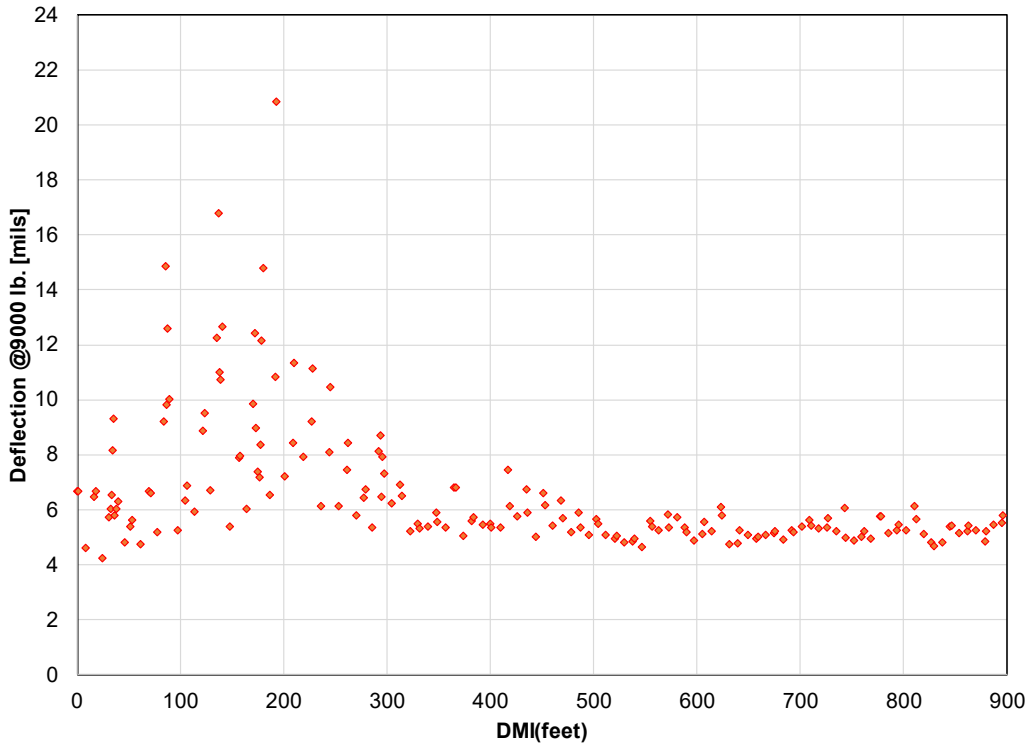

Figure 13 Location 2 FWD deflections

The Location 3 segment, shown in Figure 14, had a total of 74 points covering 25 slabs. Figure 15 shows the measured deflections in the entire segment. It was also observed that the large deflections were measured on the repaired slabs. The highest deflection in the segment was recorded to be 17.3 mils whereas the lowest deflection was 3.9 mils.

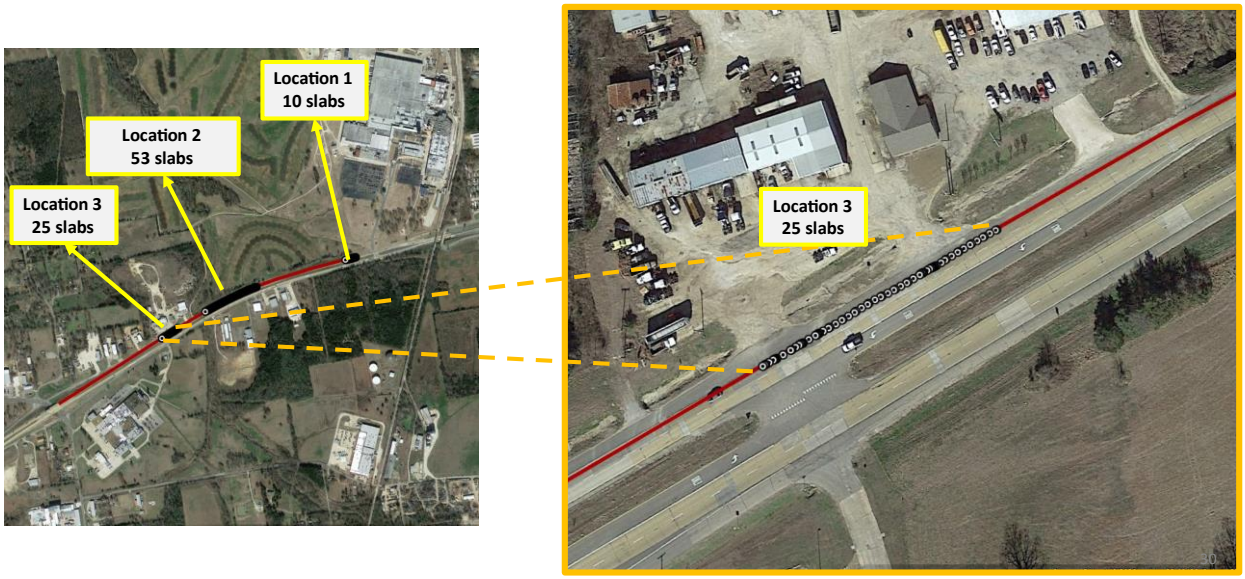

Figure 14 FWD drops in Location 3

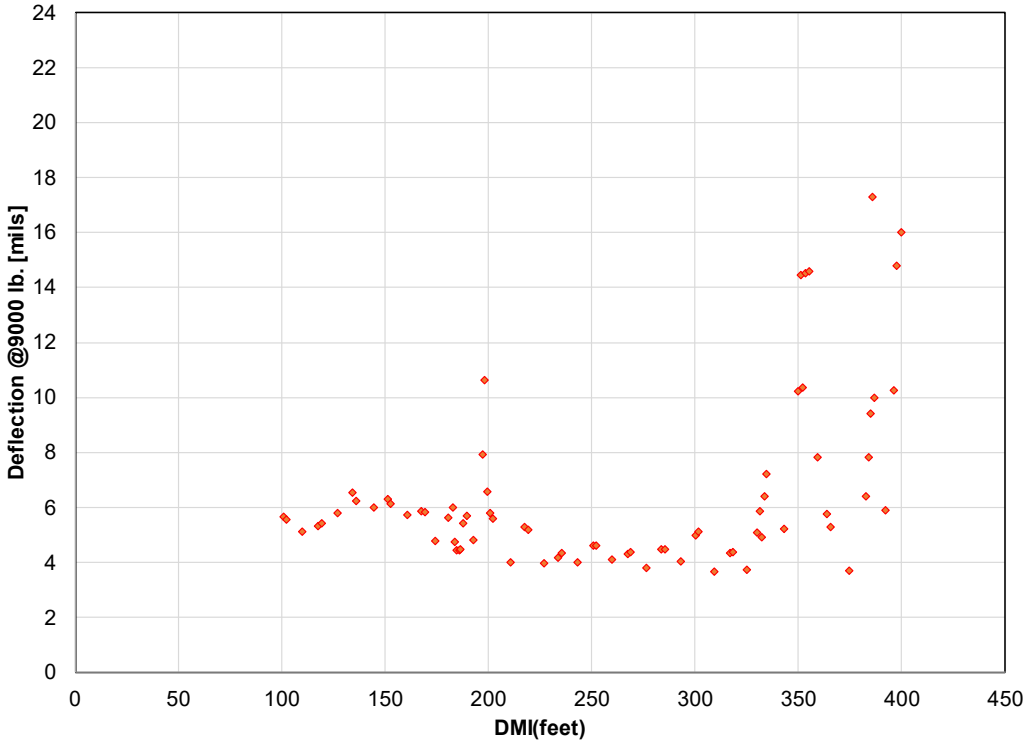

Figure 15 Location 3 FWD Deflections

In summary, the deflection data from the three segments shows that average overall deflection is 6.4 mils. The average deflection at the mid-slab and the joints of the original CPCD are 5.4 mils and 6.4 mils, respectively. Meanwhile, for the repaired slabs, the average deflection at the mid-slab and the joints are 8.1 mils, and 8.9 mils, respectively. These differences in deflections in original and repairs slabs clearly indicate the deficiencies in the current TxDOT repair practices.

From the FWD data, the modulus of subgrade reaction and LTE were calculated. The average value of LTE was about 83% with standard deviation of 10.6%. Meanwhile, the average value of modulus of subgrade reaction estimated from the AREA method was about 72 psi/in. The distribution of the calculated values is shown in Figure 16.

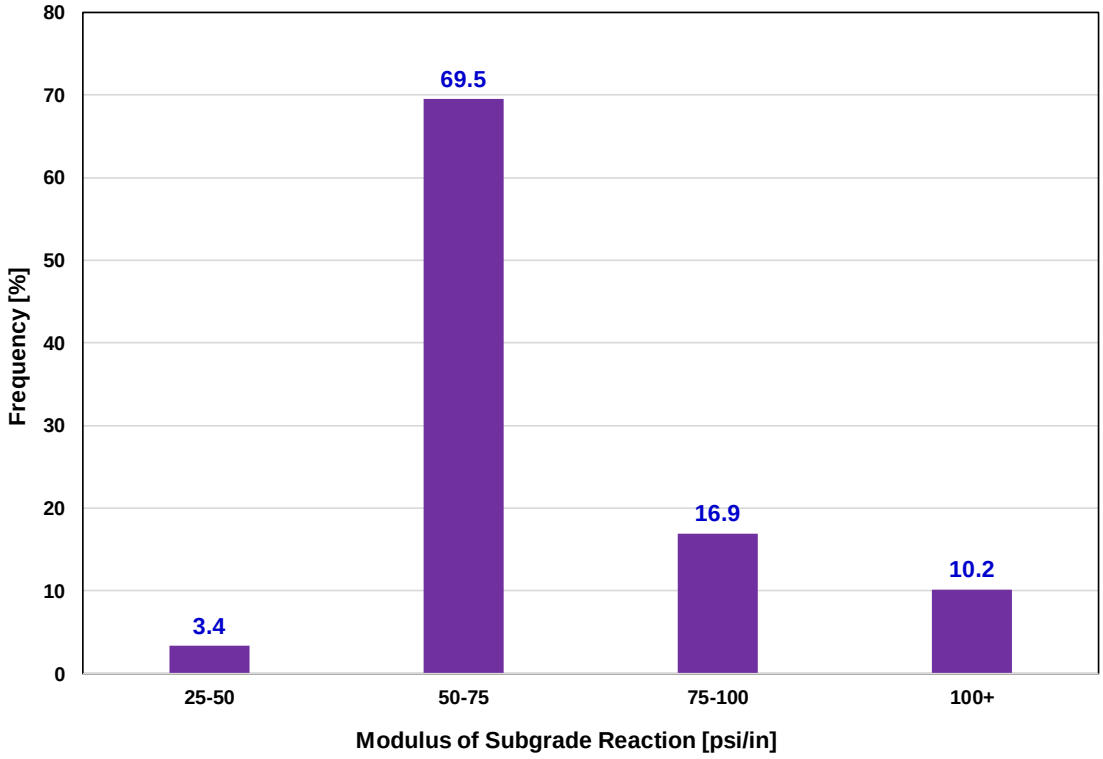

Figure 16 Modulus of subgrade reaction

It can be observed that most of the modulus of subgrade reaction values fall within 50-75 psi/in accounting for 70% of the data points evaluated and about 17% are within the 75-100 psi/in range. A typical value assumed for new CRCP design is 300 psi/in; however, it can be observed that only about 10% of the data points are above 100 psi/in. This indicates that the slab support in this project is inferior to the slab support provided by the current 2 base structures, which justifies the implementation of concrete overlay.

To identify the effects of the lower subgrade support in the measured deflections, the average mid-slab deflection was compared to the statewide average deflections in CRCP obtained from the dataset collected in the previous rigid pavement database projects. It can be seen in Figure 17 that the average mid-slab deflection of this 9-in CPCD section at 5.4 mils, represented in blue

round marker, is higher than the deflection of a typical 9-inch CRCP. The “equivalent” CRCP slab thickness is about 6.5-in. In other words, the structural capacity of the existing CPCD here is, even though the slab is 9-in thick, it is structurally equivalent to 6.5-in CRCP with one of the current 2 base types. Again, this justifies a concrete overlay as a logical rehabilitation option.

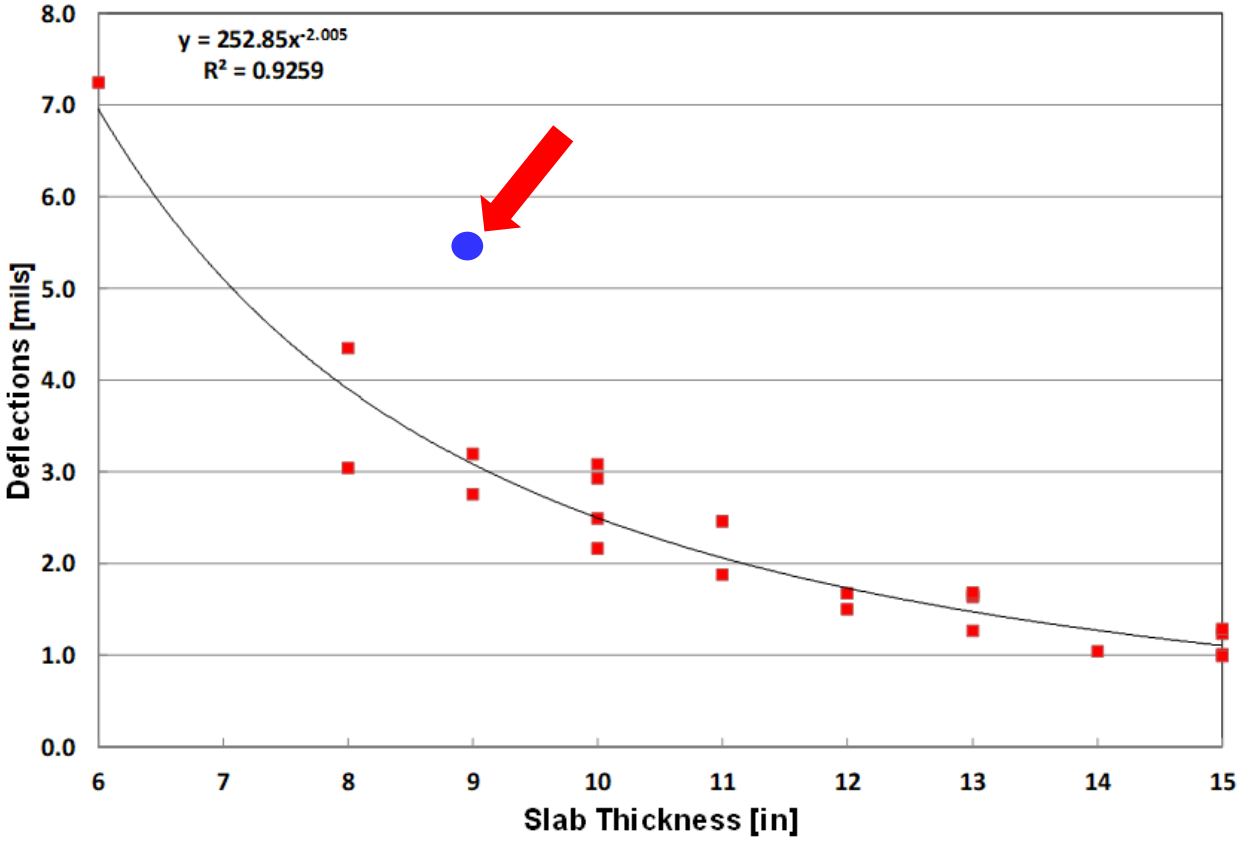

Figure 17 Relationship between slab thickness and deflections from the database project

2.4 Development of PCC Overlay Design

The existing CPCD's structural information obtained is used to design the overlay thickness utilizing the TxBCO-ME program developed in Project 0-6910. The design traffic was calculated based on the information obtained from ms2soft. This was estimated by using historical traffic data and projecting the traffic volume up to its design life. Figure 18 shows the graph of traffic projection. Based on the regression, traffic volume will increase by about 24 million ESALs from 2020 to 2050.

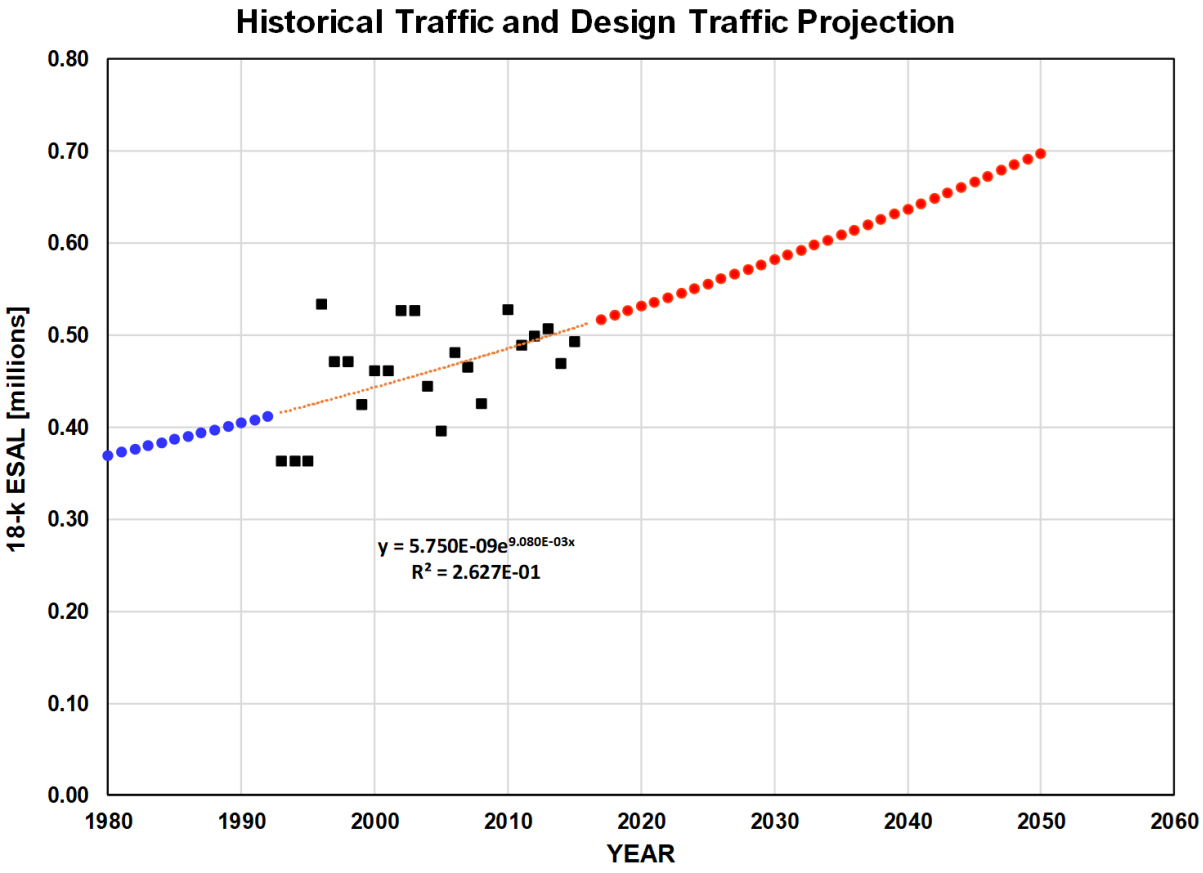

Figure 18 Design Traffic Projection for US 82 (Loop 286)

Table 2 shows the design criteria used in the Overlay Design. For an overlay thickness of 4 inches, the program calculated 1.7772 distress/mile by the end of its design life (30 years). It should be noted, however, that the transfer function generated for this program only utilizes a few datapoints due to the limited number of Overlay Projects in Texas. Hence, the prediction of the total number of distresses/miles may have some variability.

Table 2 Design criteria used for the PCC overlay design

Project Information	
District	PAR
County	Lamar
Highway	Loop 286
CSJ	1690-01
Direction	WB
Reference Marker (Begin)	705+0.6
Reference Marker (End)	706+0.5
Design Traffic	
Design Life (yrs.)	30
Total Number of Lanes in One Direction	2
Total Design Traffic in One Direction (Million ESALs)	24
Support Condition	
Composite k (psi/in.)	72
Performance Criteria	
Number of Distresses per Mile	10
Concrete Layer Information	
BCO System Type	CRCP over CPCD
Overlay Thickness (in.)	4
Existing Concrete Thickness (in)	9
28-day Modulus of Rupture (psi)	570
28-day Modulus of Elasticity (ksi)	5000
Analysis	
Total Number of Distresses/miles	1.7772

From the inputs mentioned, two overlay design thicknesses were proposed. The first is a 4-inch overlay and second is a 5-inch overlay. Table 3 shows the proposed bonded concrete overlay designs. After careful consideration, including the project cost and potential long-term effects of the 2 slab thicknesses, a 5-inch overlay thickness was selected. Figure 19 shows the reinforcement detail for a 5-inch overlay.

Table 3 Proposed Bonded Concrete Overlay Design

Slab thickness	Longitudinal		Transverse		Steel Percentage
	Number of bars	Spacing	Number of bars	Spacing	
4-in	#6	10-in	#6	4-ft	1.10%
5-in	#5	6-in	#5	4-ft	1.02%

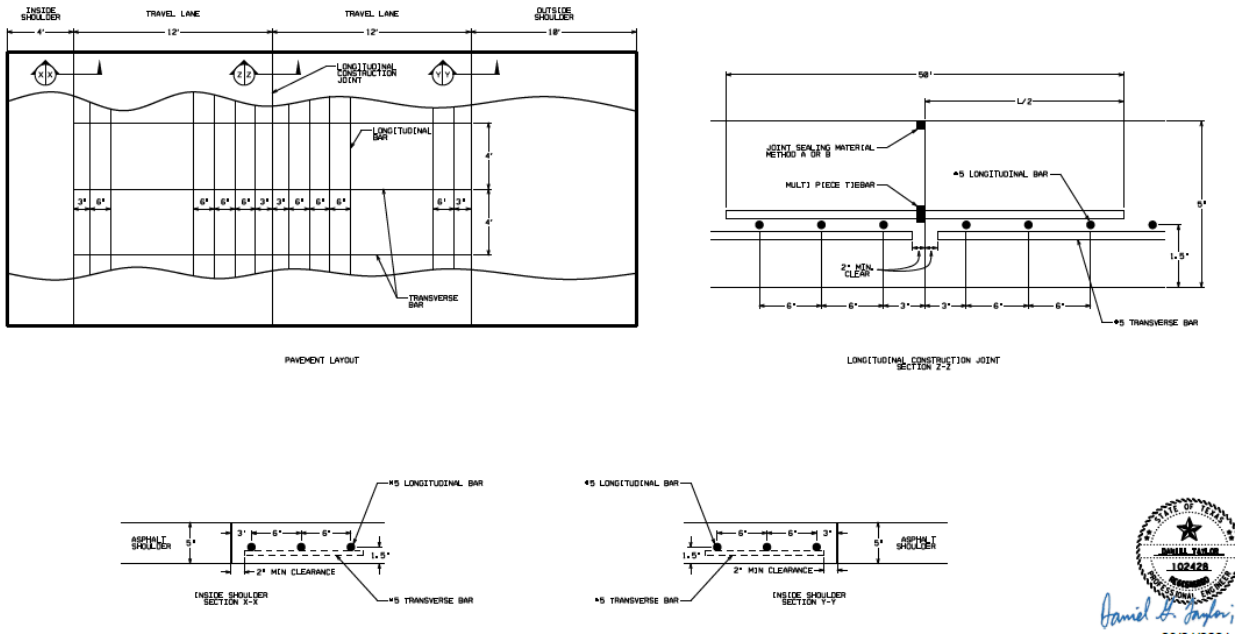

Figure 19 Reinforcement detail for 5-in overlay slab thickness

Chapter 3 CRCP BCO Construction and Evaluation of Material Properties

3.1 Pavement Information of the Section

Table 4 summarizes the project information for CSJ 1690-01-134. The section limits are from [33.6859, -95.5635] to [33.6823, -95.5775]. This section is at the westbound of Loop 286 between Kiamichi Railroad and FM 79. The section length of 4778-feet (approximately 0.9 miles).

Table 4 Pavement Information of CRCP Overlay

Attribute	Information
CSJ	1690-01-134
District	Paris
County	Lamar
Highway	US 82 (Loop 286)
Reference Marker	Start – 706+0.412 End – 706-0.853
Date of construction (Westbound Outside Lane)	Late May and early June 2023
Date of construction (Westbound Inside Lane)	Late August 2023
Pavement Type	CRCP BCO over CPCD
Slab Thickness	5-in. CRCP + 9-in CPCD
Shoulder Type	2-in Asphalt shoulder
Base Type in Existing Pavement	1-in ACP + 8-in flexible base
Drainage Type	Open Ditch
Steel Design	#5 longitudinal steel with a 6-in spacing. Steel Percentage: 1.02% of 5-in thick overlay

Figure 20 shows the typical section of the overlay, while Figure 21 provides details about the transition section. The transition section, which ensures a smooth change in surface elevation between existing and overlaid slab surfaces, is positioned at both the beginning and end of overlay section. Each transition measures approximately 8.5 slabs in length (about 127 feet) and 5-in elevation change, which is a 0.33% slope.

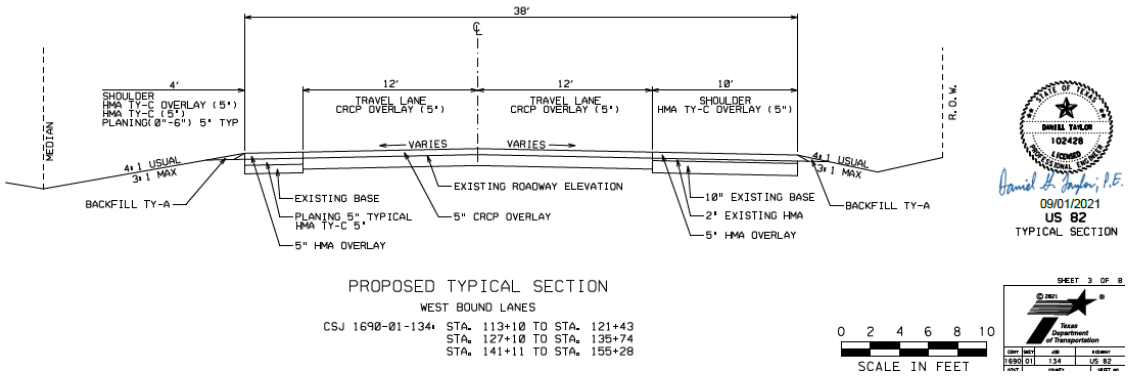

Figure 20 Proposed Typical Section of an Overlay

In Figure 21, the details of the transition section are illustrated. As shown, the existing slabs are milled down by 3 inches in order to provide space for reinforcement and gradually increase the thickness of the CRCP overlay, resulting in a 0.33 % slope. Additionally, hook bars are installed in accordance with the PS&E at the transition section.

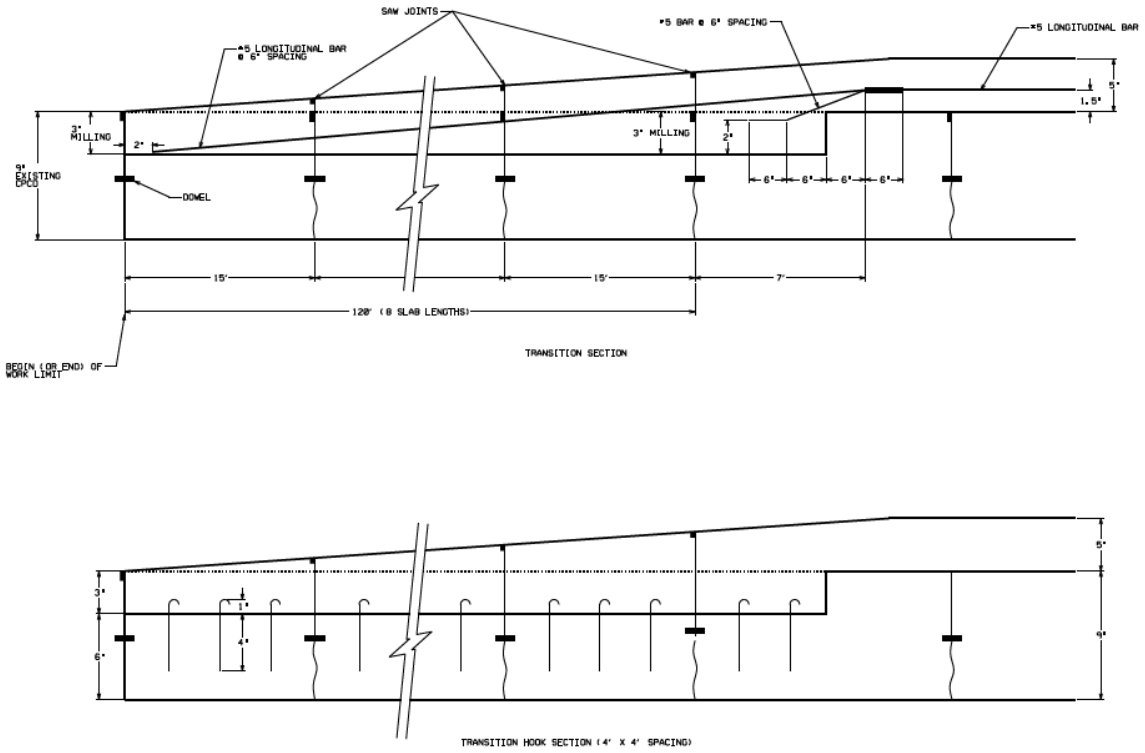

Figure 21 Transition section details of the CRCP Overlay

3.2 Material Properties

The concrete mixtures used in both outside lane and inside lane was the Class K concrete. The design slump was 5.5 in., and the water/cement ratio was 0.45. Cement used was Type I/II from Ashgrove, and twenty percent (20%) of cement was replaced by Class F fly ash from Eco Materials. The source of coarse aggregate was from Martin Marietta – Bridgeport, which met the coefficient of thermal expansion (COTE) of less than 4 in/in/°F. The details of the mixture proportions and material properties of the concrete are shown in Table 5.

Table 5 Concrete Mix Design

Component	Outside Lane	Inside Lane
Design Slump Range	5.5 inch	5.5 inch
Cement (Type I/II)	452.0 lb.	452.0 lb.
Fly ash- Class F	113.0 lb.	113.0 lb.
Coarse Aggregate (Martin Marietta-Bridgeport)	1820.0 lb.	1820.0 lb.
Fine Aggregate	1365.0 lb.	1365.0 lb.
Water	250.0 lb.	250.0 lb.
Water/Cement Ratio	0.45	0.45
Water Reducer (WR-A/D)	18.0 oz.	18.0 oz.
Non-Chloride Accelerator (NCA)	72.0 oz.	0.0 oz.
High Range Water Reducer (HRWR)	11.0 oz.	11.0 oz.

Figure 22 presents the compressive strength data for concrete samples from the outside lane, tested at various intervals: days 1, 2, 3, 7, and 10. On the first day, the average compressive strength of the concrete was recorded at 2700 psi. This strength showed a gradual increase, reaching 3100 psi on the second day and 3200 psi on the third day. By the seventh and tenth days, the compressive strengths were measured at 3500 psi and 4200 psi, respectively.

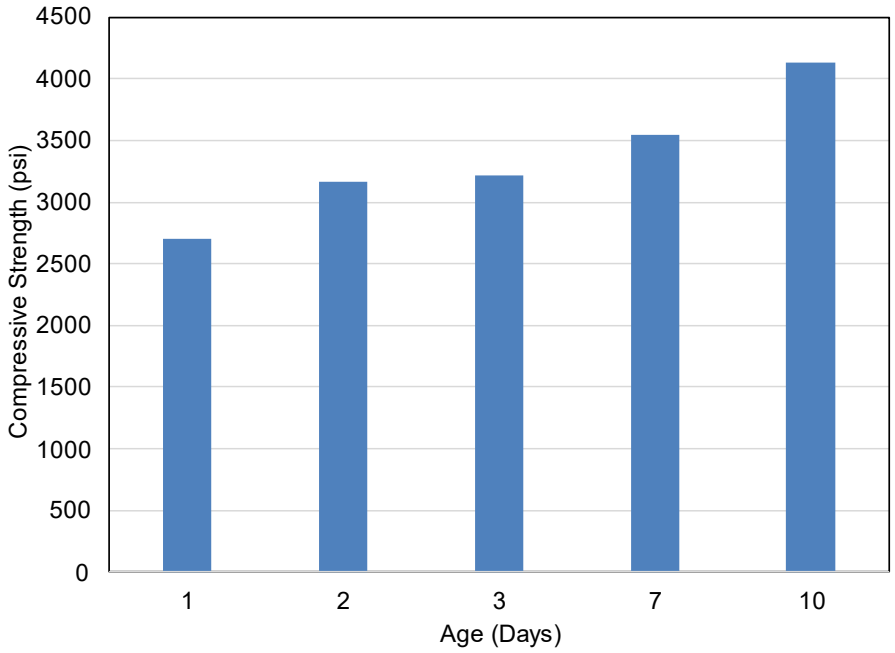

Figure 22 Compressive Strength of concrete sample with respect to age for outside lane

Similarly, Figure 23 displays the compressive strength results for concrete samples from the inside lane, tested on days 3, 4, 6, and 8. The average compressive strength for the three-day-old concrete was 3200 psi. This value rose to 3400 psi by the fourth day. On the sixth and eighth days, the compressive strengths were 3700 psi to 3800 psi, respectively.

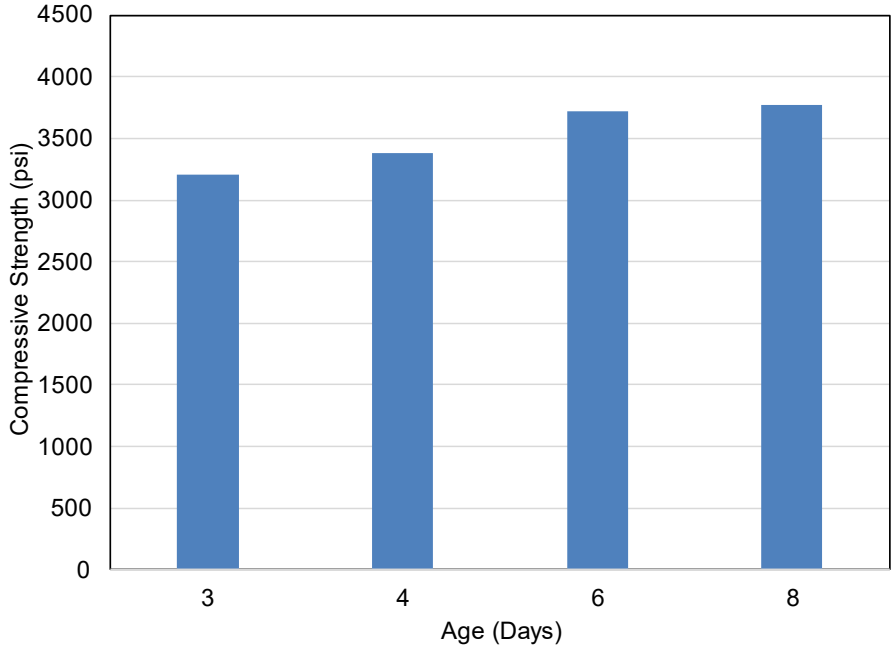

Figure 23 Compressive strength of concrete sample in respect to age for inside lane

3.3 Paving Sequence

The construction of the outside lane and inside lane was done separately, and the paving sequence for both the lanes were different. The actual paved length was measured to be 4452-ft.

Figure 24 shows the paving sequence in the construction of the CRCP overlay for the outside lane. The construction was divided into 6 segments. All concrete placements were done during daytime and the direction of the paving was from east to west. Segment 2 and Segment 3 were placed on May 30, 2023, followed by the placement on Segment 1A on May 31, 2023. On June 2, Segment 1B was placed, while the leave-out was placed on June 9, 2023, followed by the placement of exit to FM 79 on August 9.

In general, transverse saw-cuts are not made in CRCP, except at transverse construction joints; however, in this project, saw-cuts were made in Segments 1A, 2 and 3 above right on top of the existing contraction joints. This practice of saw-cuts in CRCP stopped and no more saw-cuts were made in the rest of the project, except for the first segment in the inside lane construction. The blue dotted line in the figure indicates that the encompassing segments are with saw-cuts performed. The implication of this saw-cut is discussed later in the results.

The instrumentation was made in Segment 1A. Sensors were installed in three (3) sections. The details will be discussed in the next section.

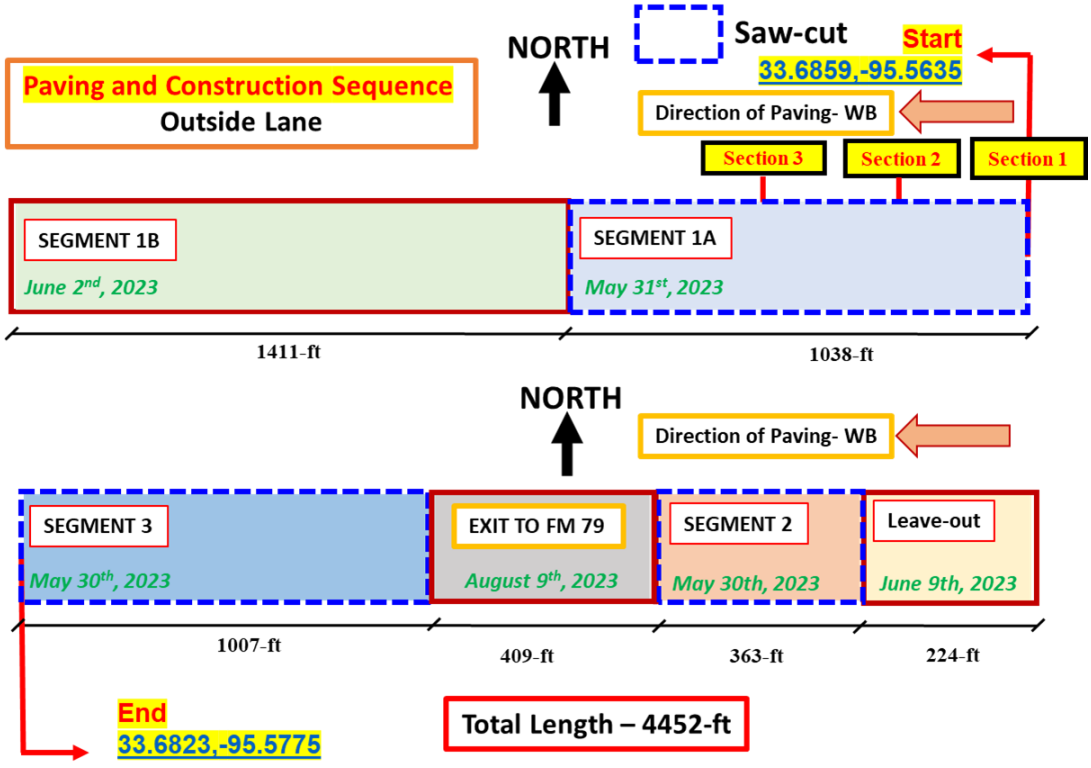

Figure 24 Map showing the paving and construction sequence of CRCP overlay for outside lane

Similarly, Figure 25 shows the paving sequence in the construction of the CRCP overlay for the inside lane, which was done in 3 segments. As with the outside lane, all the placement in the inside lane was done during the daytime, and the direction of the paving was westbound. Segment 1 was placed on August 25, 2023, followed by Segment 2 and Segment 3, which were placed on August 29, 2023, and August 31, 2023, respectively.

Saw-cuts were performed for the first 45 slabs, covering approximately 670 feet in length from the start of Segment 1. These saw cuts were made at the locations of the existing CPCD joints, indicated by the blue dotted line. No saw-cuts were made for Segment 2 and Segment 3. At the end of the project in the transition area, saw-cuts were supposed to be made; however, it did not happen. Sensors were installed in one section, and the details of sensor installation will be discussed in the following sections, along with sensors installed in the outside lane.

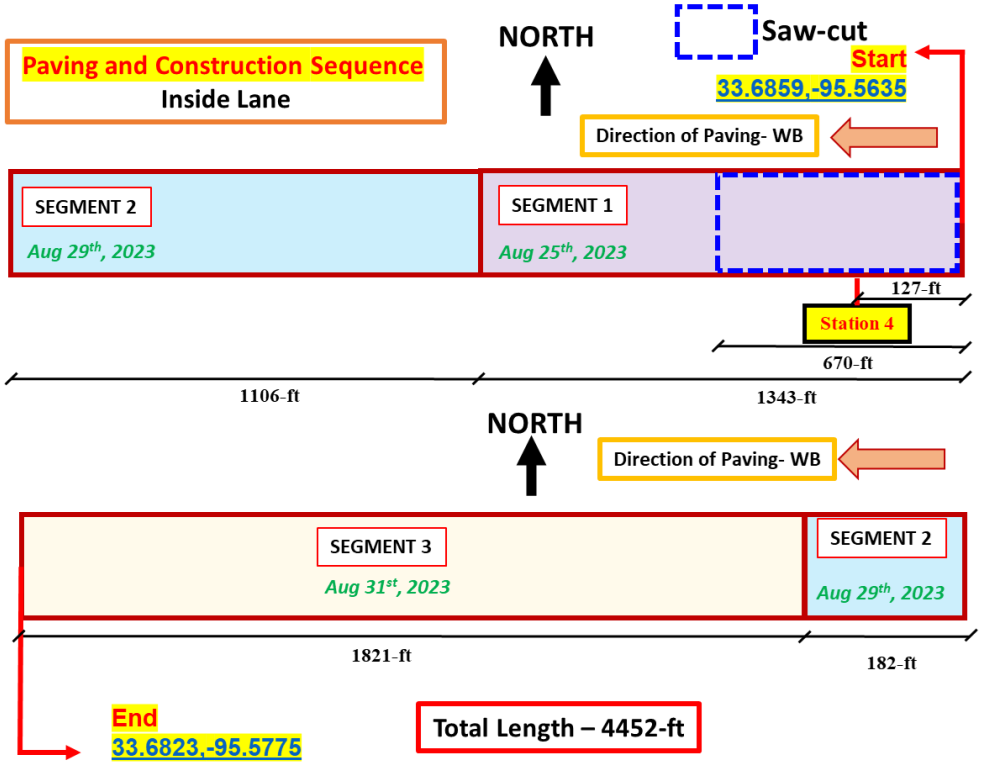

Figure 25 Map showing the paving and construction sequence of CRCP overlay for inside lane

3.4 Field Testing Program

Field instrumentation was carried out to investigate the concrete overlay behavior at specific locations. Four (4) test sections were set up as shown in Figure 26. These sections are as follows: Section 1 at the beginning of the transition of outside lane; Section 2 at the end of the transition of outside lane whereas Section 3 at a typical overlay section which is about 600 feet from the beginning of the transition in the outside lane. Section 4 was selected at the end of transition of inside lane.

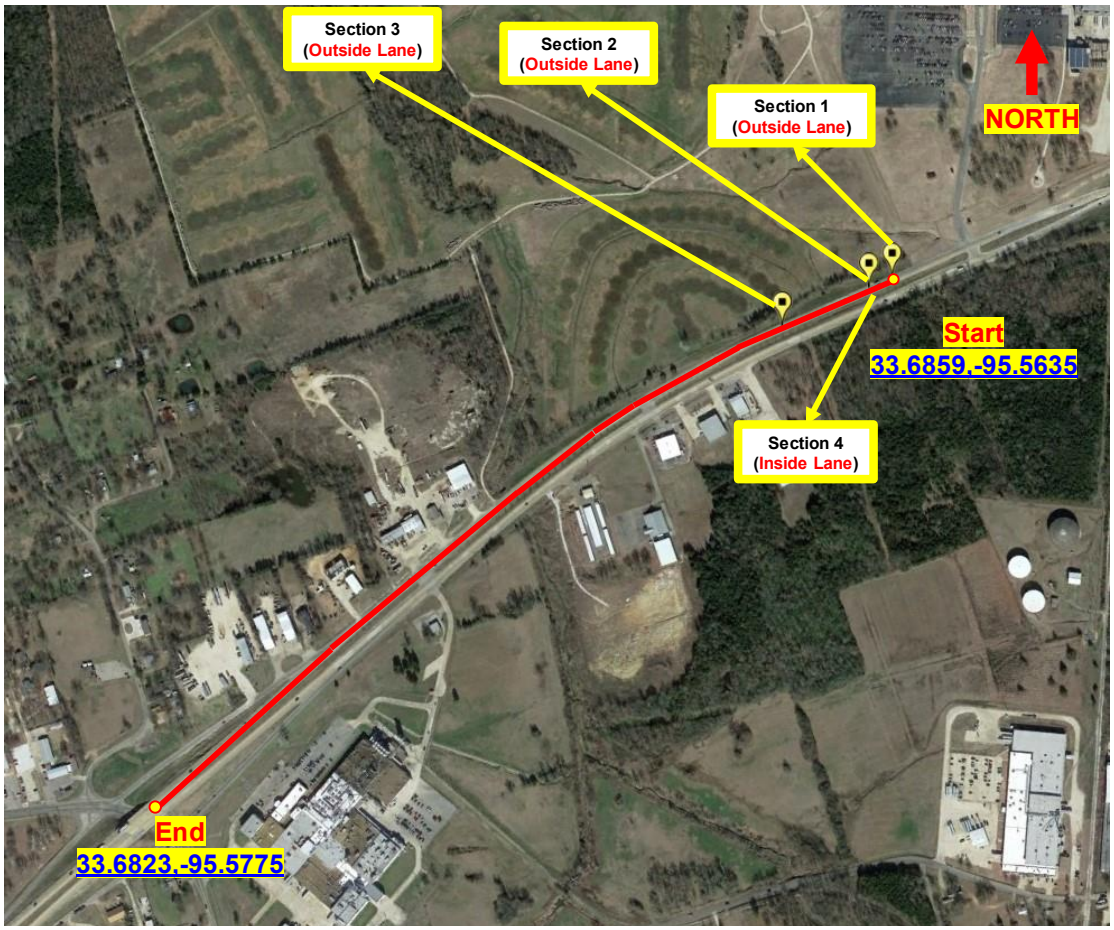

Figure 26 Map showing four location of gage installation

In CRCP bonded concrete overlay on CPCD, the transition zone presents a unique location where significant levels of interactions take place between two different pavement types. Understanding the behavior of and interactions between the two pavement types is critical to developing design details of the transition zone. With this, the start and end of the transition as shown in Figure 27 are the first two instrumented test sections in the outside lane (Sections 1 & 2, respectively). The third test section is located about 600 feet from the beginning of the transition where the pavement structure is a 5-inch CRCP overlay on a 9-inch CPCD. This is to obtain information that will characterize the behavior at a typical CRCP overlay section and its

interactions with the existing CPCD. All these three sections were instrumented in outside lane. For the inside lane construction, instrumentation was performed at the end of transition (Section 4). This was to compare the interface behavior of concrete overlay at the end of the transition at the inside and outside lanes due to the use of different concrete mix designs.

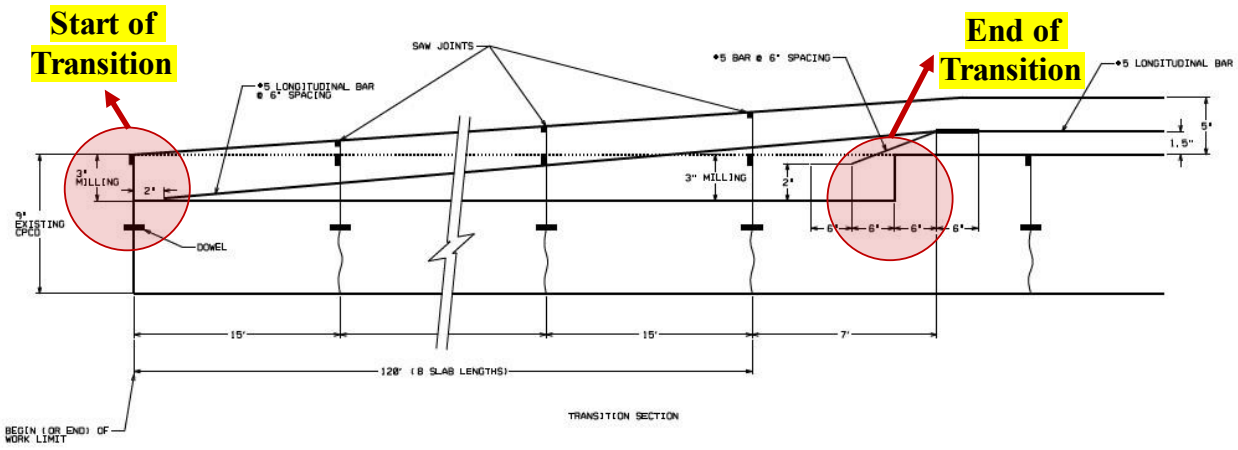

Figure 27 Instrumented test locations at the transition section

3.4.1 Field Instrumentation

3.4.1.a Weather Station

In analyzing pavement behavior, especially concrete and steel strains, corresponding weather information helps understand why concrete and steel behave the way they do. For example, rainfall usually lowers concrete temperature, while increasing concrete volumes. To obtain accurate weather information at the project site, a wireless weather station from Davis Instruments was installed as shown in Figure 28.

Figure 28 Davis weather station installed in field test site

3.4.1.b Datalogger

The data collection from all the gauges installed in the field test sections was carried out using data loggers. CR1000X from Campbell Scientific was used for this purpose. The data logger was assembled to maximize the efficiency of the data collection for given gage layouts. Figure 29 shows the image of the datalogger installed in the field.

Figure 29 Datalogger (CR1000X; Campbell Scientific)

3.4.1.c Thermocouple (TC)

Concrete, as with any materials, undergoes volume changes as temperature varies. In addition, temperature variations through the slab depth induce curling behavior of the concrete slab, which could cause cracking and debonding. In addition, concrete overlay provides insulation effect on the existing CPCD, which would reduce the amount of curling. Thus, to understand temperature effects on behavior of concrete overlay and the existing CPCD, thermocouples were installed at various depths in both the CRCP and CPCD layers. Type T thermocouple was used to measure the concrete temperature variation through the concrete slab depth. The thermocouples were installed at 1-in, 2.5-in, 3.5in, 5-in, 6-in, 9.5-in, and 13-in from the overlay surface. Figure 30 shows the typical installation of thermocouple with various depths from the surface of the slab.

Figure 30 Typical Installation of Thermocouple

3.4.1.d. Vibrating Wire Strain Gauge (VWSG)

Concrete strains provide essential information on the behavior of concrete at early ages due to temperature and moisture variations. Variation in concrete strains due to environmental loading is a continuous process, and measuring concrete strains in short intervals will aid to understanding the concrete behaviors. For this purpose, a Vibrating Wire strain gauge (VWSG) from Geokon was used. Two types of VWSGs were installed: (1) 6-in VWSG embedded at various depths of the concrete slab and (2) 2-in VWSG installed vertically at the interface between the existing CPCD and CRCP overlay to investigate the interface behaviors between them. A significant increase in vertical tensile strain may indicate debonding at the interface. The strain measured with this instrument is based on the vibrating wire principle. According to the vibrating wire principle, when there is deformation in the concrete it will lead to the movements of the VWSG flanges. When there is movement of the VWSG flanges, a tensioned wire vibrates at a frequency that is proportional to the strain in the wire. The strain is then calculated by squaring the frequency value and applying manufacturer (Geokon) constant. Figure 31 shows the typical setup of the VWSGs in the field.

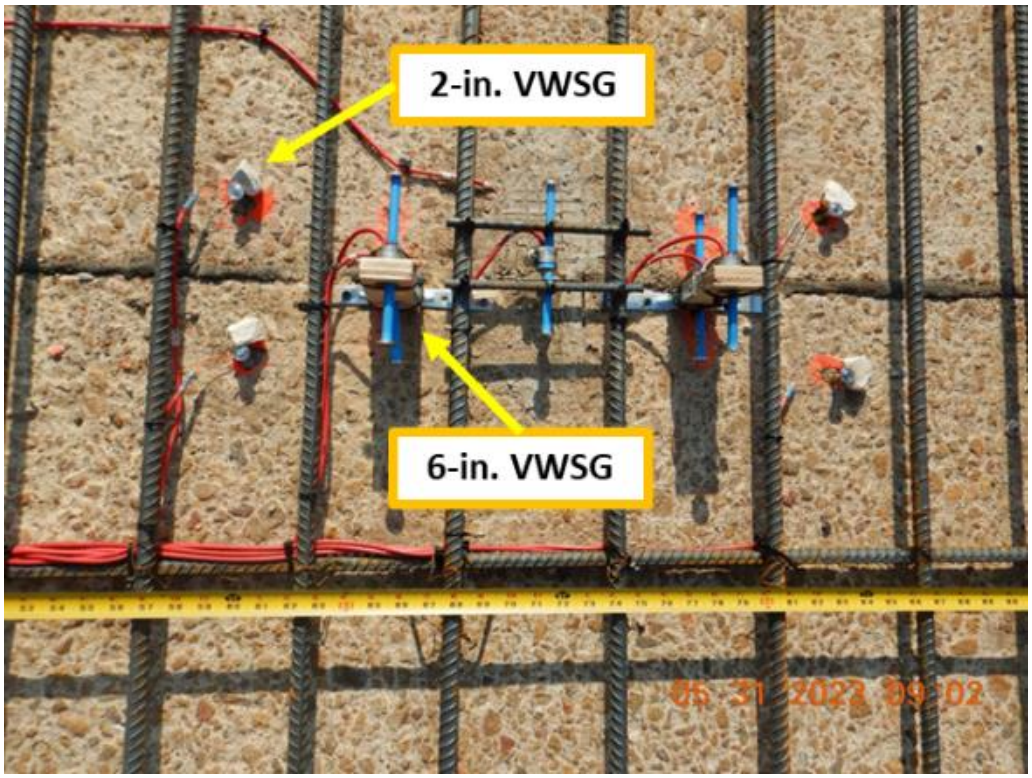

Figure 31 Typical Installation of Vibrating Wire Strain Gauge

3.4.1.e Crackmeter

To evaluate the effect of the CRCP overlay placement on the transverse contraction joint movements in the CPCD layer, crack meters were installed on the edge of the existing CPCD slab. Both horizontal and vertical displacements of the concrete at a joint were measured. The crack meter operates on the same principle as VWSG. It can measure the movements of concrete quite accurately. The measured displacements may also be compared with the internal behavior of concrete measured by the VWSG, to ascertain the reasonableness of both sets of data. Figure 32 shows the typical installation of the crack meters. During the installation, anchor bolts that are fixed using a rapid-setting epoxy are installed on the exposed side of the concrete slab. Concrete displacements were recorded at specific time intervals and collected through the data logger.

Figure 32 Typical Installation of crackmeter in the field

3.4.2 Gauge Installation Setup

Figure 33 shows the plan and cross-sectional view of gauge installation for Sections 1 and 2. For Section 1, two (2) units of 6-inch VWSGs were installed at the existing CPCD joint, with a half of the sensor length embedded into the existing CPCD, while the other half exposed to with the new concrete when the overlay is placed. The strain data obtained from these 2 sensors will provide information on the interaction between CPCD and CRCP overlay at the transverse construction joint (TCJ). Two (2) units of 2-inch VWSGs were installed vertically at the interface between the existing CPCD and CRCP overlay. One (1) unit of horizontal and one (1) unit of vertical crack meters were installed at the edge of the slab to measure the movements of the slab at the beginning of the transition section. Figure 34 and Figure 36 show the actual sensors installed in Section 1.

For Section 2, four (4) units of 6-inch VWSGs were installed. Two of these sensors were placed at the same elevation as the longitudinal steel and at a spacing between longitudinal steel. The other two sensors were embedded at the existing CPCD, with a half of the length of the sensors embedded into the CPCD and the other exposed to the new concrete when the overlay is placed. In addition, four (4) units of 2-inch VWSGs were installed vertically at the interface between the existing CPCD and CRCP overlay. Two (2) of these sensors were located 6 inches before the end of the transition (down) where the CPCD slab thickness is 6 inches and the other 2 were located 6 inches after the end of the transition (up) where the CPCD slab thickness is 9 inches.

Furthermore, a thermocouple assembly was installed 114 inches before the end of the transition where the thickness of the CPCD layer is 6 inches and the thickness of the CRCP overlay is about 7.4 inches. In the assembly, seven (7) probes were attached to measure slab temperatures at 7 different depths namely: top, middle, and bottom of existing CPCD; interface between CPCD and CRCP overlay; and, top, middle, and bottom of CRCP overlay. Lastly, crack meters were installed at the last CPCD joint before the end of the transition. One (1) unit of the horizontal and two (2) units of vertical crack meters were installed to measure the horizontal and vertical movements of the CPCD slab, respectively, before and after the CRCP overlay. Figure 35 and Figure 36 show the actual sensors installed in Section 2.

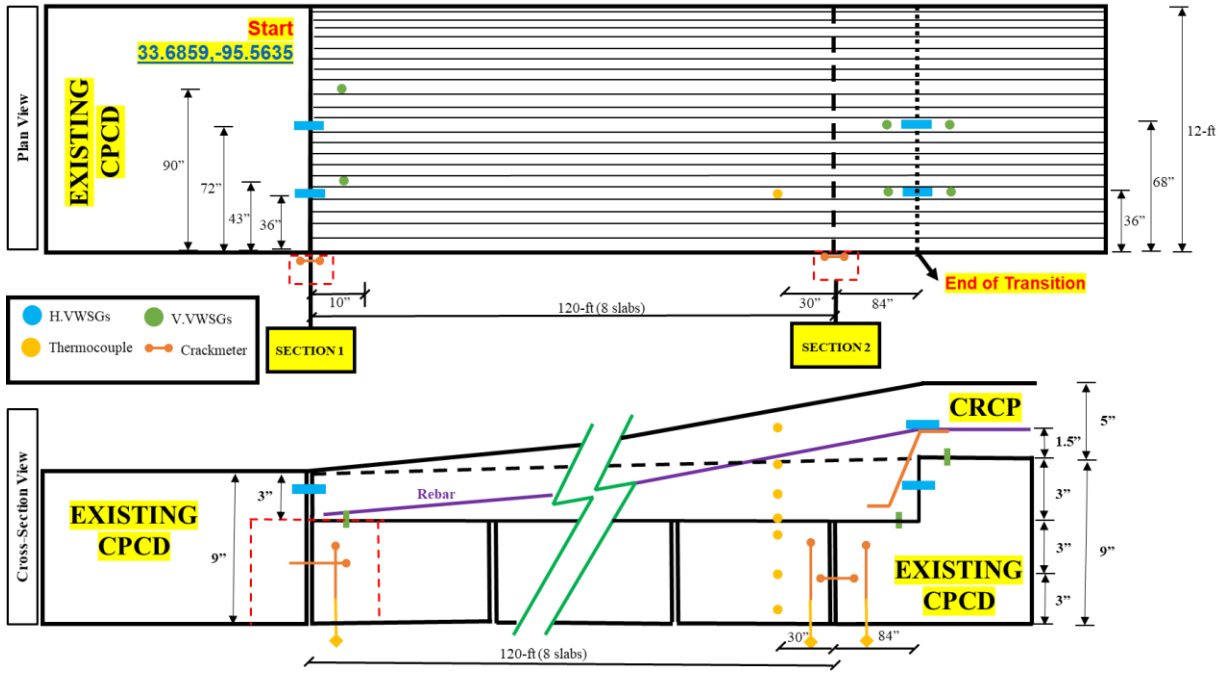

Figure 33 Gage Installation layout plan for section 1 and section 2

(a)

(b)

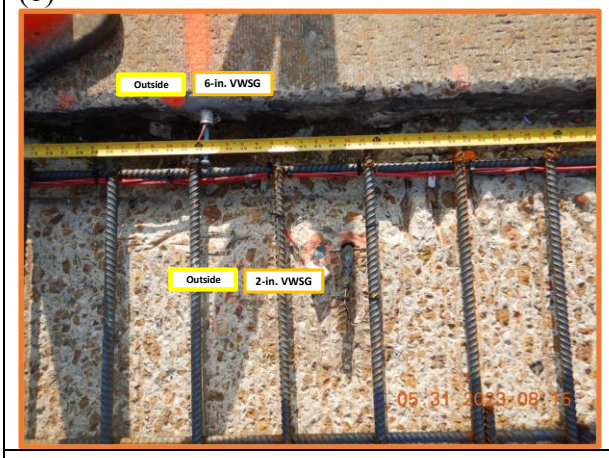

(c)

(d)

Figure 34 Field gauge installation at section 1

(a)

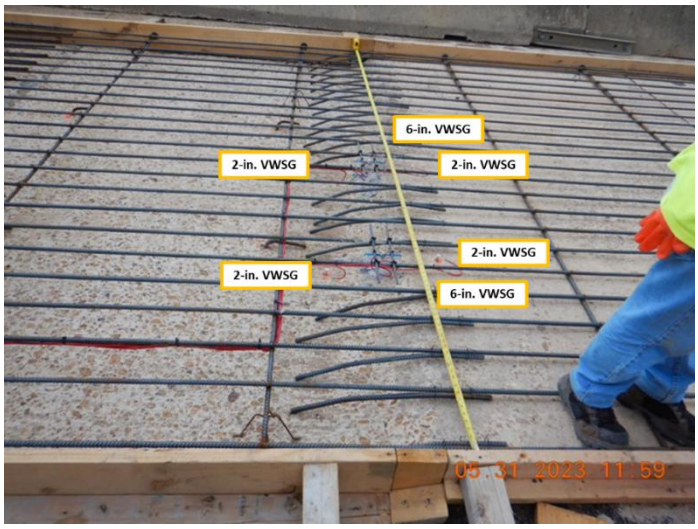

(b)

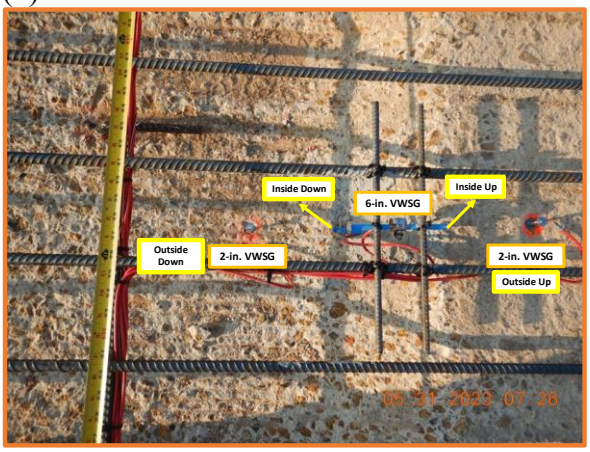

(c)

(d)

Figure 35 Field gauge installation at section 2

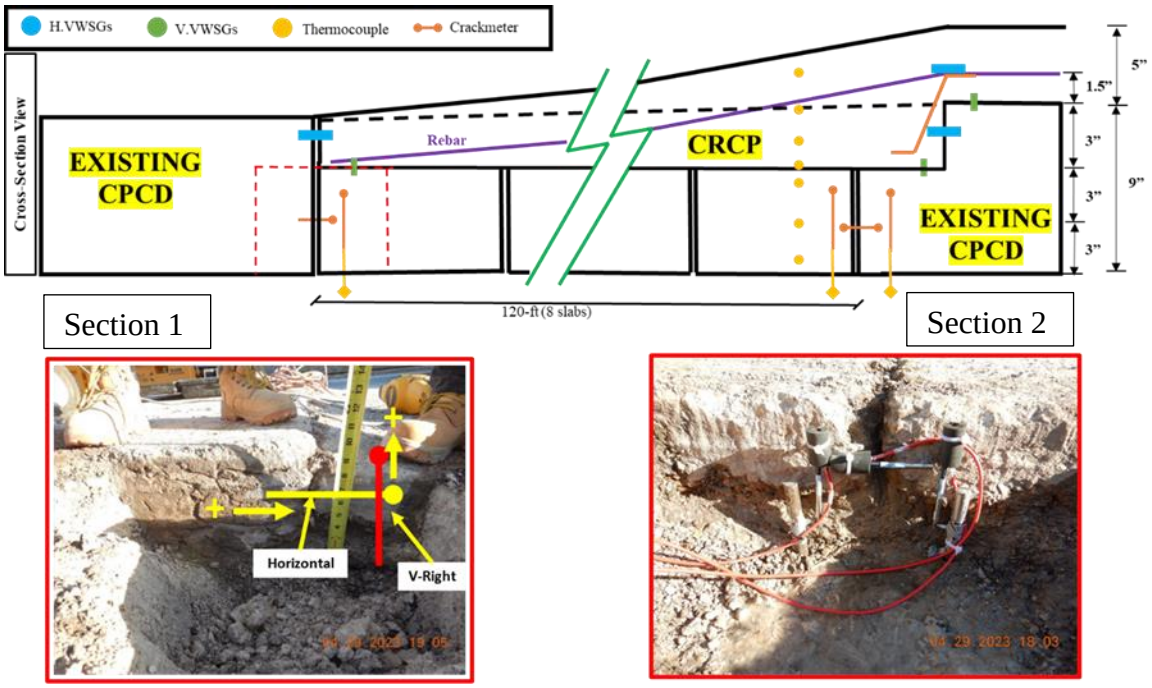

Figure 36 Installation of Crackmeter for section 1 and section 2

Figure 37 shows the plan and cross-sectional view of gauge installation for Section 3 which is located 600 feet from the start of the transition as mentioned earlier. A total of 11 gauges were installed and embedded in this section. Six (6) units were 6-inch VWSGs installed at various locations of the CRCP overlay and one embedded at the top of the existing CPCD. 4 units of 2-inch VWSGs were installed at the interface between CPCD and CRCP layers, in which 2 units were installed on both sides of the joint. Lastly, one assembly of thermocouple having seven (7) probes was installed throughout the entire depth of the CPCD and CRCP layers. These probes measure temperature at 7 different depths namely: top, middle, and bottom of existing CPCD; interface between CPCD and CRCP overlay; and, top, middle, and bottom of CRCP overlay. Figure 38 shows the actual gauges installed at Section 3.

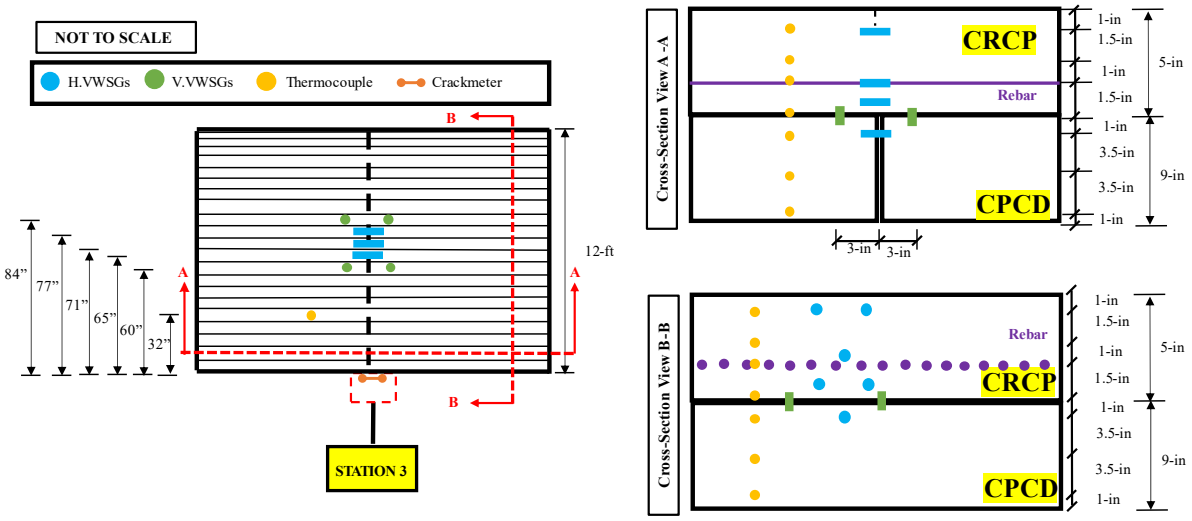

Figure 37 Gage installation layout plan for section 3

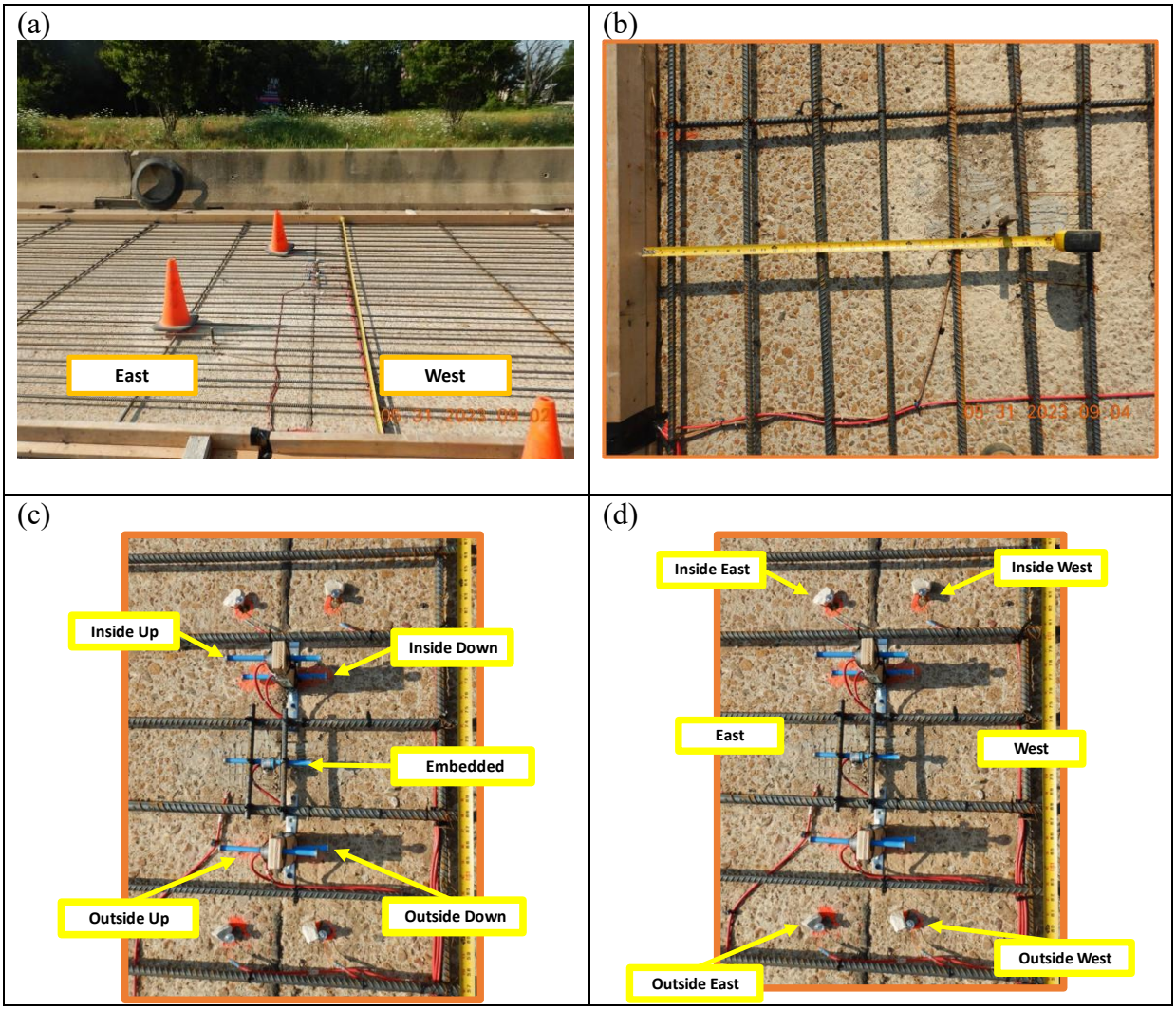

Figure 38 Field gauge installation of sensors at section 3

In addition, Figure 39 shows the crackmeter installed at Location 3. A total of four crack meters were installed. Two units of crack meters were installed horizontally, 3 inches from the top and 3 inches from the bottom of the CPCD slab. Two units of the crack meters were installed vertically near the top surface of the CPCD slab, and each positioned on opposite sides of the joint.

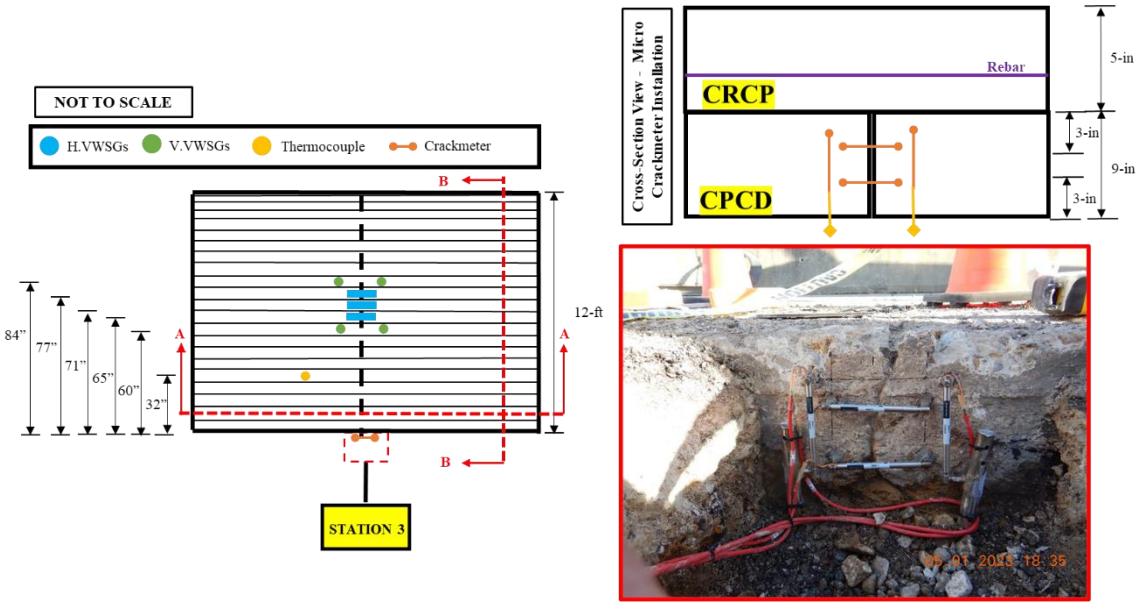

Figure 39 Installation of crackmeter at section 3

Similarly in Section 4, four units of 2-inch VWSGs were installed vertically at the interface between the existing CPCD and CRCP overlay. As shown in Figure 40, two (2) of these sensors were located 6 inches before the end of the transition (down) where the CPCD slab thickness is 6 inches and the other two (2) were located 6 inches after the end of the transition (up) where the CPCD slab thickness is 9 inches. As mentioned earlier, this installation aims to compare the vertical strain results with Section 2. Figure 41 shows the actual sensor installation in Section 4.

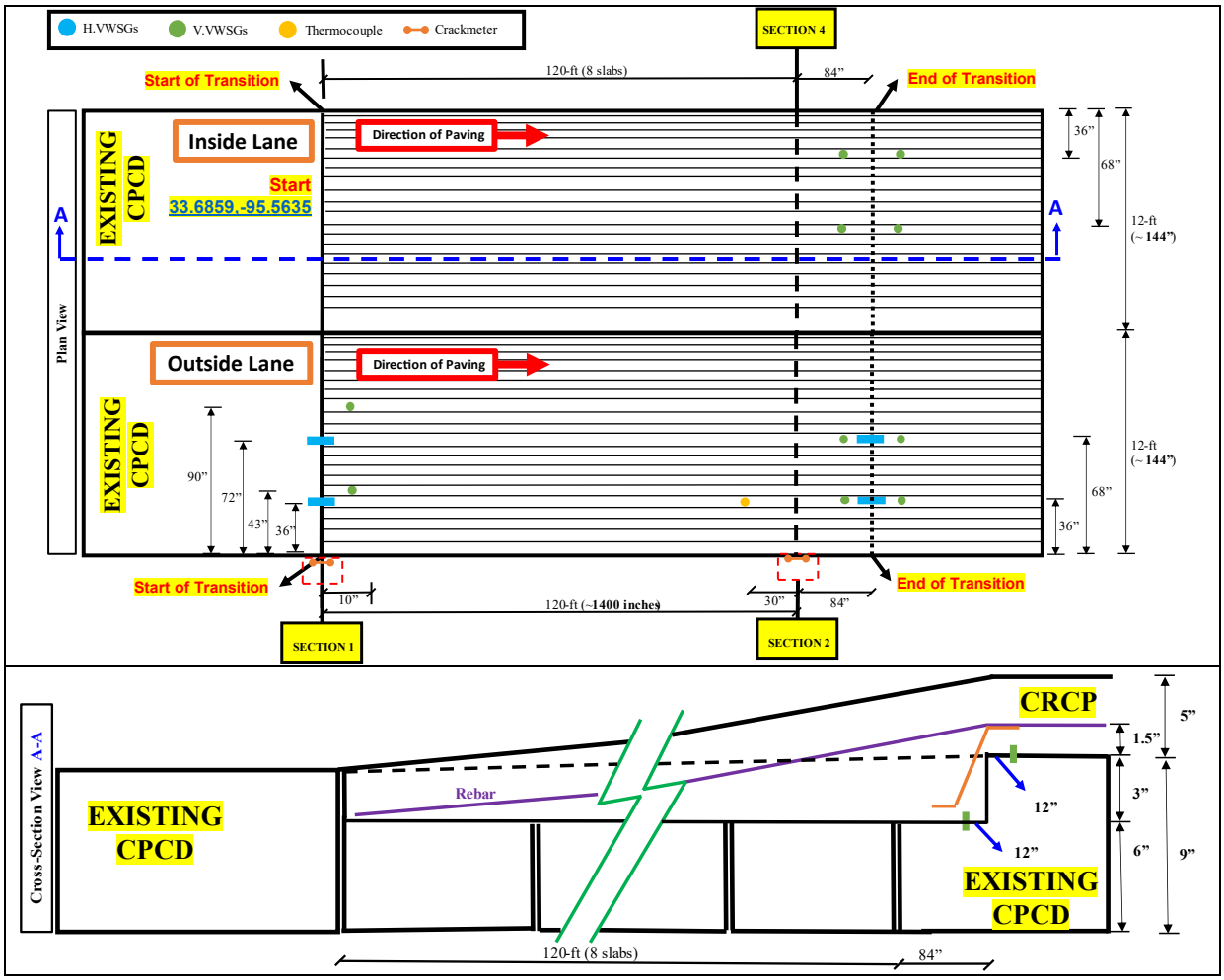

Figure 40 Gage installation layout plan for section 4

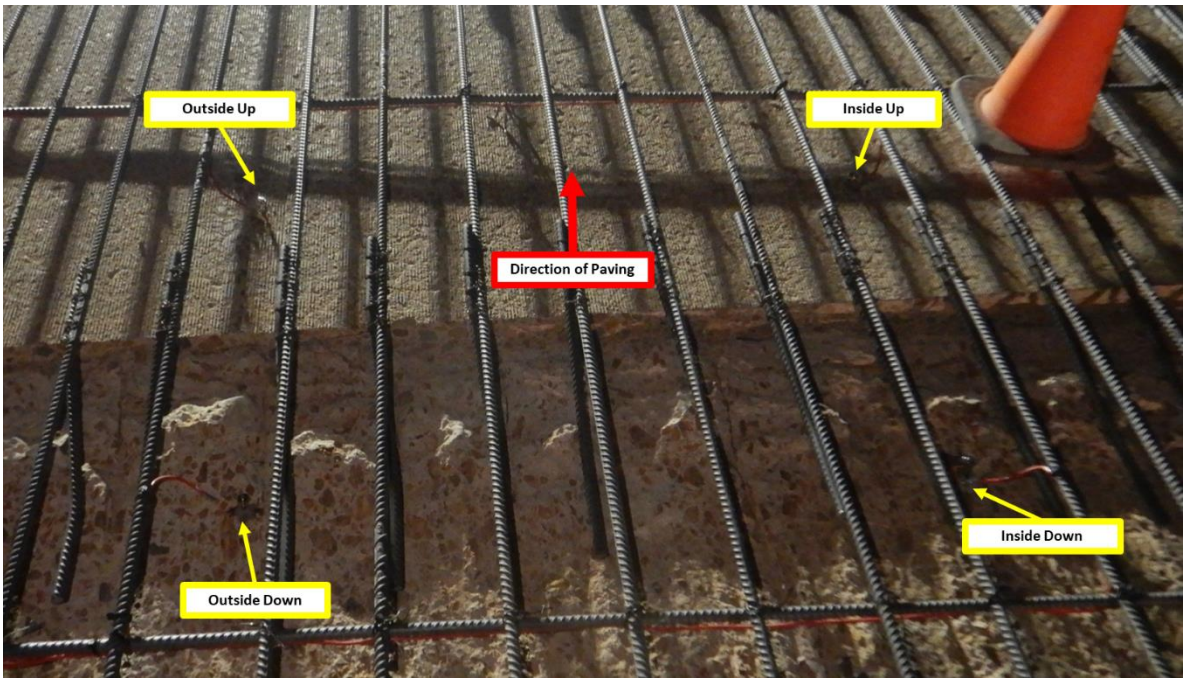

Figure 41 Field gauge installation of sensors at section 4

3.5 Construction

The concrete placement details are presented in this section, along with photos taken during the construction. Table 6 shows the concrete placement information of the test section and Figure 43 shows the construction information for both outside and inside lanes.

Table 6 Placement Information of the Test Sections

ID	Time of Concrete Placement
Section 1 - Start of Transition (Outside Lane)	5/31/2023 11:45 AM
Section 2 - End of Transition (Outside Lane)	5/31/2023 12:45 PM
Section 3 – Regular Section (Outside Lane)	5/31/2023 03:15 PM
Section 4 – End of Transition (Inside Lane)	8/25/2023 5:00 AM

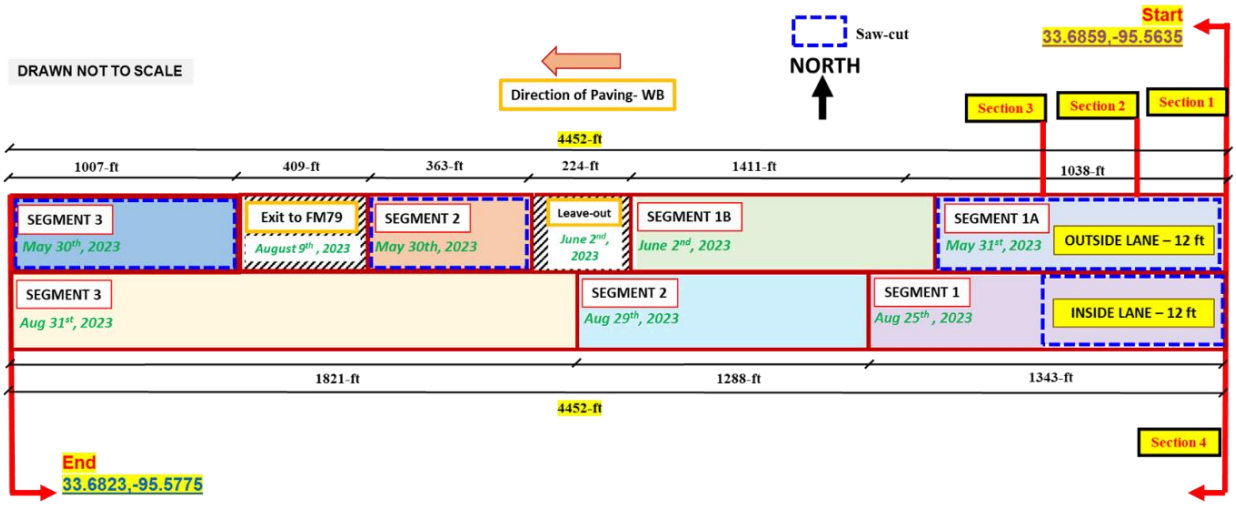

Figure 42 Construction information of both outside and inside lane

Figure 43 shows the concrete placement on the outside lane. Figure 43-(a) was taken just before the placement of concrete on 31st May 2023. Figure 43-(b) and Figure 43-(c) show the protection of the sensors with concrete and preliminary consolidation of the concrete before the concrete placement, respectively. This was to ensure that concrete placement would not affect the sensors during placement and consolidation as shown in Figure 43-(d), Figure 43-(e), and Figure 43-(f).

Figure 43 Concrete placement and consolidation on outside lane.

Figure 44 shows the finishing and tining activities after consolidation.

(a)

(b)

Figure 44 Finishing and Tining of CRCP Overlay after concrete placement.

Figure 45 shows the curing operation. It is observed that there are areas with deficient curing. The grey areas were more dominant on the inside of the outside lane. The insufficient application of curing compound may not prevent moisture loss from the concrete surface, potentially increasing temperature loss and shrinkage of concrete.

(a)

(b)

Figure 45 Curing compound application after concrete placement.

The day after concrete placement, saw-cuts were made on the CRCP overlay as shown in Figure 46 even though saw-cuts are not needed in CRCP. As pointed out earlier, the saw-cut was made only on Segments 1A, 2 and 3. The effect of the saw-cut in crack propagation was monitored and will be discussed in the discussion of the results.

(a)

(b)

Figure 46 Saw-cut on Segment 1A, Segment 2 and Segment 3

It was also observed that in some areas, the surface of the existing CPCD was not in SSD condition prior to the concrete placement. The need for SSD condition or damp condition on the existing surface is necessary to establish a good bonding at the CPCD and CRCP interface. However, as seen in Figure 47 -(a) to Figure 47-(d), there were areas where the surface of existing CPCD dried up before the concrete was placed. Those dry areas were mostly in the left half of the outside lane.

(a)

(b)

(c)

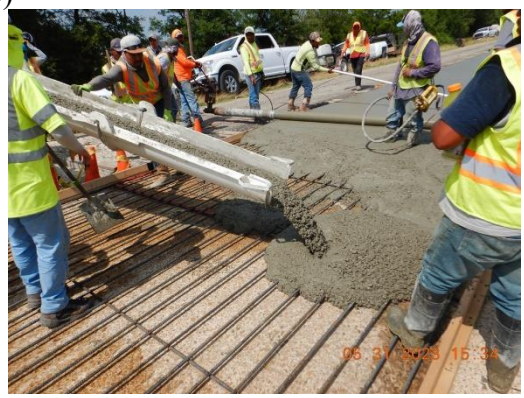

(d)

Figure 47 Surface condition during concrete placement

Figure 48 shows the concrete placement on the inside lane on Segment 1. Figure 48-(a) was taken right before the placement of concrete on August 25, 2023. Figure 48-(b) and Figure 48-(c) show the concrete placement after the first batch of concrete arrived on the field, and Figure 48-(d) shows the covering of the sensors with concrete by hand. Figure 48-(e), and Figure 48-(f) show the consolidation of concrete during the placement.

(a)

(b)

(c)

(d)

(e)

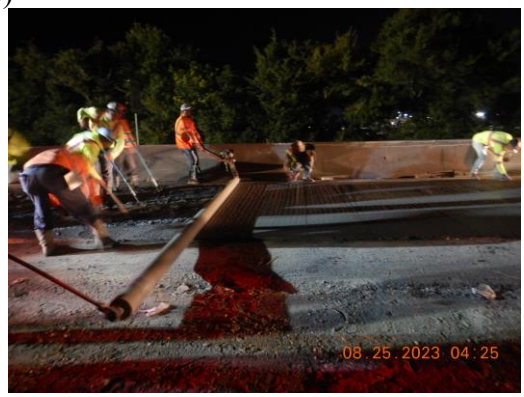

(f)

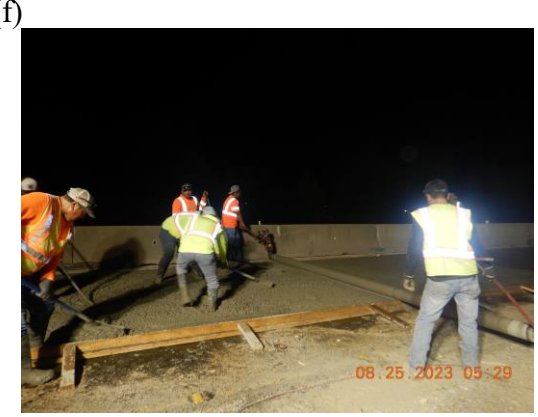

Figure 48 Concrete placement and consolidation on inside lane

Figure 49 shows the finishing and tining activities after consolidation.

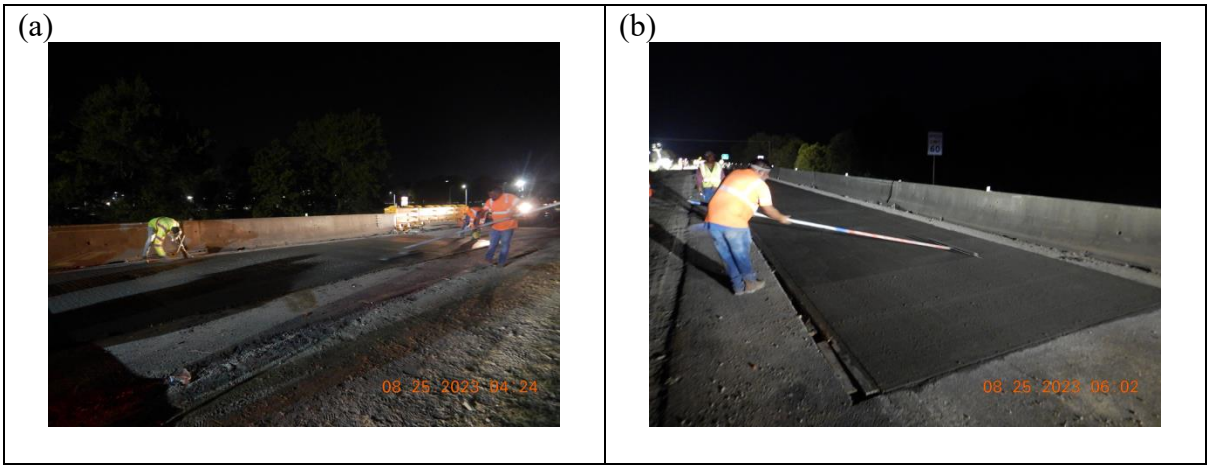

Figure 49 Finishing and Tining of CRCP overlay after concrete placement

Figure 50 shows the curing operation and the condition of curing membrane. It shows that the curing membrane was in a rather non-uniform condition.

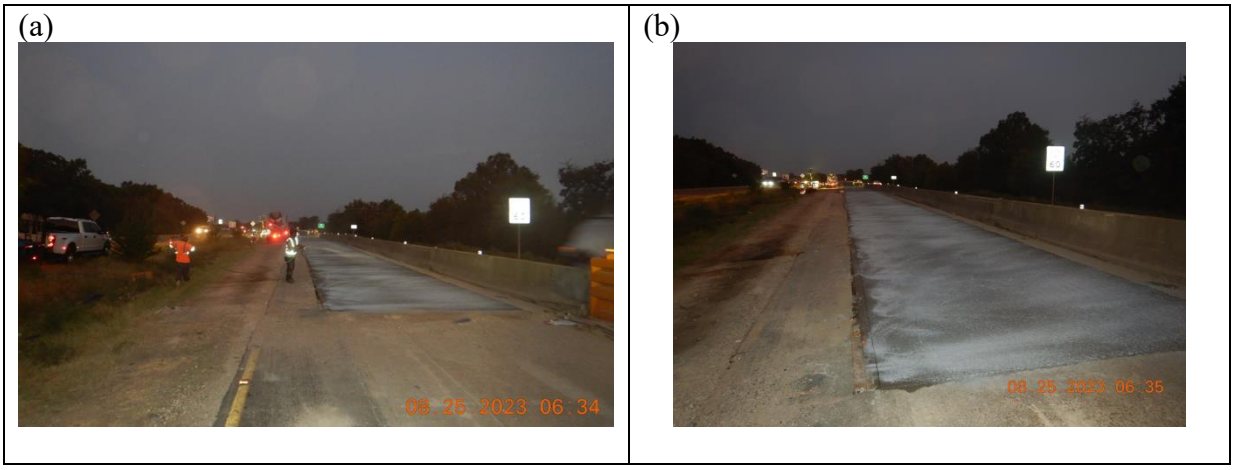

Figure 50 Curing compound application after concrete placement

Chapter 4 Early Age Bonded Concrete Overlay Behavior

The early age behaviors of the bonded concrete overlay were obtained from the data acquired from the instrumentation at the four Sections described in Chapter 3. The obtained data were processed and analyzed. The physical interpretations of the data are presented and discussed in this chapter.

4.1 Weather Data

Air temperature, rainfall, relative humidity, and wind velocity were measured using the wireless weather station. It was placed close to Section 2 which generally represents the actual weather condition at the test section. Figure 51 presents the recorded air temperature and rainfall data that were collected between May 17 and June 21, 2023. The temperature was measured in Fahrenheit(°F) and rainfall in inches. It can be observed that the air temperature a few days before and after the concrete placement at Segment 1A on outside lane were relatively similar. The decrease in temperature was primarily attributed to the rainfall events that occurred on those days. For instance, on June 3 when one inch of rainfall was recorded, the air temperature dropped to 65°F. There were minor rainfall events after that, but the air temperature went up again until the next heavy rainfall events almost two weeks from the concrete placement. The period of interest in the data analysis is the first week from the concrete placement, and the temperature drops on June 3 due to the rainfall event may have an impact on the behavior of the concrete overlay which will be discussed later.

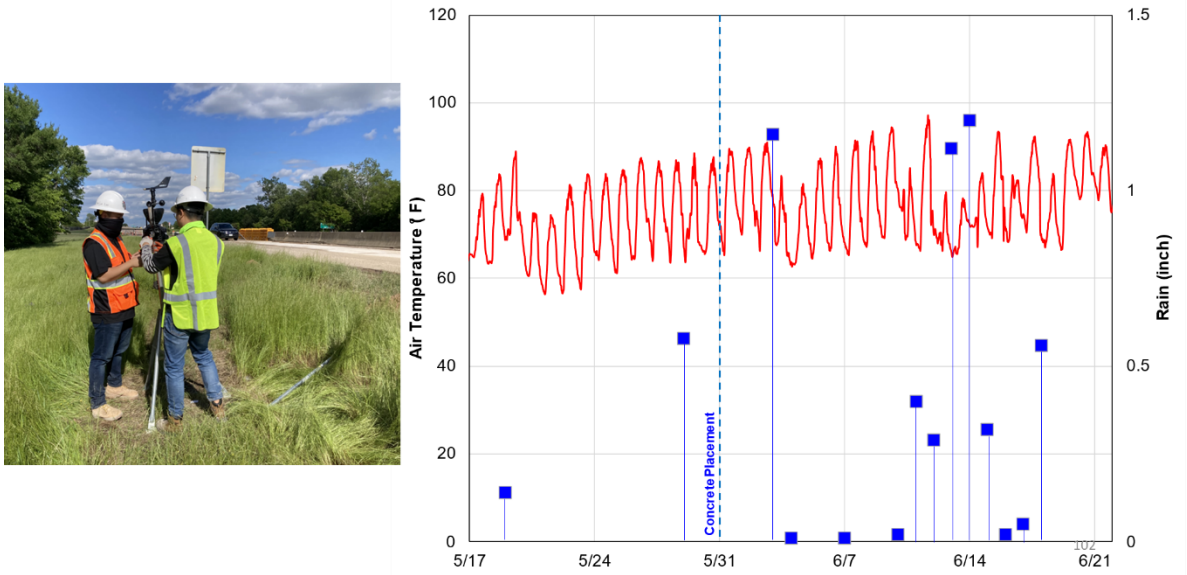

Figure 51 Air temperature and rainfall measured using weather station

4.2 Evaluation of Pavement Temperature Profile

The investigation of the temperature profile in this pavement structure will aid in better understanding of the behavior of the CRCP overlay as well as its interaction with the existing CPCD layer. As discussed earlier, there are two assemblies of temperature gages that were installed in the test section. The first one (at Section 2) is located before the end of the transition where the existing CPCD is 6 inches thick after milling and the CRCP overlay thickness is 7.4 inches. The second one (at Section 3) is located at the regular section where the thickness of the existing CPCD is 9 inches and the CRCP overlay thickness in 5 inches.

The temperature probes were positioned such that it will obtain temperature data at the top, middle and bottom of both the CRCP and CPCD layers and one at its interface. Temperature data from these seven (7) probes will provide temperature gradients through the pavement slab depths at a specific time period as well as over the time period of interest.

Figure 52 and Figure 53 present the temperature variations of the concrete at various depths in the slab on Sections 2 and 3, respectively. To make the temperature data presentation clearer before and after concrete placement, two scales in the temperature were used: one on the left y-axis presents concrete temperatures in CPCD, while the right in CRCP overlay. The numbers in the legend represent depths from the surface of CRCP overlay. More specifically, the lines with blue, yellow, and green represent temperatures in CRCP, while the others represent temperatures in CPCD. For example, in Section 2 three sensors at 3-, 5-, and 7-in depths were in CRCP overlay (See Figure 35).

Before the concrete placement, the difference in existing CPCD thickness (i.e., Section 2 @ 6 inches vs. Section 3 @ 9 inches) has also influenced the range of temperature variation of the slab under the same air temperature variations, where the thicker slab at Section 3 have higher temperature variations than Section 2. It was also observed that the difference in the temperature variation of the top and the bottom of the thinner slab (Section 2) is lesser compared to the variations observed in Section 3, which shows that the bottom of the CPCD layer has smaller temperature variations than at the top of the CPCD layer.

Another observation is the change in temperature variation at the CPCD layer after the concrete overlay placement. It can be seen that there was a substantial reduction in temperature variations, which can be attributed to the insulation effect that was provided by the concrete overlay on the CPCD.

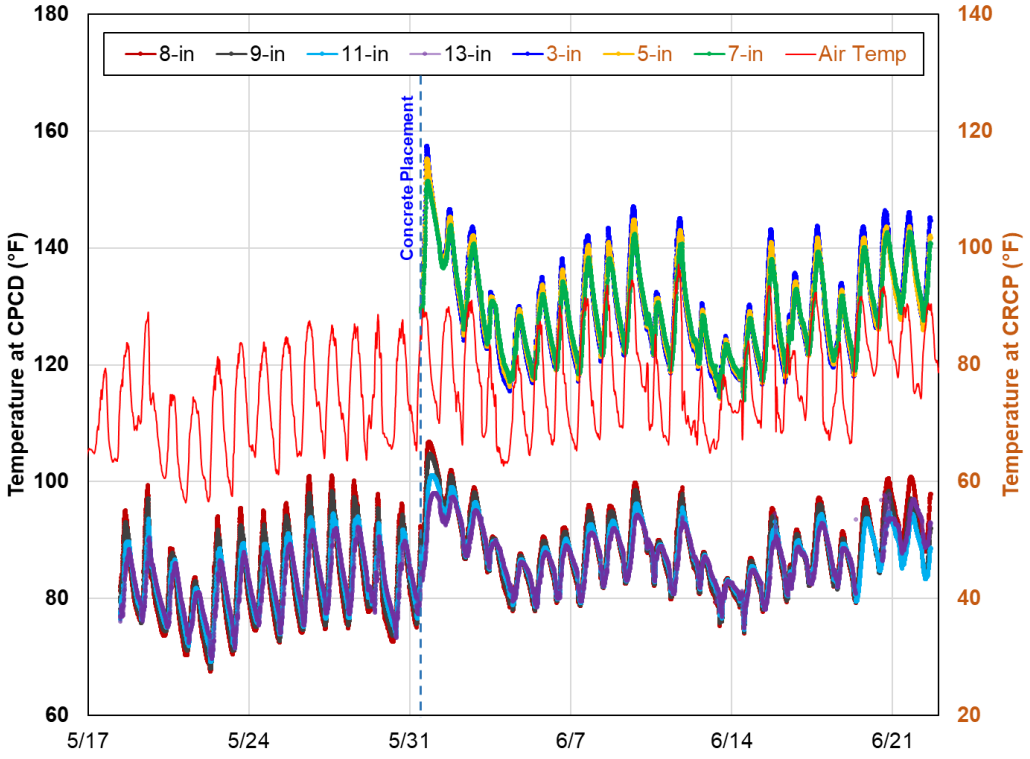

Figure 52 Temperature variation throughout the depth of concrete slab at Section 2

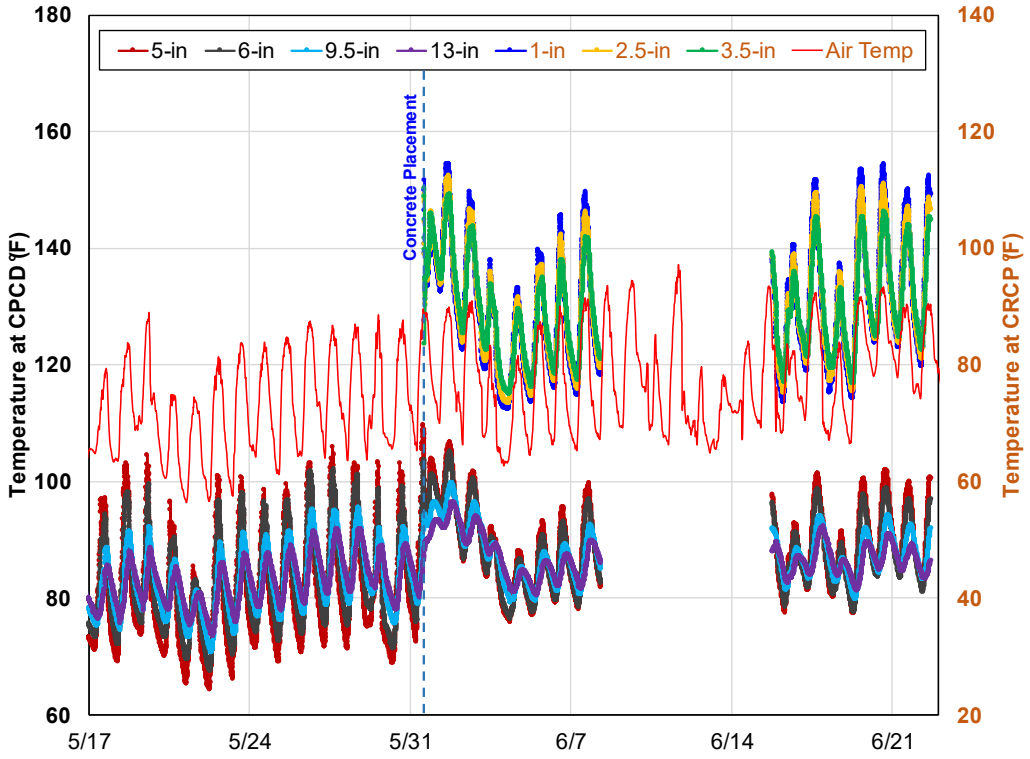

Figure 53 Temperature variation throughout the depth of concrete slab at section 3

It is known that an overlay provides a certain level of insulation to the existing pavement layer. In order to investigate the insulation effects, two sets of a day's temperature data were analyzed from the dataset. The first set was a day before the concrete placement, while the second set was a day after the concrete placement. To make the insulation effect investigation valid, the two sets of air and concrete temperatures and environmental conditions should have the following characteristics: (1) at the top of the concrete slab, the peak temperatures must be similar, (1) at the top of the concrete slab, the range of the concrete daily temperature variations should be similar, (2), and (3) there should be no rainfall event during the days of interest.

For Section 2, May 26 and June 7 temperature data satisfied the above 3 requirements and the temperature gradients are shown in Figure 54. It should be noted that Section 2 is located at, before concrete placement, the temperature at 8-inch depth on May 26 is the temperature at the surface of the existing CPCD, while, on June 7, the temperature at 3-inch depth is the temperature at 2.4 inches from the surface of the overlay and the temperature at 8-inch depth is the temperature at the interface between CPCD and CRCP. The range of temperature variation at the surface is relatively similar at around 25 degrees. However, the range of temperature variation at the bottom of the slab after concrete placement has reduced from 15 degrees to 11 degrees. Also, the range of temperature variation at the interface is 15 degrees which is 10 degrees lower (40% reduction) under the same air temperature before the concrete overlay was placed. This reduction of temperature variation on the existing slab is expected according to the concepts of heat transfer.

For Section 3, May 22 and June 16 temperature data are comparable as shown in Figure 55. Before concrete placement, the range of temperature variation on May 22 was 35 degrees at the surface and 11 degrees and the bottom of the existing CPCD. On June 16, after concrete overlay placement, the range of temperature variation was 24 degrees at the surface and 5 degrees at the bottom of the existing CPCD. In addition, the range of temperature variation at the interface was 13 degrees (60% reduction).

It is also noted that, while the air temperature and occurrence of rainfall event was included in the selection of comparable dates before and after concrete overlay placement, there are other factors that may also have influenced the slab temperature profiles. As such, this comparison is only indicative and not absolute, and it just aims to illustrate that the behavior of the CPCD due to temperature variation is reduced due to the insulation effect provided by the CRCP overlay.

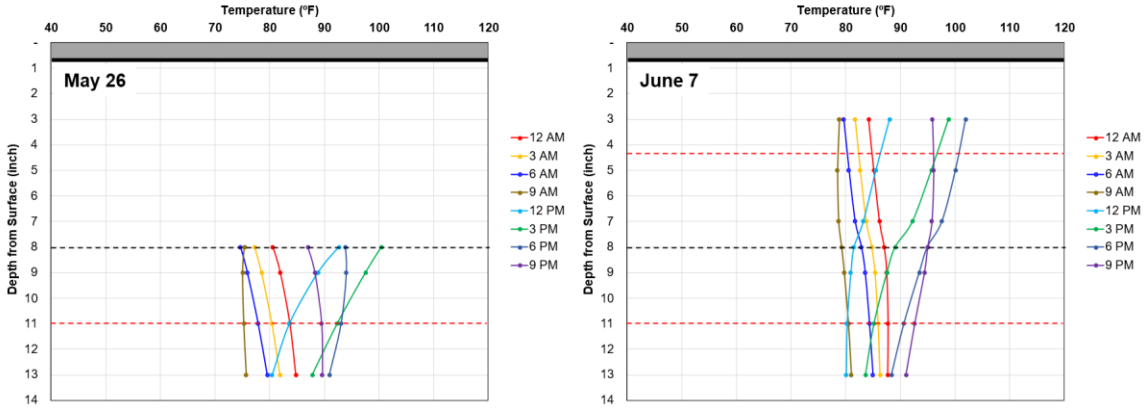

Figure 54 Temperature variation before and after concrete placement in Section 2

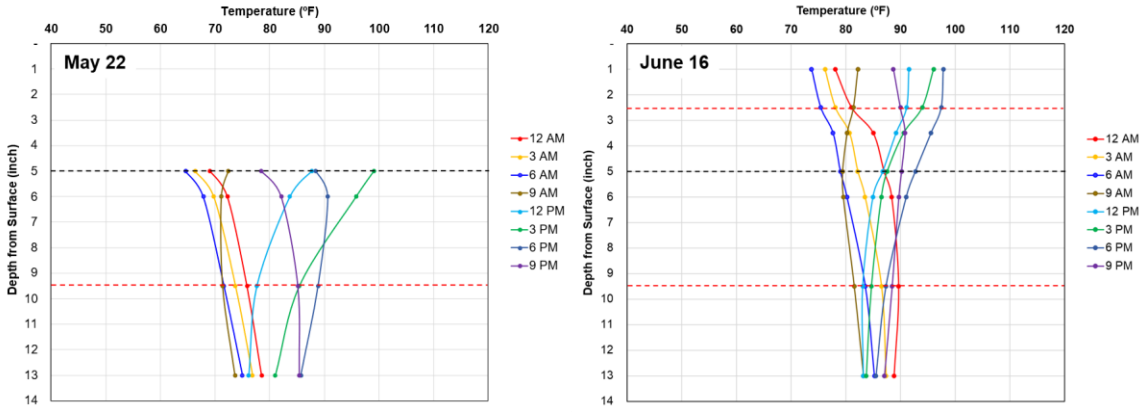

Figure 55 Temperature variation before and after concrete placement in Section 3

4.3 Characterization of CPCD Joint Movements

Compared with the movements of concrete at transverse cracks in CRCP, CPCD joint movements are relatively larger. It is because the dowel bars are supposed to allow free movement of concrete slabs from temperature variations. This section investigates the joint movements at the existing CPCD before and after the CRCP overlay placement. It can be recalled that the crack meters were installed in all three Sections.

4.3.1 Section 1 – Start of Transition

As shown in Figure 56, two crackmeters were installed in Section 1. One crackmeter was installed horizontally and the other vertically on the milled section, where the slab thickness of the CPCD is 6 inches. The round markers in yellow and red in the illustration indicate where movements of the slab were measured, either horizontally or vertically. As for the signage for slab movements, when the horizontal crack meter moves towards the right direction, the value will be positive (+), indicating that the slab is moving away from the transition joint, increasing joint width. As for the vertical crack meter, the positive (+) values indicate that the slab is moving in the upward direction.

The recorded data from Section 1(start of the transition) is presented in Figure 56. Here, the primary y-axis is joint movement measured in mils. The secondary y-axis provides information on concrete temperature at a depth of 3-inch from the milled section where the horizontal crackmeter is installed. The x-axis provides the date and time it was recorded. It can be observed that there was minimal horizontal movement recorded before and after concrete placement. The same is true with the vertical movement of the slab. There was no significant effect that resulted from the concrete overlay. At this location, the thickness of the overlay was 3 inches, equal to the depth of the milling since this is the beginning of the transition. However, as will be discussed later, the horizontal movements at this joint are quite small. If the dowels were properly installed, they are not supposed to restrain slab movements in the longitudinal direction. The daily joint movement in the longitudinal direction at this joint should be in the range of 9 mils to 14 mils. This range was estimated with the assumption that the subbase friction will reduce the free slab movements by 20 % to 50 %, as well as the thermal coefficient of concrete at 5 microstrains/ºF. Prior to the overlay placement, the maximum joint movement was 4 mils, which suggests that dowels restrained concrete movements, and this joint was locked. On the other hand, vertical movements are not small, indicating that locking joints still experience warping movements, even though their magnitudes are much smaller than those at joints with working dowels, which will be discussed later.

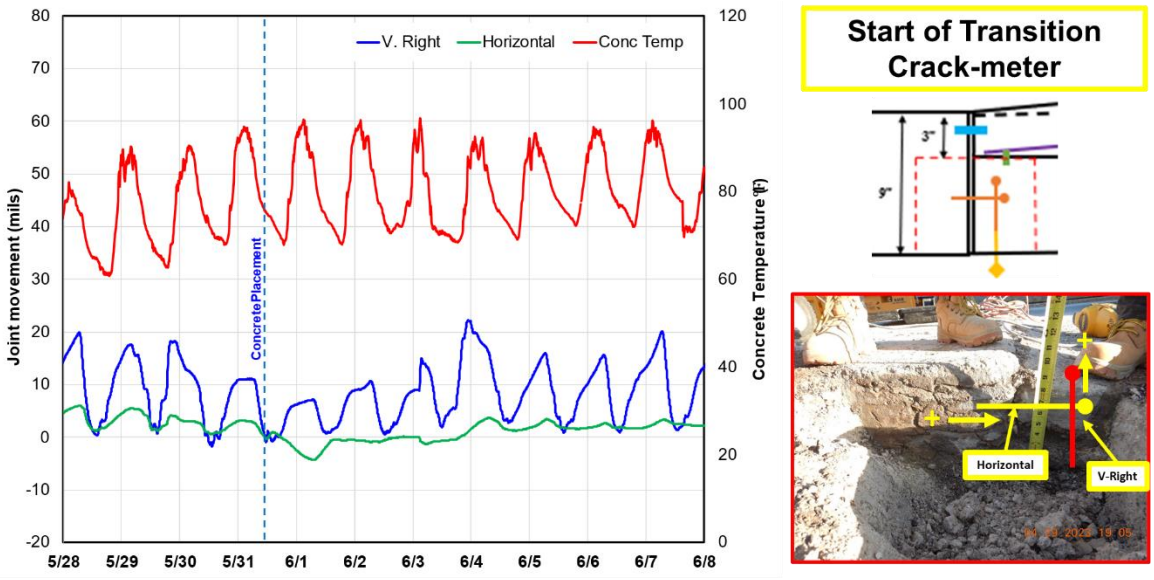

Figure 56 Crackmeter data analysis at section 1

4.3.2 Section 2 – End of Transition

As shown in Figure 57, three crackmeters were installed in Section 2. Section 2 is a joint located 120 feet from the start of transition and 7 feet before the end of transition. This section has 6 inches of existing CPCD and 7.7 inches of CRCP overlay thickness above the joint. The horizontal joint movement is measured 3 inches from the milled surface of the existing CPCD, while the vertical joint movements were measured 2 inches from the milled surface of the existing CPCP and 2 inches away from the joint. The positive (increasing) values of the horizontal displacement indicate that the sensor is expanding and thus the joint width is expanding. Meanwhile, the positive (increasing) values of the vertical displacement indicate that the sensor is moving upward, i.e., the slabs are curling up.

It is observed that, compared with the slab movements after the overlay concrete placement, the slab movements before the concrete overlay placement were significantly larger, as much as up to 20 mils for longitudinal movements and 40 mils for vertical movements, while those after the overlay concrete placement were about 8 mils for both movements Temperature insulation effects and the restraints provided by the longitudinal steel in CRCP overlay on concrete volume changes in the existing CPCD are considered to be responsible for this substantial reduction in slab movements. This manifests the benefits of longitudinal steel in concrete pavement in reducing slab movements from temperature and moisture variations. Compared with the slab movements observed in Section 1, those in this Section are much larger, especially before the placement of overlay concrete. It appears that dowels are not locked in this joint. Another observation is that substantial reduction in vertical movements were recorded in this joint after overlay placement, while not much difference was observed in Section 1. It is recalled that in Section 1, longitudinal steel was not continuous through the joint; rather, it was terminated at the

joint. This indicates the role of longitudinal steel in restraining concrete volume changes. The last observation is a rather small difference between data from 2 gages, which indicates a good quality of gage installation practice.

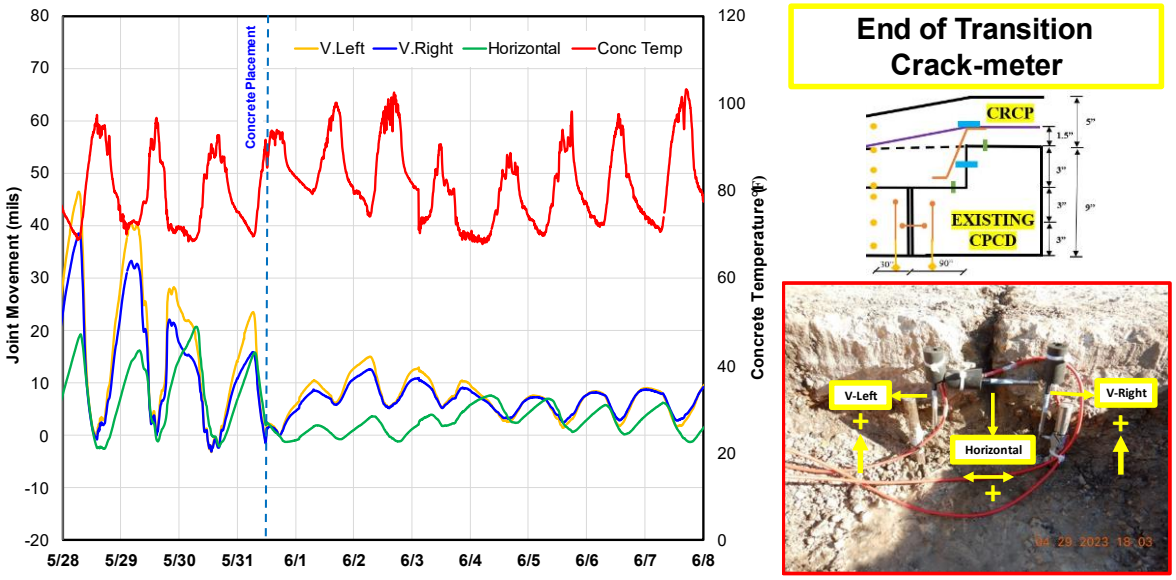

Figure 57 Crackmeter data analysis at section 2

4.3.3 Section 3 – Regular Overlay Section

Figure 58 shows slab movements data as well as the installation of four crackmeters at Section 3. which is located 500 feet from the start of the transition in the outside lane, and it is a representative of a regular overlay section where the thickness of the existing CPCD is 9 inches and the CRCP overlay thickness in 5 inches. Two crack meters measured the horizontal joint movements: one at 3 inches from the surface of the CPCD layer (H.Top) and the other at 3 inches from the bottom of the CPCD layer (H.Bottom). The other two crack meters measured the vertical movement of the CPCD on the left (V.Left) and on the right (V.Right) side of the joint.

Compared to Section 1 and Section 2, this section recorded the least horizontal movements, even smaller than those in Section 1, where the joint was suspected of being locked. It appears that this joint was also locked. The vertical movements prior to overlay concrete placement are comparable to those for Section 1. However, after overlay concrete placement, they were reduced substantially in the beginning, followed by increased vertical slab movements, which could be due to the formation of a transverse crack in CRCP overlay on top of this joint. However, their magnitude is much smaller, about 1/3 of those observed in Section 1, which again manifests the effects of continuous longitudinal steel above this joint. On more observation is that, prior to the overlay concrete placement, vertical movements at this joint were not small, indicating that locked joints restrain longitudinal concrete movements more effectively than vertical movements. In other words, even when the joint is locked, the joint experiences some level of warping and curling, which reduces warping and curling stresses in concrete slabs. This explains

why very few transverse cracks have been observed in CPCD in Texas, even when some joints are locked. Another evidence of warping and curling being allowed in the locked joint is that the longitudinal movements observed in the two gages in Figure 58 shows warping and curling behavior. For example, in the morning of May 29, while the temperature increases, the longitudinal slab movements recorded were contraction in the top gage and expansion at the bottom gage.

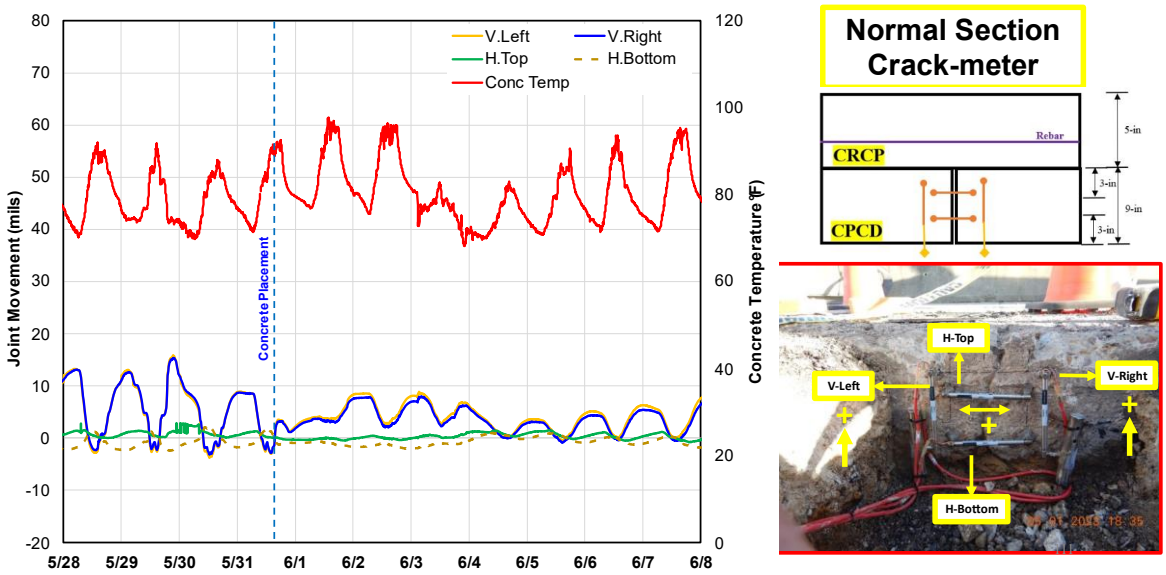

Figure 58 Crackmeter data analysis at section 3

The findings from joint movement data can be summarized as follows:

- Placement of CRCP overlay on CPCD reduces temperature gradients in CPCD, which also lowers curling behavior of the existing CPCD.
- Longitudinal steel in CRCP overlay also reduces slab displacements in CPCD, especially vertical displacements.
- It appears that dowels in some transverse contraction joints were not properly installed, resulting in locking of the joints. Locked joints reduce longitudinal slab movements more substantially than vertical movements, which still reduces warping and curling stresses and could explain why very few transverse cracks are observed in CPCP projects in Texas.

4.4 Vibrating Wire Strain Gauges

This section will discuss the strain behaviors of concrete and the CRCP/CPCD interface behavior.

4.4.1 Section 1 – Start of Transition

Figure 59 and Figure 60 show the typical installation of vertical VWSGs and longitudinal VWSGs at Section 1 as well as obtained data, respectively. A total of 4 VWSGs were installed at Section 1 – start of the transition. Two vertical VWSGs were installed at 2 locations ("outside" and "inside") in the outside lane as discussed in Chapter 3. As can be seen in Figure 59, the data shows that little variations were observed in vertical strains at outside. On the other hand, it is observed that in the morning of June 4, around 150 microstrains of vertical strain were observed inside. The distance between outside and inside is 47 inches, and it appears that there was a large difference in bonding behavior between the concretes in the two locations.

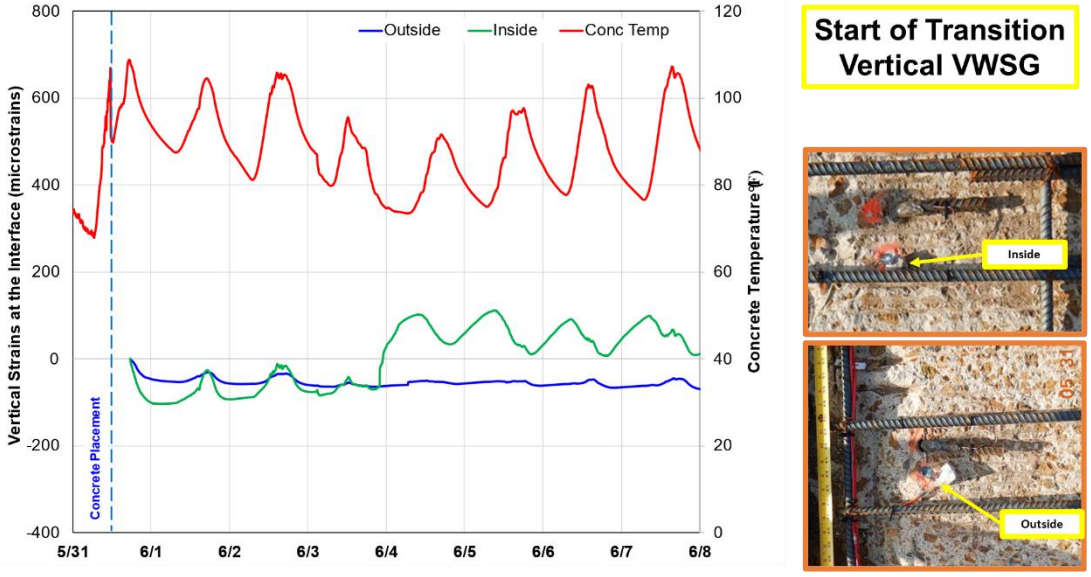

Figure 59 Vertical VWSG data analysis at section 1

The longitudinal concrete strains at Section 1, as shown in Figure 60, are already in tension and are undergoing daily cycles – as temperature goes up, the concrete strains move into compression direction, vice versa. . This is a typical behavior expected at transverse construction joints. It is also observed that the magnitude of longitudinal strains at "inside" is larger than that at "outside," which is consistent with the vertical strain behavior at the interface, where the strains at "inside" were larger than those at "outside.".

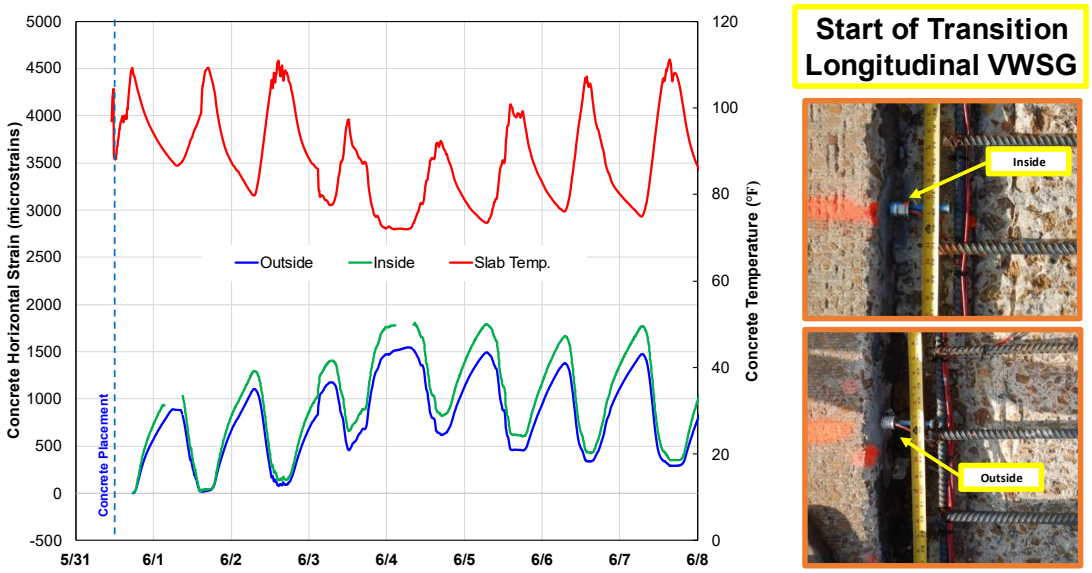

Figure 60 Longitudinal VWSG data analysis at Section 1

4.4.2 Section 2 – End of Transition

Figure 61 depicts the standard setup and data analysis for both vertical VWSG and longitudinal VWSG in Section 2. Notably, all four vertical VWSGs registered negligible strain from the concrete placement on May 31, 2023, until June 3. It's worth recalling our earlier discussion in Section 4.1(Figure 51), where a significant 1-inch rainfall event occurred on June 3, contributing to a sustained reduction in concrete temperature.

The abrupt vertical movement at the overlay interface, potentially triggered by the plummeting slab temperature and other factors, resulted in a rapid increase in vertical strain. At 6 inches after the end of the transition segment, the outer sensor indicated approximately 2500 microstrains, while the inner sensor recorded about 1200 microstrains. These substantial strain values strongly suggest debonding at the interface after the transition segment.

Meanwhile, at 6 inches before the end of the transition segment, vertical strains displayed minimal increases, emphasizing that significant vertical movement at the interface occurred primarily at the area after the transition segment. However, it's noteworthy that the "Outer-Down" sensor exhibited a strain increase of 250 microstrains on June 4, coinciding with a further surge in vertical strains of up to 3500 microstrains at the locations after the transition segment ("Outside-Up" and "Inside-Up" sensors).

.

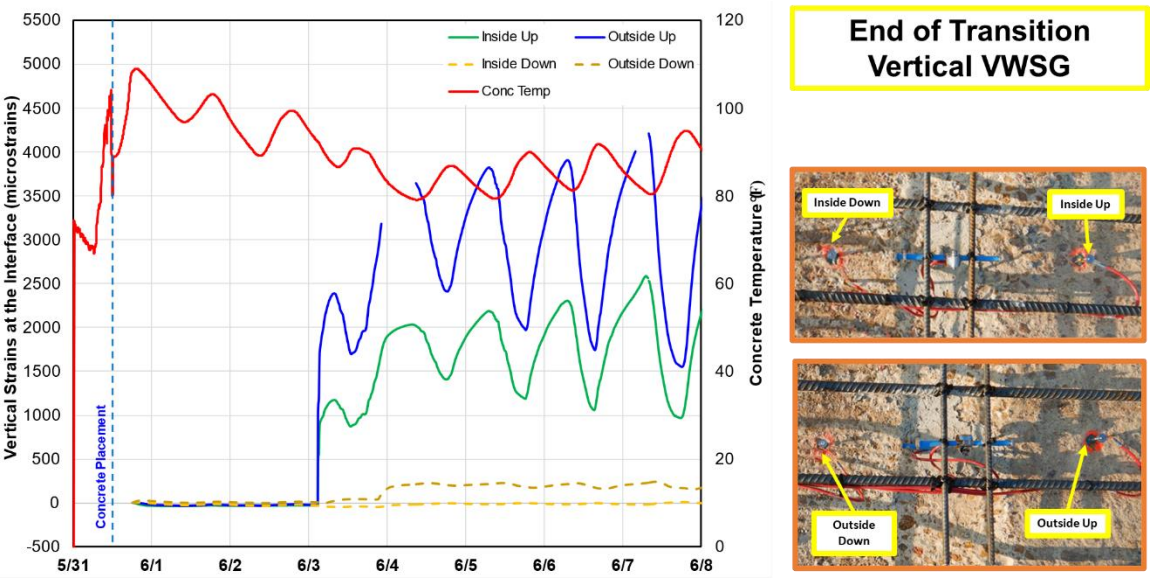

Figure 61 Vertical VWSG data analysis at section 2

Prompted by these observations, researchers conducted a comprehensive visual survey in the vicinity of the sensors. This investigation revealed a transverse crack located 15-20 inches away from the vertical strain gages installed after the end of the transition segment. The documented crack pattern is presented in Figure 62, suggesting that this transverse crack likely developed due to excessive vertical strain at the CRCP-CPCD interface in the section beyond the transition segment.

a.

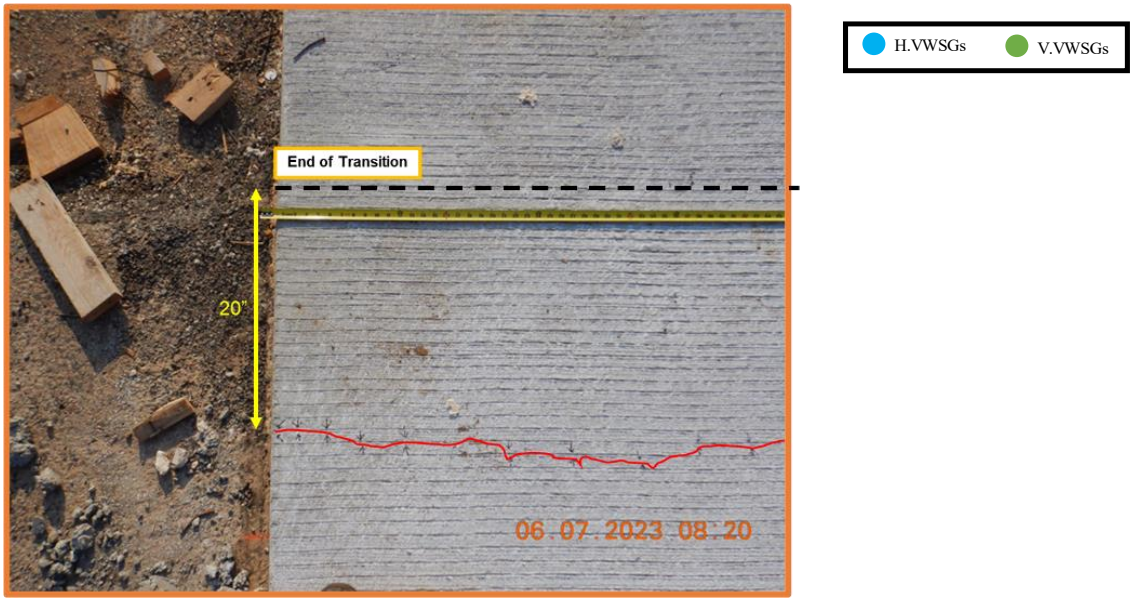

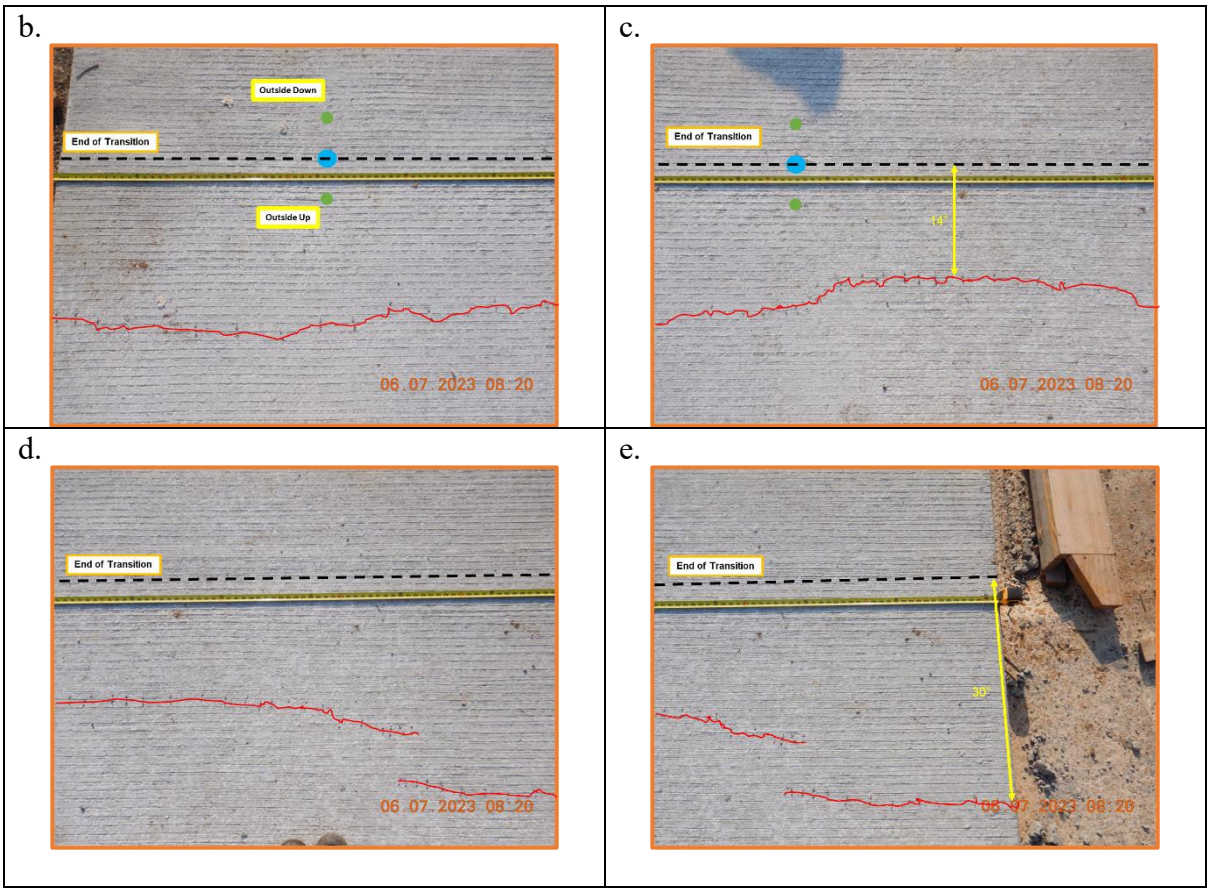

Figure 62 Crack propagation near the end of transition at Section 2

Figure 63 illustrates the longitudinal concrete strain behaviors at the termination of the transition segment, with two "Up" sensors installed at the mid-depth of the concrete overlay and another two "Down" sensors, where half of their length is embedded in the existing CPCD, and the remaining half in the CRCP overlay, as depicted in Figure 64. This dual-sensor arrangement provides insights into the interface behavior at the transition's conclusion.

From the time of concrete overlay placement until June 3, all four longitudinal VWSGs recorded compressive strains, characteristic of concrete undergoing the hydration process. However, a notable shift occurred on June 3, simultaneous with the vertical strain surge to 2500 microstrains. The two longitudinal VWSGs situated at the interface recorded an escalating tensile strain. The outer longitudinal sensor exhibited a higher tensile strain of approximately 80 microstrains compared to the inner longitudinal sensor, which showed about 0 microstrains. While these values do not clearly indicate debonding, they suggest tensile behavior in the interface, likely resulting from debonding beyond the end of the transition segment.

Conversely, the longitudinal sensors at the mid-depth of the overlay continued to record compressive strains, indicating an absence of cracks traversing the sensor locations in the overlay layer. This phenomenon, distinct from observations in US 75 in Sherman, raises the idea of significant drying shrinkage in the concrete overlay as the underlying cause.

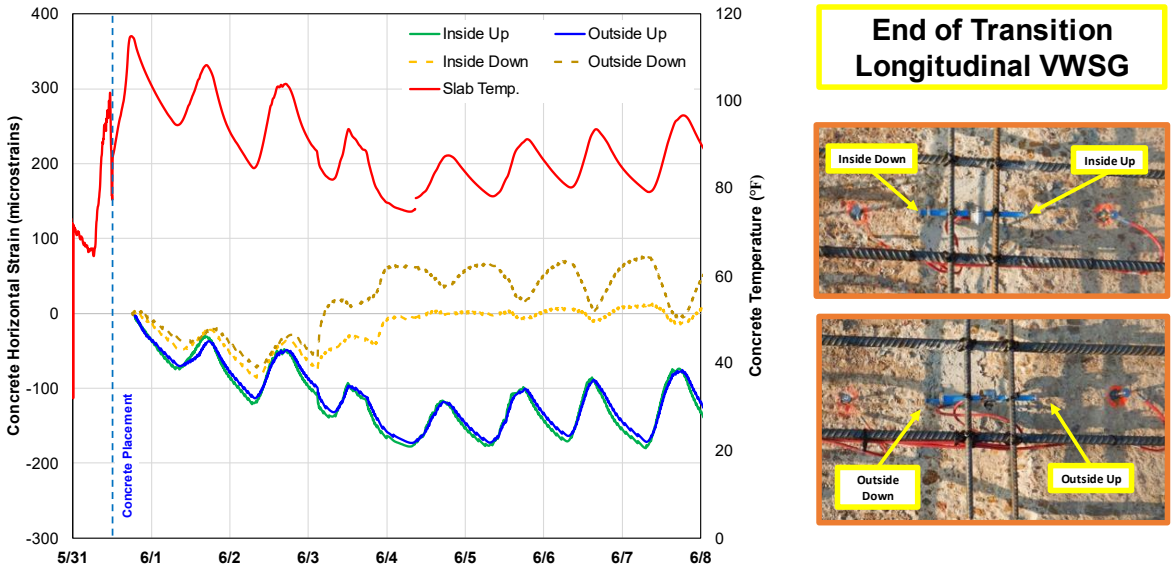

Figure 63 Longitudinal VWSG data analysis at Section 2

Figure 64 Longitudinal VWSG installation at Inside Up and Inside Down in Section 2

4.4.3 Section 3 – Regular Overlay Section

Figure 65 and Figure 66 show the installation of vertical and longitudinal VWSGs at Section 3. As shown in Figure 65, except outside west, the 3 other vertical sensors are in compression but are showing trends that it is moving towards the tension side. It is important to note that this section was saw-cut exactly at the location where the sensor was installed. From the data on longitudinal VWSG and vertical VWSG we can see the sensor recorded peak strains on June 2. This means the saw cut which was made right after the concrete placement led to crack propagation. The crack propagated across the slab and the sensors recorded the strains. In the

case of longitudinal VWSG both inside up and outside up followed same pattern and recorded as high as 1000 microstrains. This implies that there was comparatively larger longitudinal movement experienced on the top of CRCP overlay. Similarly, inside down and outside down followed same pattern and recorded strains as high as 750 microstrains. This was compared with the embedded longitudinal VWSG data which is observed in between top and bottom. This points out the fact that there is substantial longitudinal movement going on existing CPCD. In the case of vertical VWSG at the interface, similar inference can be made.

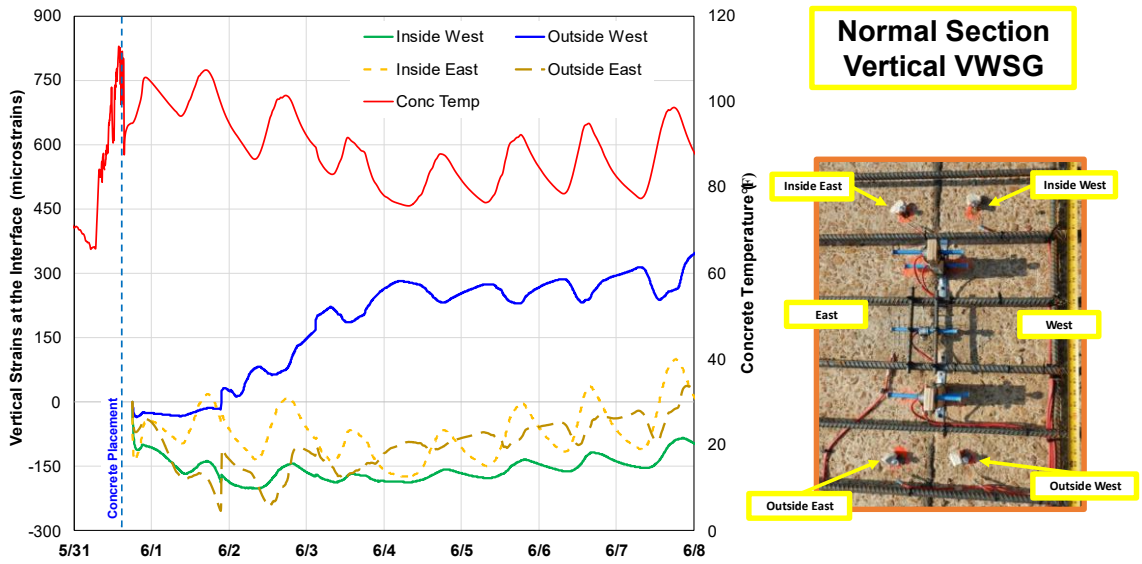

Figure 65 Vertical VWSG data analysis at Section 3

Figure 66 shows the longitudinal strain behaviors at various depths in the CRCP overlay. It can be observed that the strain near the surface of the overlay (Inside Up and Outside Up) have higher strains compared to the strain behaviors at the bottom of the overlay layer (Inside Down and Outside Down). The difference in strain behaviors at the top and bottom of the CRCP overlay is indicative of the curling and warping behavior that exists in the overlay layer.

Another observation is the strain behavior at the top of the existing CPCD layer (Embedded). The strain magnitudes between the top of the CPCD layer and bottom of the CRCP overlay layer are close but there is a slight difference. It is presumed that when the interface is properly bonded, the strain close to the interface will be similar or very close in magnitude and trends. One may also argue that the locked joint condition which was identified earlier may have influenced the difference in strain behaviors. Nevertheless, this data implies that the interface is not behaving under as a fully bonded condition.

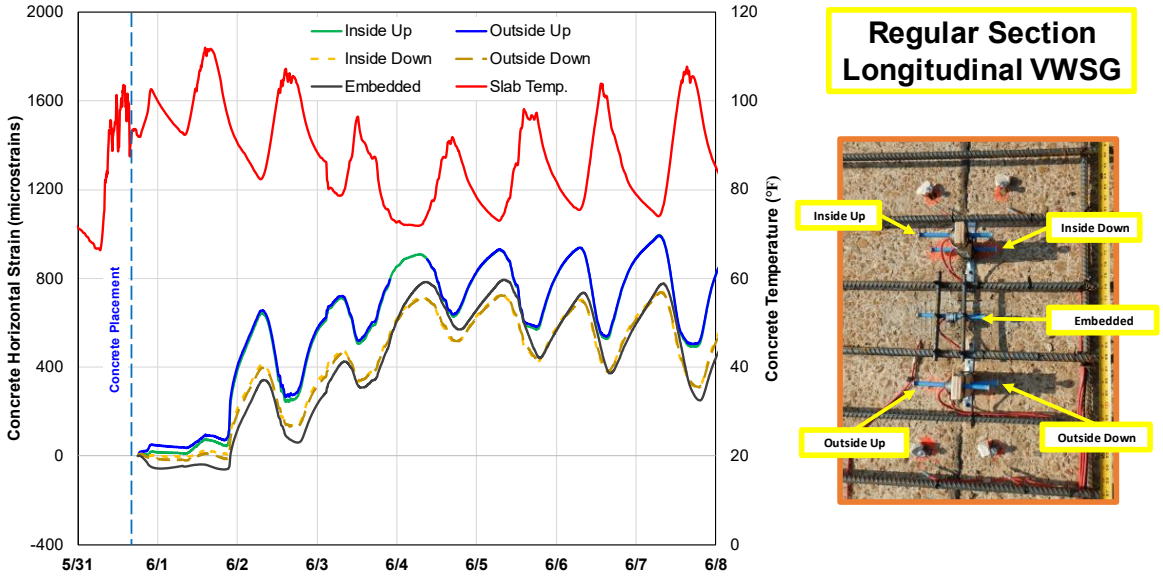

Figure 66 Longitudinal VWSG data analysis at Section 3

4.4.4 Section 4 – End of Transition at the Inside Lane

Figure 67 illustrates the standard setup and data analysis for the VWSG at Section 4, located at the end of the transition. On August 25, 2023, during the concrete placement, only two of the VWSGs remained functional. Consequently, the data from the other two gauges, which were situated in the outside up and outside down positions, is not included in this report. The VWSGs installed in the 'inside up' and 'inside down' locations exhibited relatively low vertical strains from the outset. The strain values fluctuated between zero microstrains and a range of -25 microstrains to +50 microstrains during the first 21 days following concrete placement. Given the minimal magnitude of these recorded microstrains, it may imply that there was no significant vertical movement at the overlay interface which will indicate that there was no sign of debonding which was observed at the same location on the outside lane. This finding is validated by the absence of cracks in this area.

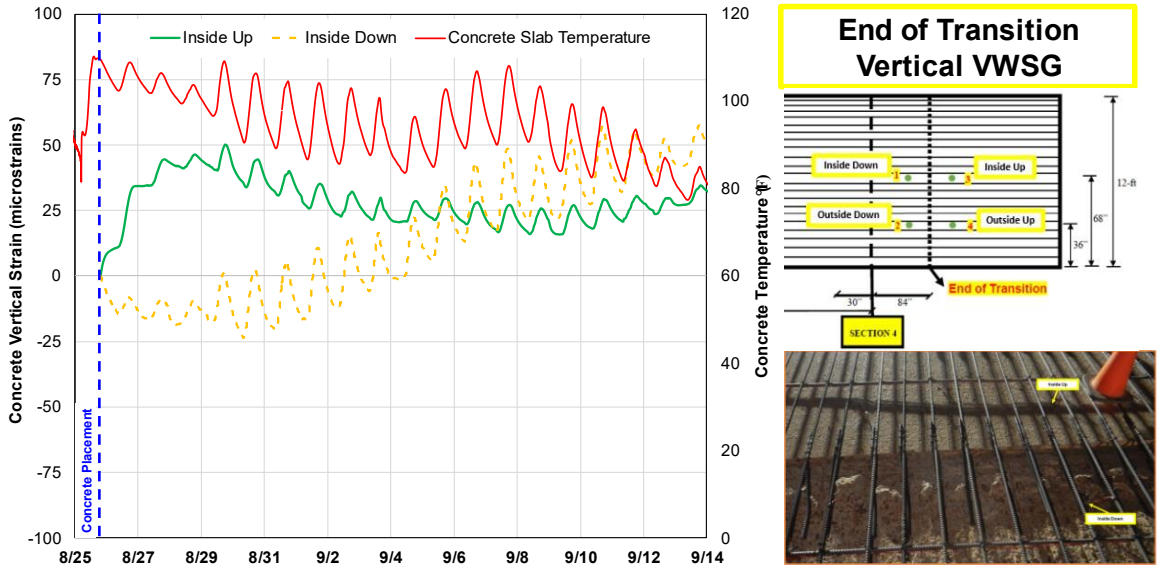

Figure 67 Vertical VWSG data analysis at Section 4

4.4.5 Comparison of Vertical VWSG between Section 2 and Section 4

The installation of VWSGs in Section 4 during the construction of the inside lane primarily aimed to detect any discrepancies in the results compared to those observed in Section 2. Since both sections represented the end of a transition, a thorough understanding of their behavior was deemed essential. Figure 68-(a) presents an analysis of Section 2 and Figure 68-(b) Section 4 for the first 21 days following concrete placement. To facilitate a clear comparison, data from only two VWSGs, specifically 'inside up' and 'inside down,' are considered.

The analysis clearly shows that Section 4 exhibited relatively higher deformation compared to Section 2. This difference, as previously discussed in Section 4.4.2, is attributed to the crack observed adjacent to Section 2. Notably, the 'inside down' VWSG readings for both sections demonstrated very similar trends, with an initial recording of -25 microstrain. This comparative analysis leads to an important conclusion: in the absence of cracks, the end of a transition, such as Section 4, is expected to behave in a manner similar to this section.

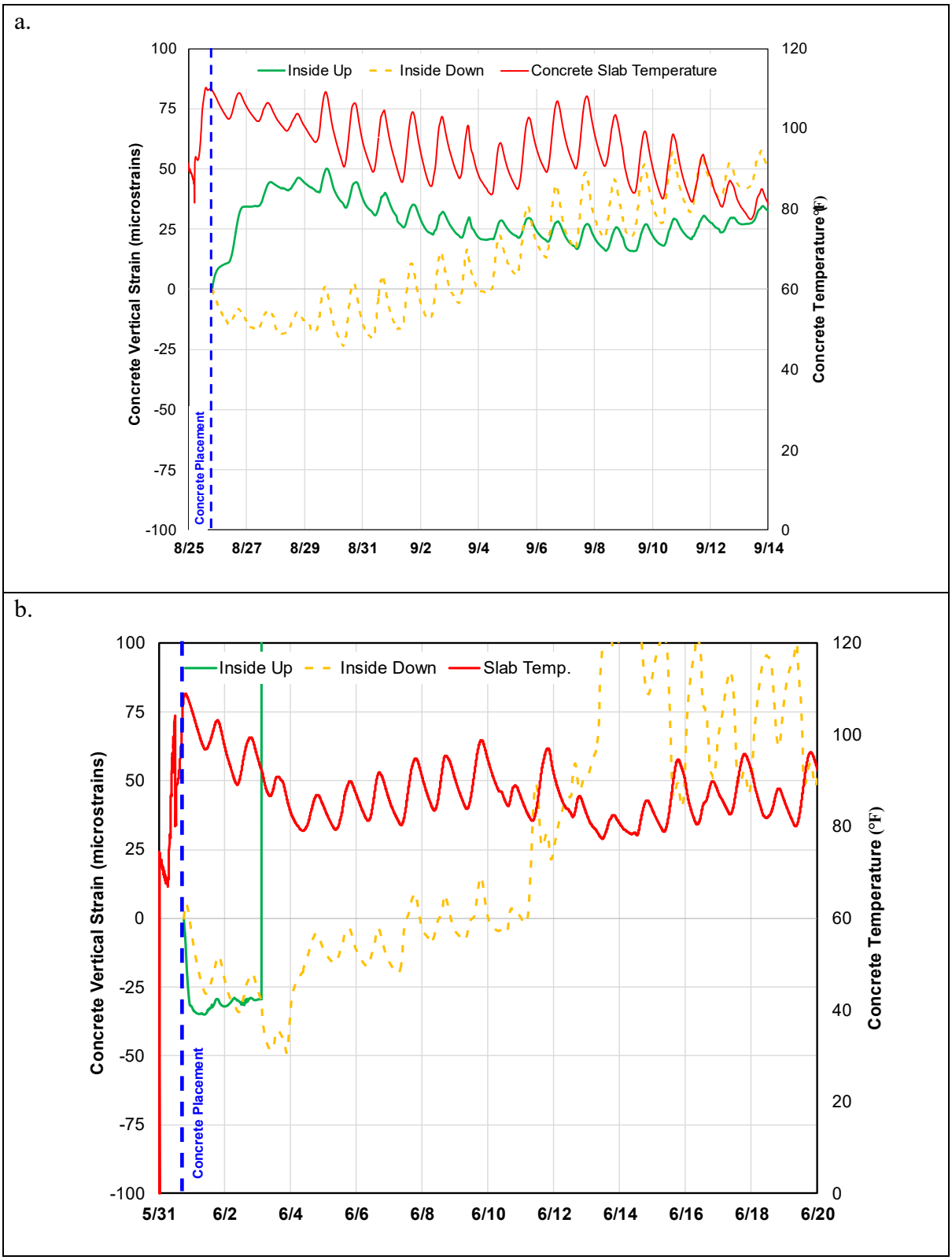

Figure 68 Comparison of vertical strains in Section 2 and Section 4

Chapter 5 Bonded Concrete Overlay Performance

This chapter discusses the performance of the bonded concrete overlay evaluated up to January, 2024. Since the overlay construction was completed in early September 2023, the information presented in this Chapter is preliminary in nature, and the monitoring of the long-term performance will be conducted for TxDOT's rigid pavement database project (0-7147). The findings to be made will be included in the rigid pavement database report. In this Chapter, structural evaluations of the overlay with Falling Weight Deflectometer (FWD), along with cracking and other pertinent performance indicators observed, will be discussed.

5.1 Slab Deflection on Bonded Concrete (CRCP) Overlay

Following the construction of CRCP overlay of the outside lane in May/June 2023, the post-overlay FWD test was conducted. The drops were made at the same location as the previous FWD test on CPCD. The GPS information recorded during the FWD testing was utilized to locate the testing points. The deflection on CRCP overlay was compared with the deflection measured on existing CPCD. However, only Location 2 and Location 3 are the segments where the deflection before and after the overlay shall be compared. Location 1 was not part of the overlaid section; therefore, it is excluded from the analysis.

Figure 69 shows the FWD deflections on newly overlaid 5-inch CRCP at Location 2. Comparing it with FWD deflections on 9-inch CPCD, FWD results showed improved uniformity even at the locations where there are large deflections recorded on the CPCD. The blue dots, which represent FWD drops on CRCP overlay ranged between 2 mils to 4 mils. It can be observed that, regardless of the variability in deflections on the CPCD layer, the deflections measured on the CRCP overlay are relatively consistent. For instance, if we compare the deflections of the segment between DMI 0 to 300 and between DMI 300 to 900 after the overlay, there is minimal difference in the measured deflections on CRCP overlay, even though there was a large difference in deflections on CPCD between the two segments. This indicates the capability of bonded CRCP overlay on improving the structural condition of CPCD.

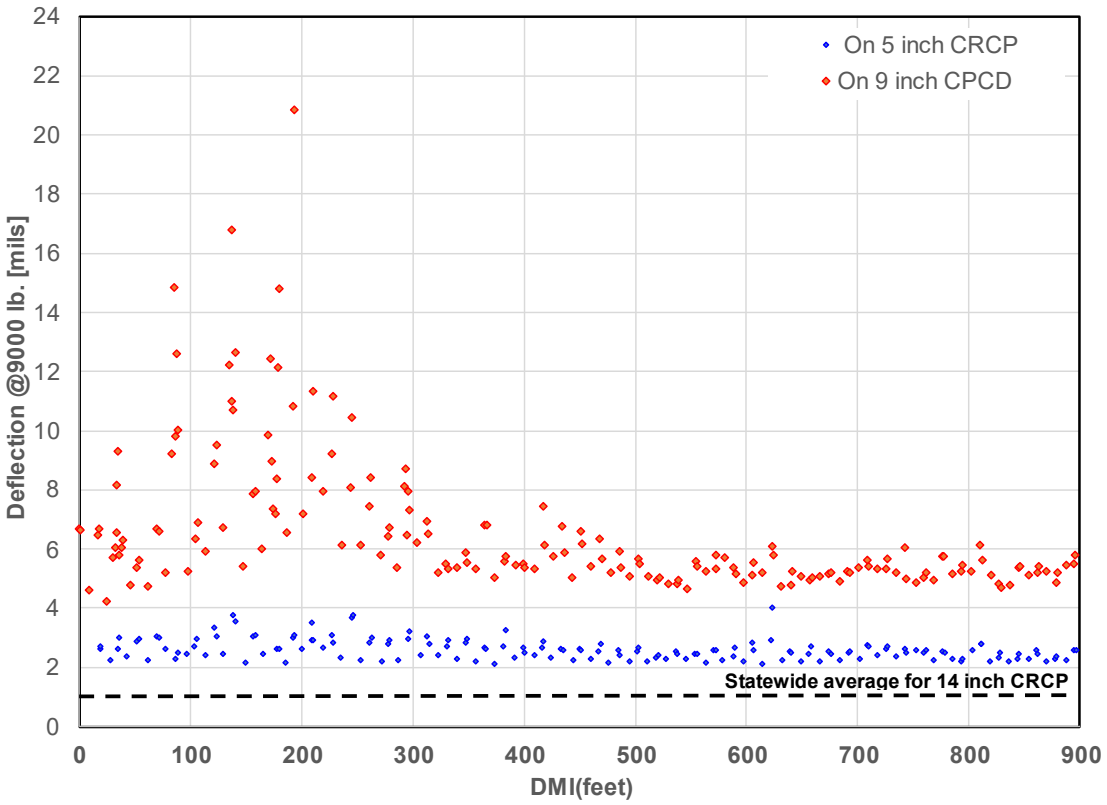

Figure 69 Comparison of FWD deflection between 9-inch CPCD and after placing 4-inch CRCP in location 2

Figure 70 shows the FWD deflections on CPCD and 5-inch CRCP at Location 3. As was observed in Location 2, 5-in CRCP overlay reduced not only the deflections themselves, but the variability in slab deflections. This improvement in the deflection characteristics implies better long-term performance of the overlayed CRCP. Although the average deflection on the CRCP overlay is larger than the statewide average of 1.25 mils for a 14-inch CRCP, the reduction in deflection compared to the existing CPCD is notably significant. The significant reduction in deflection by the placement of CRCP overlay was also observed in previous BCO projects in US 281 Wichita Falls and Loop 610 South in Houston.

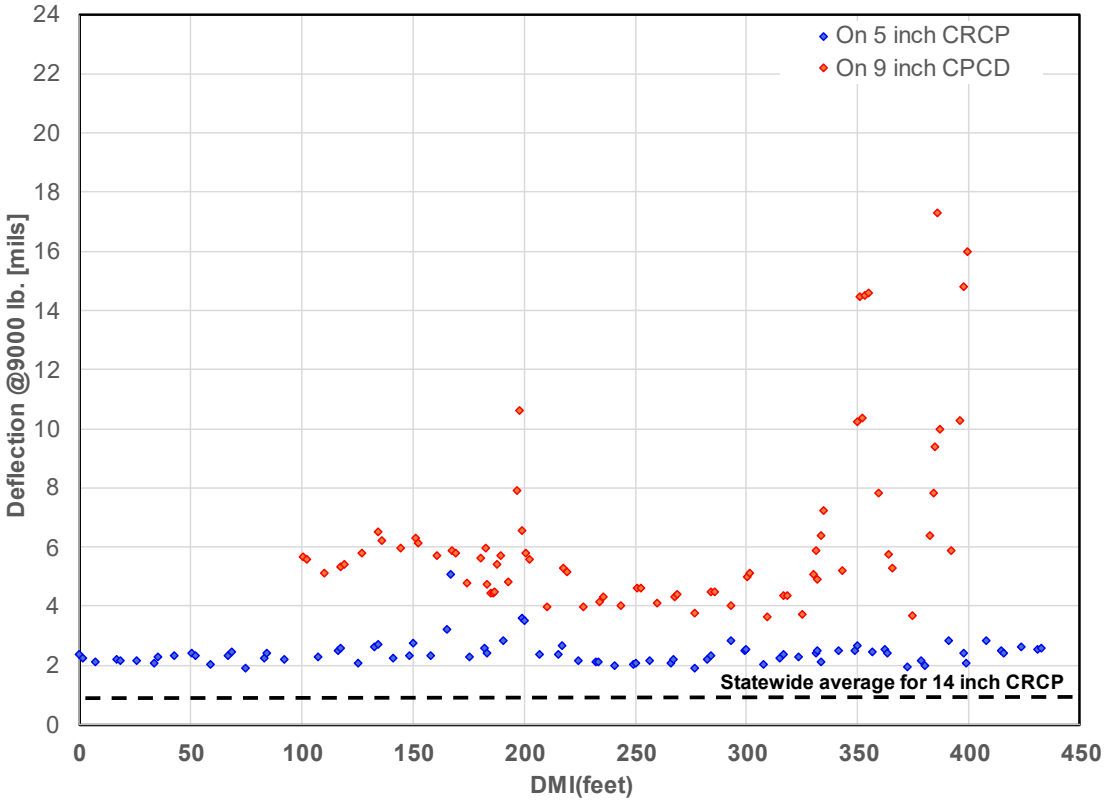

Figure 70 Comparison of FWD deflection between 9-inch CPCD and after placing 5-inch CRCP in location 3

5.2 Observed Crack and Distresses

Following the construction of both the outside and inside lanes, surveys were conducted to evaluate cracking behavior and identify any distresses. In this project, transverse saw-cuts were made in some segments, while in the other segments, no transverse saw-cuts were made.

5.2.1 Outside Lane

Figure 71 displays the construction details for both the outside and inside lanes, highlighting several important aspects. As previously mentioned, the outside lane comprises six segments: Segment 1A, Segment 1B, Segment 2, Segment 3, the Leave-out segment, and the Exit to FM79 segment. Among these, saw-cuts were made in CRCP overlay at the locations of transverse contractions joints in CPCD for Segment 1A, Segment 2, and Segment 3 underwent sawcuts at 15-foot intervals, , indicated by blue dotted lines in the figure. These saw-cuts were not intended or a part of this research. Segment 2 and Segment 3 were completed on May 30th, Segment 1A on May 31st, and Segment 1B on June 2nd, 2023. The initial crack survey for these segments was conducted on June 2nd, 2023.

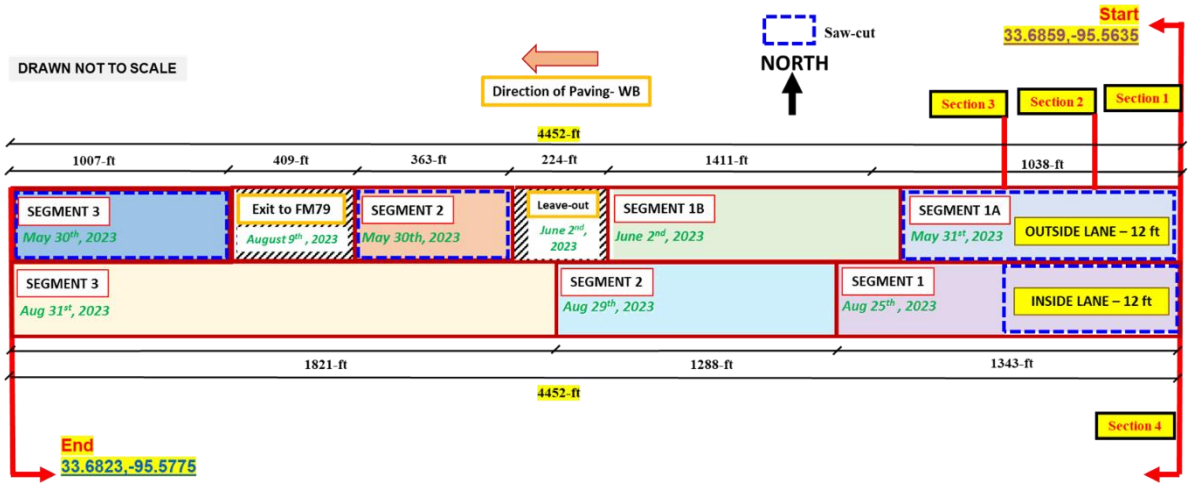

Figure 71 Construction detail on both outside and inside lane construction

Figure 72 illustrates average crack spacings during the first week post-placement. On Day 1, it shows limited crack developments in Segments 1A, 2, and 3, resulting in larger crack spacing. For example, the average crack spacing on Day 1 was approximately 135 feet for Segment 1A, 180 feet for Segment 2, and 205 feet for Segment 3. However, by Day 2, significant cracking developed across all segments, reducing the spacing to less than 20 feet. Figure 73 provides a more detailed average crack spacing after Day 2. This increased crack development could be attributed to the temperature drop on June 3rd and continued drying shrinkage of concrete. Over time, the average crack spacing across all segments stabilized, ranging between 12 and 14 feet, regardless of whether the segments were sawcut or not. This observation suggests that saw-cutting does not significantly affect later-age crack development.

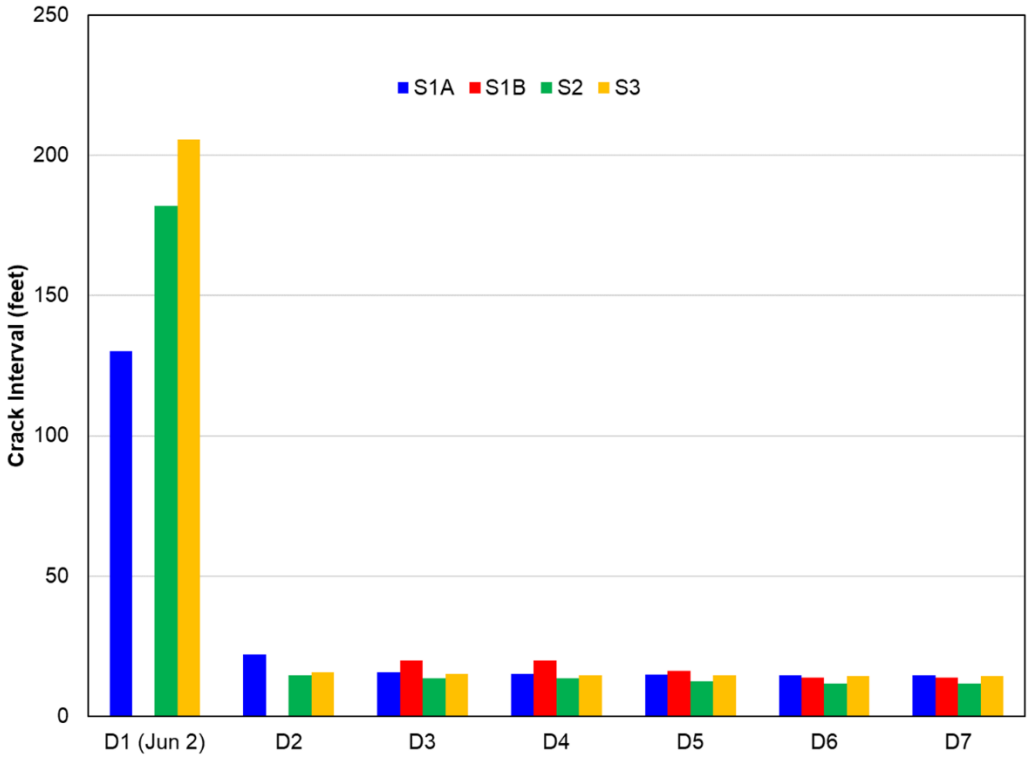

Figure 72 Crack spacing observed in different Segments

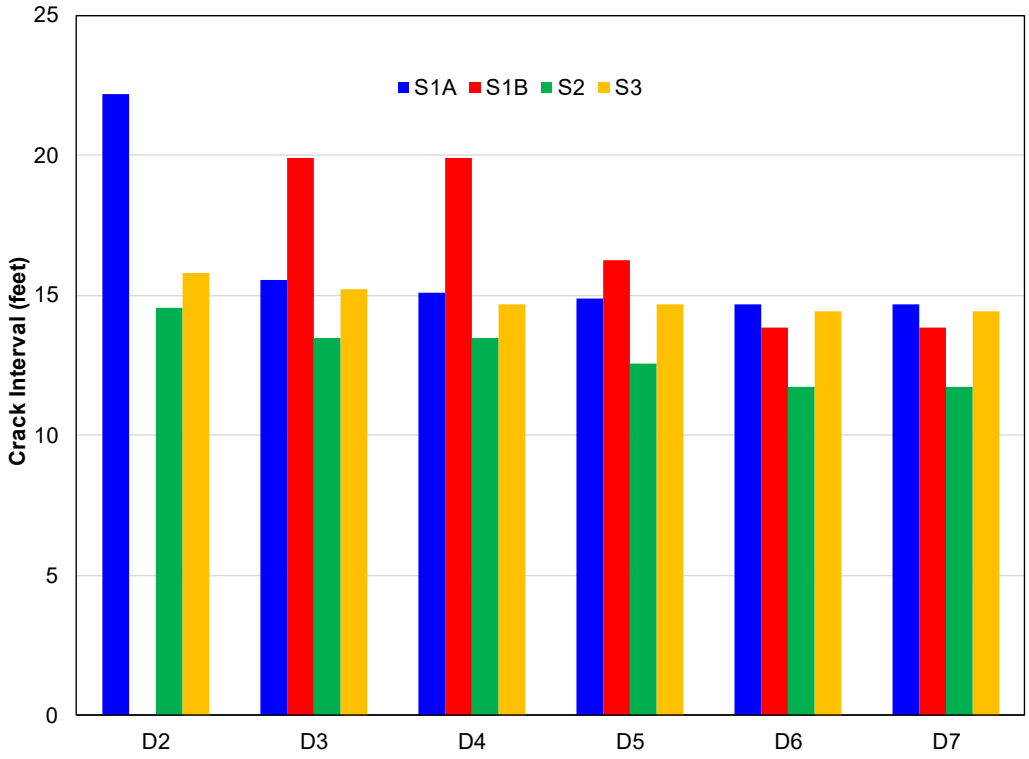

Figure 73 Graph showing Crack Interval observed in different Segment after Day 2

A notable aspect of the crack development was its location. In Segments 1A, 2, and 3, where sawcuts were made directly above the joints of the existing CPCD, cracks propagated at the sawcut locations. However, in Segment 1B, which did not undergo saw-cuts, the majority of cracks still developed at the locations of transverse contraction or repair joints in CPCD. Initial surveys identified some off-joint transverse cracks, but a review of the slab condition before overlay application revealed that these cracks also developed over repair joints. This pattern indicates that in CRCP overlays, reflection cracking is a dominant factor for transverse crack development. The finding in this study, along with the fact that the majority of transverse cracks in CRCP develop over transverse steel, indicate the sensitivity of transverse crack development to external factors in CRCP – in this case, transverse contraction joint. Additionally, crack survey revealed that, in the segment with saw-cuts, the resulting cracks have larger widths compared to the cracks that developed in the segment without saw-cuts.

5.2.1.1 Bond Test

Table 7 presents a summary of the bond tests conducted on the outside lane. A total of five slabs were identified based on visual survey conducted in November 2019. 12 coring locations were selected in those 5 slabs. Of these, 5 coring locations were on repaired areas, labeled as 'Repair' in the summary. The remaining 7 locations were on existing CPCD without distresses, marked as 'Normal' in the summary. Figure 74 **Coring Location for Bond Test on outside lane** illustrates the coring locations for each slab, both before and after concrete placement. Notably, all bond

tests resulted in failure, occurring at the interface between the existing CPCD and the new CRCP overlay.

One of the potential reasons for the failure in conducting the bond test is the condition of the existing CPCD. It was observed during coring operation that the concrete in CPCD layer is quite solid, and it took a long time to be able to core the existing concrete even by a quarter of an inch. It might be that the phase of coring for existing CPCD concrete induced bending on the 5-in concrete core, causing debonding at the interface. This needs to be further verified.

Table 7 Summary of Bond Test conducted on Outside Lane US 82(Loop 286)

Segment (Slab Number)	**Concrete Age (Days)**	**Coring Points**	**Remarks**	**Result**
Segment 1A (Slab 79)	23	3	3 Normal (*Failed During Coring Operation*)	Fail
Segment 1A (Slab 80)	23	2	2 Normal (*Failed During Coring Operation*)	Fail
Segment 1B (Slab 150)	21	2	1 Repair + 1 Normal (*Failed During Coring Operation*)	Fail
Segment 2 (Slab 203)	24	3	2 Repair + 1 Normal (*Failed During Coring Operation*)	Fail
Segment 3 (Slab 212)	24	2	2 Repair (*Failed During Coring Operation*)	Fail


Before
SLAB 80
80
01 09 2022 09 42


After
23 days old Concrete
Location 4
Normal
Location 5
Normal
06 22 2023 15 06


Before
SLAB 150
150
01 09 2022 09 54

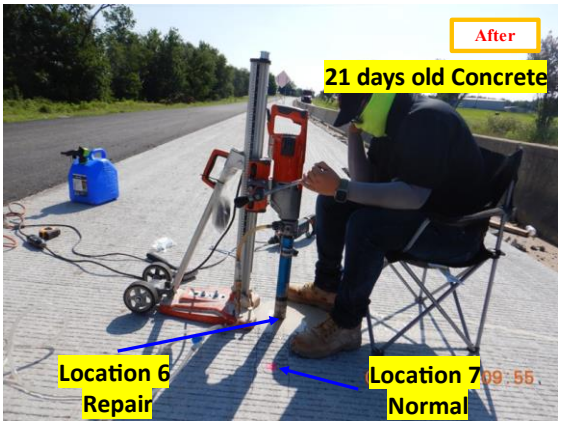
After
21 days old Concrete
Location 6
Repair
Location 7
Normal
09 55


Before
SLAB 203
01 09 2022 10 02

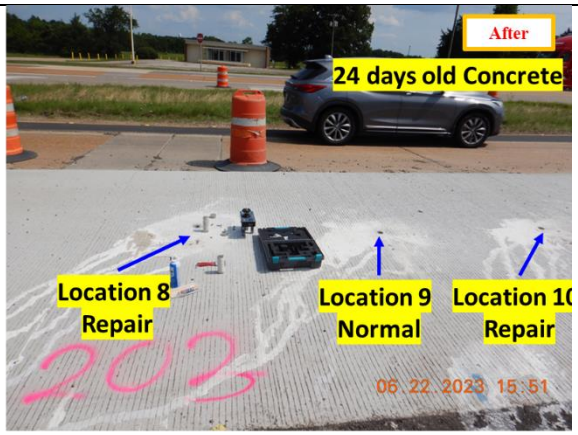
After
24 days old Concrete
Location 8
Repair
Location 9
Normal
Location 10
Repair
203
06 22 2023 15 51

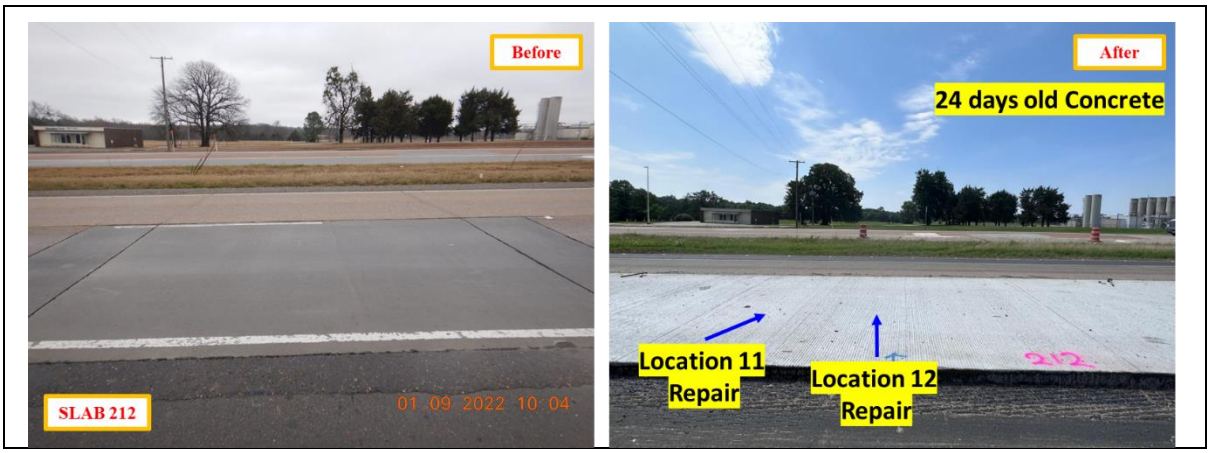

Figure 74 Coring Location for Bond Test on outside lane

5.2.1.2 Debonding

As discussed earlier, an issue of debonding in the outside lane was identified. To investigate potential debonding, a specific slab section in the outside lane was selected, and MIRA testing was performed. Figure 75 illustrates the MIRA testing on the selected slab.

Figure 75 MIRA scanning performed in a selected slab.

Figure 76 presents the MIRA testing results. The images, specifically numbers 1, 3, 4, 5, 7, and 8, indicate, in general, debonding occurred at slab corners and along the longitudinal edges. However, at the middle of the transverse contraction joints, debonding was not observed.

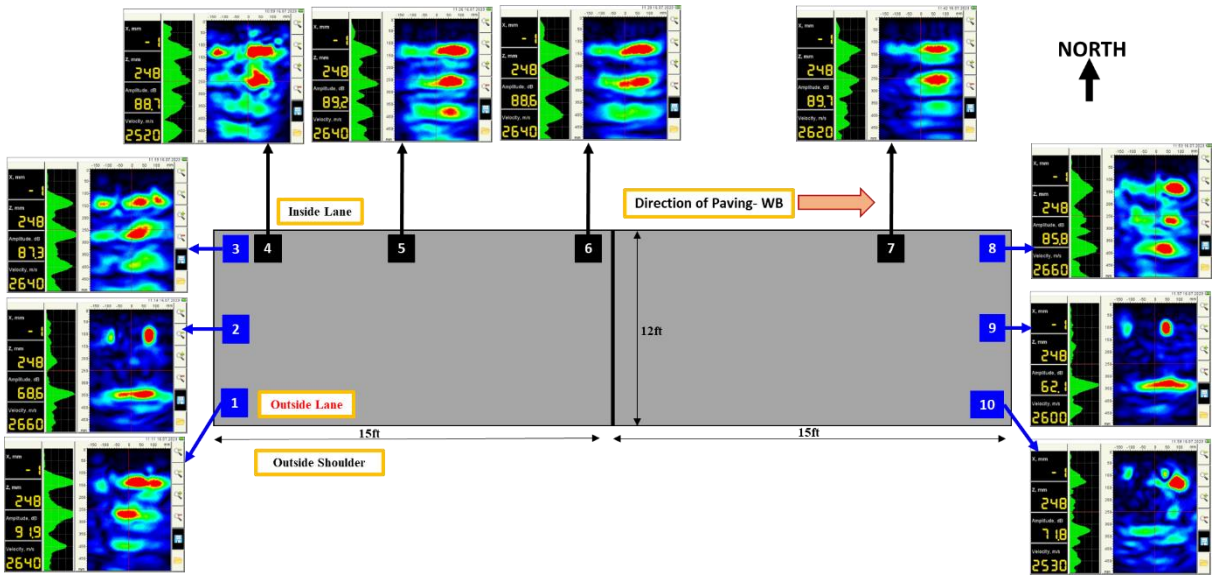

Figure 76 MIRA image of selected slab on outside lane

In MIRA images, areas in blue represent solid concrete with no large voids. On the other hand, red areas represent void or materials quite different from concrete, such as steel. Figure 77 is the image taken at Location 2, showing two longitudinal steels placed at 4-in deep and a total slab thickness of 14-in (350 mm), which is the combined slab thickness of 9-in CPCD and 5-in CRCP. And no void or debonding is observed at the interface (100 mm down from the surface).. This is evident in MIRA images numbered 9 and 10 as well.

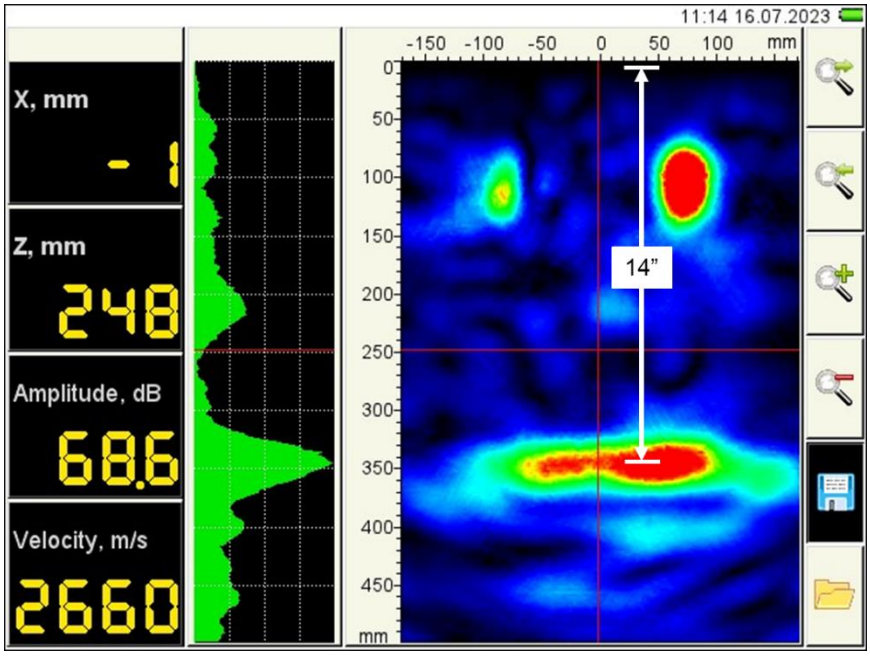

Figure 77 MIRA image with no debonding

Examining Figure 78, an image taken at location 5, the MIRA image shows debonding; a layer of separation is noticeable at a depth of 5 inches from the top, highlighting the progression of debonding. At this location, MIRA was placed longitudinally and between two longitudinal steels. It shows delamination at the bottom of the 5-in CRCP. Here, the overlay thickness was about 130 mm, or 5.2-in, a little bit larger than the design thickness of 5-in. The other 2 red dots do not represent discontinuities, such as bottom of the CPCD. Rather, they represent reflections of waves at the interface. It is noted that the middle red dot is approximately twice as deep as the top one (about 265 mm), and the third red dot is three times as deep as the top one (about 390 mm).

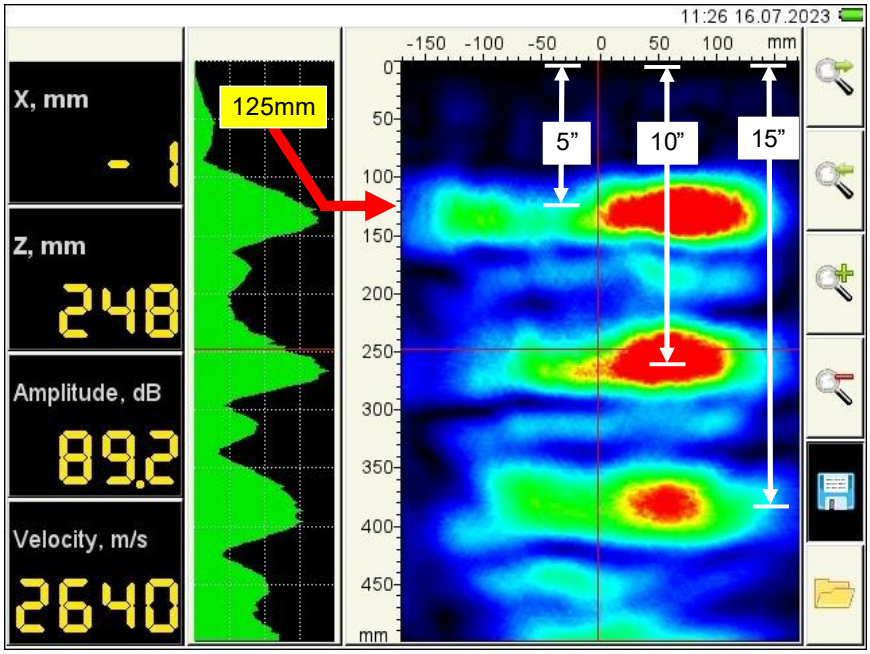

Figure 78 MIRA Image with debonding

This analysis led to identifying causes for failures in bond test and the probable debonding in the outside lane, which appears to stem from construction issues.

Review of job control testing results indicates large variabilities, especially for slump, which varied between 4 and 8.5 inches as shown in Table 8. The concrete from some trucks was so watery that, after the concrete placement, there was a thick layer of water, which resulted in different surface colors of concrete. As will be discussed later, a good bond was confirmed at the location of 4-in slump concrete. Even though no systematic field evaluations were conducted to identify the correlation between slump and bond strength, anecdotal evidence indicates a potential correlation.

Table 8 Concrete Test Result for outside lane

Segment	Date Sample	Date Broke	Core/Cyl#	Diameter (inch)	Length (inch)	Break (lbs)	Break (psi)	Avg (psi)	CRCP Station
Segment 1A	5/31/2023	6/1/2023	HES-10	3.997	8.076	25850	2060	2060	115+00
	5/31/2023	6/2/2023	HES-11	4.019	8.136	35920	2832	2887	115+00
			HES-12	4.027	8.119	37460	2941		
	5/31/2023	6/2/2023	HES-13	4.011	8.015	36960	2925	2957	120+30
			HES-14	4.017	8.112	37880	2989		
Segment 1B	6/2/2023	6/5/2023	HES-15	4.013	8.068	45600	3606	3584	126+00
			HES-16	4.017	8.104	45130	3561		
	6/2/2023	6/5/2023	HES-17	4.022	8.084	45750	3601	3626	129+00
			HES-18	4.015	8.087	46210	3650		
	6/2/2023	6/5/2023	HES-19	4.023	8.059	42620	3353	3257	132+00
			HES-20	4.022	8.056	40150	3161		
Segment 2	5/30/2023	6/9/2023	HES-21	4.02	8.111	52360	4126	4126	157+00
Leave-out	6/9/2023	6/12/2023	HES-22	4.015	8.015	31180	2463	2391	139+00
			HES-23	4.019	8.08	29420	2319		
	6/9/2023	6/16/2023	HES-24	4.017	8.08	45170	3607	3548	139+00
			HES-25	4.013	8.093	44130	3489		
Exit to FM 79	8/9/2023	8/11/2023	HES-26	4.01	8.08	39940	3162	3375	144+00
			HES-27	4.015	8.002	45420	3587		
	8/9/2023	8/11/2023	HES-28	4.05	8.091	43670	3390	3448	148+00
			HES-29	4.009	8.135	44240	3505		
Segment 3	5/30/2023	5/31/2023	HES-1	4.02	8.09	36840	2903	3051	141+00
			HES-2	4.019	8.051	40560	3198		
	5/30/2023	5/31/2023	HES-3	4.006	8.103	33800	2687	2799	150+00
			HES-4	4.019	8.062	36930	2911		
	5/30/2023	5/31/2023	HES-5	4.021	8.084	39200	3087	3183	154+00
			HES-6	4.021	8.11	41640	3279		
	5/30/2023	5/31/2023	HES-7	4.025	8.025	19410	1525	2151	157+00
			HES-8	4.016	8.064	35170	2777		
	5/30/2023	5/31/2023	HES-9	4.015	8.042	37770	2983	2983	157+00

5.2.2 Inside Lane

5.2.2.1 Bond Test

Based on the experience of bond test conducted in the outside lane, the research team opted for a trailer mounted coring machine to perform the test in the inside lane as shown in Figure 79. The primary objective of this approach was to determine if a trailer-mounted coring machine could minimize eccentricity of the drilling to prevent premature shear failure at the overlay interface or

to minimize damage to the concrete interface. To this end, three locations were selected for coring tests, as shown in Figure 80. Table 9 provides a summary of these tests in the inside lane.

Of the three coring locations, locations C2 and C3 encountered failures during the coring operation, while location C1 did not fail. The bond test at coring location C1 revealed a bond strength of 109 psi. Concrete in this location was placed on August 31, 2023, making it relatively new concrete at only 15 days old. In contrast, coring locations 2 and 3, constructed on August 29 and August 25, 2023, respectively were 17 and 21 days old, respectively, yet they failed during the coring operation. This observation led to the hypothesis that the failures were not attributable to shear failure at the interface caused by the coring method.

An alternative explanation for the shear failures at the interface between the existing and overlay slabs could be linked to construction methods, as suggested by the distresses observed in the inside lane. These findings and their correlation with the bond test results in both the inside and outside lanes are further discussed in the following sections.

Table 9 Summary of Bond Test conducted on Inside Lane US 82(Loop 286)

Segment	Coring Points	Coring Age (Days)	Remarks	Result	Slump
Segment 3	C1	15	**Peak Force**: 330 lb.F. **Disk Area**: 3.017 in2 **Bond Strength**: 109 psi	Pass	Ranged from 6.5 inch to 7.5 inch.
Segment 2	C2	17	Failed During Coring Operation	Fail	
Segment 1	C3	21	Failed During Coring Operation	Fail	

Figure 79 Trailer mounted coring machine used for Inside lane

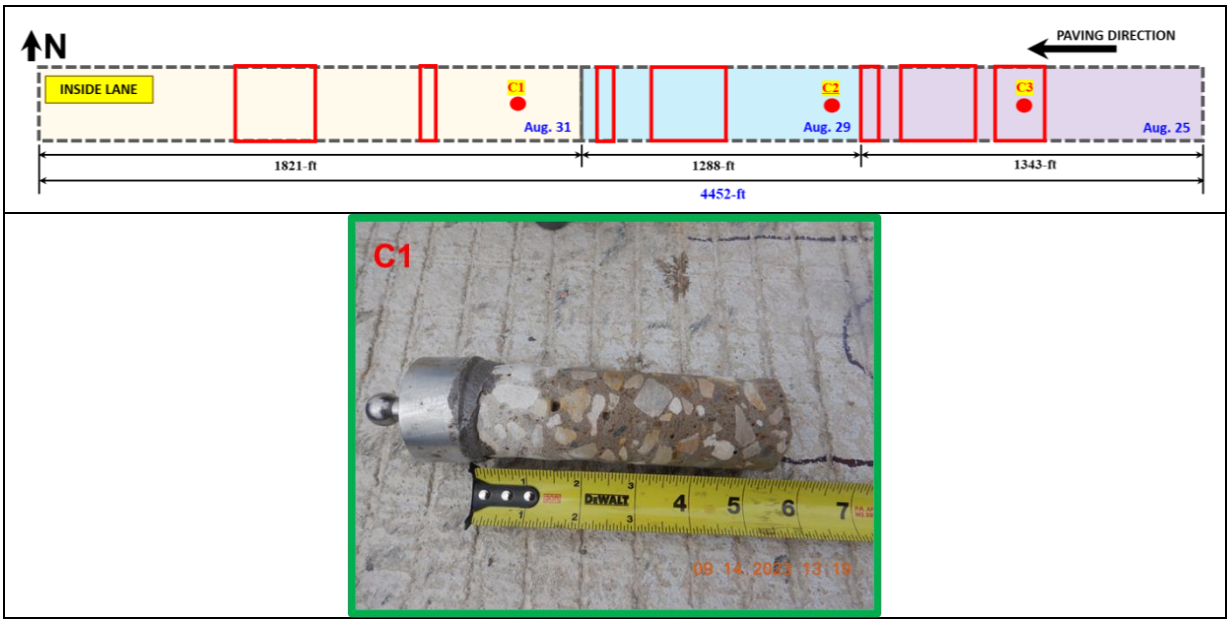

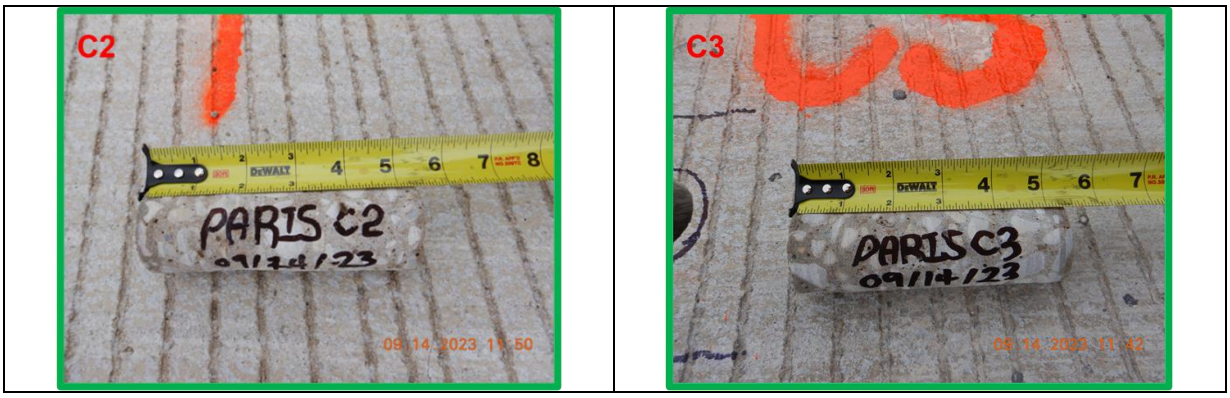

Figure 80 Coring location and bond test for Inside lane

5.2.2.2 Longitudinal cracks

Upon completion of the inside lane construction, longitudinal cracks were observed. Figure 81 shows the location of a longitudinal crack observed in the field. Table 10 provides a detailed summary of these longitudinal cracks as observed in the field.

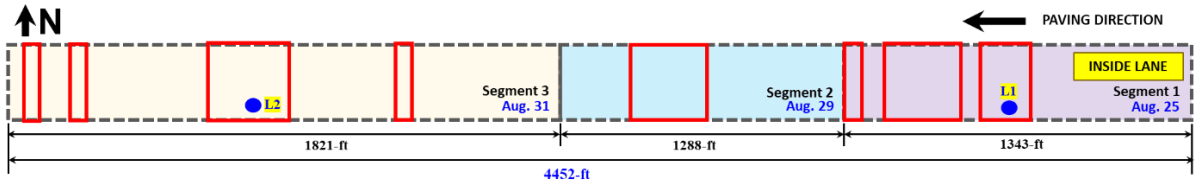

Figure 81 Location of longitudinal crack in inside lane

Table 10 Details on longitudinal cracks on inside lane

Start	End	Length	Width	Offset from CL (ft)	Segment
122+37	123+58	121	10	-2	1
124+17	125+61	144	12	0	1
126+33	126+47	14	3	-9	1
134+41	135+04	63	10	-2	2
146+03	146+30	27	3	-9	3
147+13	150+74	361	5	-7	3
153+78	153+79	1	1	-9	3
157+00	157+04	4	1	-6	3

Longitudinal cracks were notably aligned directly above the longitudinal steel, indicating that these are settlement cracks. This correlation suggests a direct link to the construction process. During construction, it was noted that the slump of the delivered concrete was higher than the required 4 inches. This observation is supported by the job control testing results as shown in Table 11. This data implies a correlation between higher slump and the occurrence of settlement cracks in the inside lane.

Table 11 Concrete Test Result for inside lane

Segment	Date Sample	Date Broke	Core/Cyl#	Diameter (inch)	Length (inch)	Break (lbs)	Break (psi)	Avg (psi)	CRCP Station
Inside Lane Segment 1	8/25/2023	8/28/2023	HES-30	4.0196	8.0376	40740	3212	3208	115+00
			HES-31	4.028	8.0456	40820	3203		
	8/25/2023	8/29/2023	HES-32	4.023	8.035	43366	3411	3376	119+00
			HES-33	4.029	8.105	42580	3340		
	8/25/2023	8/29/2023	HES-34	4.027	8.035	35600	2795	2601	123+00
			HES-35	4.013	8.077	30430	2406		
Inside Lane Segment 2	8/29/2023	9/6/2023	HES-36	4.029	8.052	58920	4625	4464	127+00
			HES-37	4.012	8.056	54400	4303		
	8/29/2023	9/6/2023	HES-38	4.006	8.068	45640	3621	3627	130+00
			HES-39	4.027	8.028	46250	3632		
	8/29/2023	9/6/2023	HES-40	4.01	8.095	40880	3237	3384	135+00
			HES-41	4.007	8.058	44520	3530		
	8/29/2023	9/6/2023	HES-42	4.012	8.053	53100	4200	3599	138+00
			HES-43	4.023	8.071	38100	2997		
Inside Lane Segment 3	8/31/2023	9/6/2023	HES-44	4.01	8.12	62660	4962	4849	141+00
			HES-45	4.001	8.127	59550	4736		
	8/31/2023	9/6/2023	HES-46	4.013	8.08	42010	3321	3191	147+00
			HES-47	4.002	8.022	38500	3060		
	8/31/2023	9/6/2023	HES-48	4.019	8.013	43360	3410	3456	151+00
			HES-49	4.023	8.029	44520	3502		
	8/31/2023	9/6/2023	HES-50	4.021	8.117	42380	3337	3371	155+00
			HES-51	4.014	8.09	43080	3404		

To investigate the nature of longitudinal cracks, two specific locations were selected. The first location, designated as L1, is in Segment 1, from 122+37 to 123+58, covering a length of 121 feet. Figure 82 illustrates the trajectory of the longitudinal crack in this segment, marked in red. MIRA scanning was conducted directly over this longitudinal crack to determine its location relative to longitudinal steel, and it was observed that the majority of the cracks were aligned with the longitudinal steel.

During a coring operation in a section of the longitudinal crack, it was ensured that the longitudinal steel was avoided. This coring process revealed the absence of a bond between the existing CPCD and the new CRCP overlay. Notably, at 123+00, the concrete slump was 7.5 inches, far exceeding the required 5.5-inch standard. This finding suggests a link between the increased slump and the debonding of the layers. The cored sample from L1, measured 5 inches

in length, revealed that the cracks were wider on the surface, further supporting the crack was caused by plastic settlement of concrete over longitudinal steel.

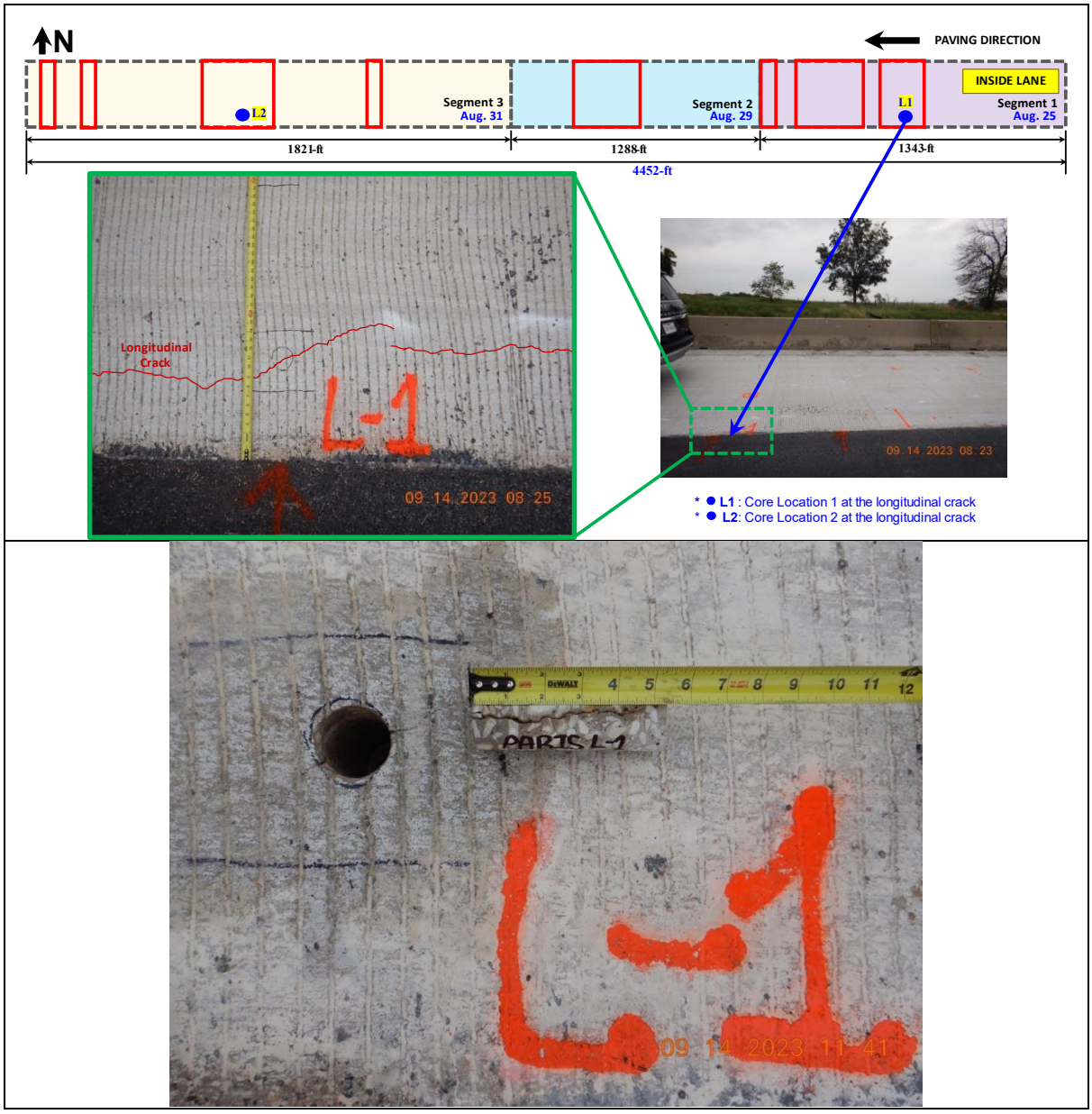

Figure 82 Longitudinal cracks observed at Location 1 on Segment 1

Similarly, location L2 falls on Segment 3 between 147+13 to 150+74, covering the length of 361 feet. As shown in Figure 83, the red mark shows the propagation of the longitudinal crack. The slump for this area, at 147+00, was measured at 6.5 inches which is still higher than the 5.5-inch requirement. These two locations establish that the increase in slump possibly led to debonding as well as plastic settlement cracks.

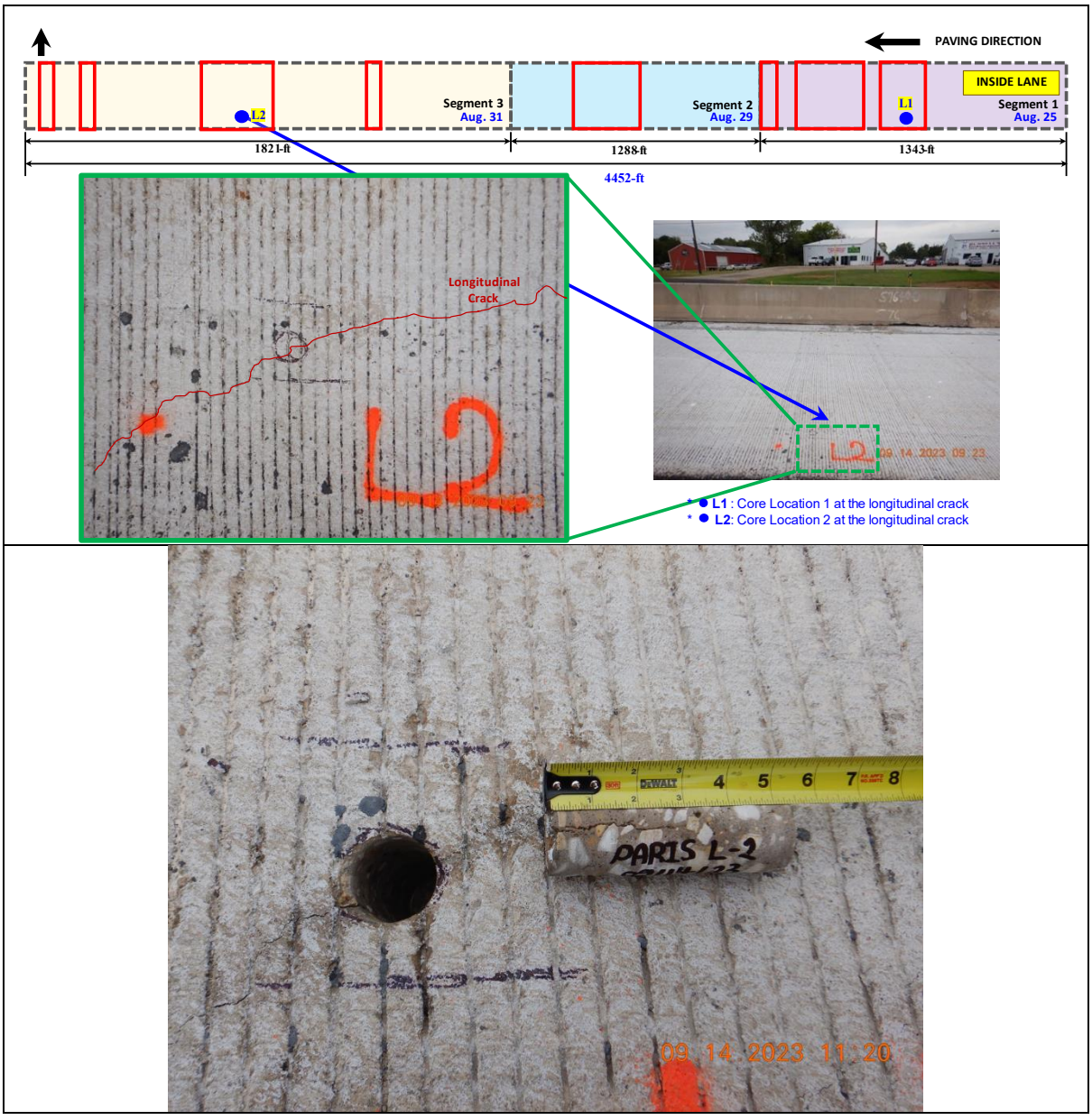

Figure 83 Longitudinal cracks observed at Location 2 on Segment 3

Chapter 6 Summary

The CRCP overlay project on old CPCD in Loop 286, Paris, is an ongoing effort to evaluate the effectiveness of CRCP as a rehabilitation method for old deteriorated CPCD, combining long-term performance with reasonable costs. Following the successful application of a 7-inch CRCP bonded overlay on CPCD under heavy truck traffic on US 75 in Sherman, a section of Loop 286 in Paris, between US 82 and US 271, was selected for a similar treatment. This research project focuses on early-age pavement performance evaluation of the CRCP overlay.

The following are the summary of the findings:

- The overall condition of the existing CPCD in Loop 286 was generally good, with no severe distresses identified. However, several repaired sections were noted in both the inside and outside lanes, specifically at the joints. This observation suggests that there were previous joint-related issues in the CPCD.
- The structural evaluation, conducted using Falling Weight Deflectometer (FWD) testing, revealed that the average deflection at the mid-slab of the 9-inch CPCD section was about 5 mils. Post-CRCP BCO construction structural evaluation has shown that there was a reduction of deflection with values between 2 to 4 mils, indicating the strengthening of the structural capacity of the pavement by CRCP overlay.
- Using the structural information obtained on CPCD and estimating 30-year design traffic, the CRCP overlay design thicknesses that were proposed are 4 inches and 5 inches. Eventually, it was decided that a 5-inches overlay will be implemented. The steel percentage of the 5-inch overlay was recommended to be 1.02%.
- Slab temperature profile has shown that the CRCP overlay provided an insulating effect on the existing CPCD that significantly reduced the range of daily temperature variation after concrete overlay placement.
- Bond strength testing indicated quite poor bond at the interface, which might compromise the long-term performance of this overlay. Anecdotal evidence shows concrete with quite a high slump was responsible for poor bonding.
- Longitudinal cracks were observed where concrete slump was rather large, and most of them were settlement cracks. Also, debonding was observed near longitudinal cracks, supporting the hypothesis that poor bonding was partly due to the use of high slump concrete.
- Transverse crack surveys showed that cracks propagated above the location of the CPCD joint, indicating that reflection cracking is a dominant mechanism in CRCP bonded overlay on CPCD.
- It appears that some transverse contraction joints in the existing CPCD were locked. It is possible that these locked joints are not limited to this project. It could be that locked joints may be a statewide issue.

The age of this overlay is less than 9 months, and its performance evaluations made in this study are thus quite preliminary in nature. Further evaluations, including forensic evaluations of longitudinal cracks and debonding, will be conducted under the current rigid pavement database project and the findings will be included in the technical memorandums and the final report of the rigid pavement database project.

References

AASHO. (1962). *The AASHO Road Test Report 5*. Highway Research Board. Wasington, D.C., USA

Choi, P., Ryu, S., Zhou, W., Saraf, S., Yeon, J., Ha, S., & Won, M. (2013). *Project Level Performance Database for Rigid Pavements in Texas, II,* Texas Tech University. Center for Multidisciplinary Research in Transportation. Lubbock, TX, USA

Ryu, S. W., Won, H. I., Choi, S., & Won, M. C. (2013). Continuously reinforced bonded concrete overlay of distressed jointed plain concrete pavements. *Construction and Building Materials*, 40, 1110-1117.

Ryu, S., Won, H., & Won, M. C. (2011). *Continuously Reinforced Bonded Concrete Overlay of Distressed Jointed Concrete Pavements.* Texas Tech University. Center for Multidisciplinary Research in Transportation. Lubbock, TX, USA

TxDOT. (2023). *Condition of Texas Pavement - PMIS Annual Report FY 2020-2023*. Texas Department of Transportation. Austin, TX, USA

Appendix A: Additions and Amendments to Pavement Manual

This document describes recommended additions and amendments to Section 4 – Bonded Concrete Overlay in Chapter 10 – Rigid Pavement Rehabilitation of TxDOT Pavement Manual.

4.2 Bonded Concrete Overlay (BCO) Procedures

- Second and third sentences in the third paragraph under "1. Repair distresses in the existing pavement." need to be revised as follows:

  When distresses are caused by localized weak slab support, it is necessary to restore the slab support by removing all loose base materials and by replacing them with new concrete per Item 361.

- First and second paragraphs under "3. If needed, place steel." need to be revised as follows:

  When constructing a CRCP BCO, reinforcing steel should be placed per design standards in the plan set. Since the slab thickness of the overlay layer is usually smaller than normal CRCP, the placement depth of the longitudinal steel should be within the vertical tolerance of longitudinal steel, which is ±0.5-in. Otherwise, potential problems including insufficient cover depth and resulting corrosion, or too large crack spacing, will result.

- The first 5 paragraphs under "4. Place and cure concrete." need to be replaced with the following:

  The concrete materials to be used for BCO must be carefully selected. In general, the less volume change potential, the better the performance will be. Thermal volume change potential of concrete depends on coarse aggregate properties – the more calcareous components in coarse aggregates, the less thermal potential of the concrete. Some documents state that the thermal properties of the new concrete must be compatible with those of the existing concrete. It doesn't have to be rather, the use of calcareous coarse aggregate, such as crushed limestone, is strongly encouraged. Another benefit of using calcareous coarse aggregate is the lower modulus of concrete. Lower modulus of concrete results in smaller concrete stresses, thus enhancing bond and overall improvements of BCO performance.

  Concrete design strength should be as stipulated in the governing specifications. Concrete design strength for BCO is usually higher than that of normal Class P concrete. However, higher strength should be achieved by appropriate uses of chemical admixtures and with a proper water/cement ratio, not by too much cement or the use of Type III cement. Use of too much cement could increase the concrete setting temperature and also drying

shrinkage, both will adversely impact bond strength and overall performance of BCO. For assistance in the development of concrete mix designs, contact Rigid Pavements and Concrete Section in the Materials and Tests Division.

- The last paragraph under "4. Place and cure concrete." needs to be replaced with the following:

  The duration of construction is critical mostly in urban areas or highways with heavy traffic. Compared with reconstruction, BCO is quicker thanks to a limited number of operations. A fast-track BCO takes this concept further: by utilizing special materials, the BCO could be opened within 6 to 24 hours after concrete placement.